THE EFFECT OF COBALT ON THE STRUCTURE AND PROPERTIES OF A Ni - Mo HOT WORK DIE STEEL

THE EFFECT OF COBALT ON THE STRUCTURE AND PROPERTIES OF A Ni - Mo HOT WORK DIE STEEL

A Thesis submitted at the
University of Aston in Birmingham for the
Degree of Doctor of Philosophy

Jeffrey Richard Holloway B.Sc

April 1970

SYNOPSIS

The possibility of improving a commercial 3% nickel 3% molybdenum hot work die steel by progressive additions of up to 10% cobalt has been explored. Several of the major property requirements for hot work steels have been studied and the effect of cobalt determined. Further development of the steel has been based on economics whereby cobalt was used to replace its cost equivalent of molybdenum. A series of ausformed alloys have also been investigated and a die wear test used as the criterion of performance of all these steels.

The results indicate that cobalt is essentially neutral in its effect on the retention of austenite after quenching and air cooling. Tempering resistance increases with increasing amounts of cobalt and the rates of nucleation and agglomeration of the alloy carbides are increased in the presence of cobalt. Analysis of the extracted carbides from the tempered samples has shown that cobalt does not alter the general form of the precipitated carbides and no evidence can be cited for its partition to the carbide phase. Fracture toughness is reduced after tempering above 200°C and the tensile properties greatly increased. Cobalt increases the A_1, A_3 and M_s temperatures. Both pearlitic and bainitic incubation during the isothermal decomposition are reduced and the transformation rates in each region are increased by cobalt. Hardenability is reduced due to the promotion of the bainite transformation. The die wear test shows a significant improvement in die wear properties with the addition of up to 3% cobalt, thereafter the effect being only marginally advantageous.

Reducing the molybdenum content of the basic steel leads to an increase in die wear. For the economically balanced steels, however, the cost per unit forging is reduced by up to 17% and several steels are suggested for further investigation and industrial trials.

The action of cobalt in steels has been reviewed and several explanations proposed to account for the observed effects. Most of the results can be successfully explained on the basis of cobalt reducing the surface energy of the carbide-ferrite interface but the elevation of the transformation temperatures remains unanswered on this basis. All the results can be rationalised if it is accepted that cobalt lowers the fault energy of the austenite and these high faulted regions act as sinks for the carbon atoms or nucleation sites for the martensite transformation.

CONTENTS

1. INTRODUCTION

Hot work die materials form an important and specialised category of die materials used in drop forging practice. During a production run, die lives vary from 1,000 to 50,000 pieces depending on the shape, size and complexity of the particular forging. Since die costs account for about 10% of the total cost of a forging, the cost per unit forging can be substantially influenced by any variation in die performance and may affect the feasibility of the whole operation.

It is difficult to obtain reliable statistics for the amount of steel consumed as hot die steels. In the United Kingdom the quantity is of the order of 10,000 tons per annum and the annual expenditure of the forging industry on dies is estimated at £7.5m. However, in common with other tool steels the importance of this group of materials should not be judged by the quantity used as the materials are unique.

Since the conditions under which the hot work steels are required to work impose exacting demands upon their properties, it is not surprising to find that these steels form a bewildering collection of miscellaneous compositions and heat treatments. The only standard British die steels are found in BSS 224, 1938 and 1949 which specifies four steels:-

i) a plain carbon steel containing 0.6% carbon

ii) a 1% nickel steel

iii) a 1.5% nickel 0.75% chromium steel

iv) the most commonly used die steel, No.5, containing 0.5-0.6% carbon, 1.25-1.75% nickel, 0.5-0.8% chromium and 0.2-0.4% molybdenum.

Although this last steel is the most important, there are many others that are used, in particular those containing 1-5% chromium and 7-10% tungsten respectively. In the United States, on the other hand, the situation is more regularised in that the American Iron and Steel Institute have an identification and type classification. The hot work die steels specified under this system of classification are found in Group 500 or under the AISI designation of "H" steels.

A tentative and highly simplified calssification of tool steels has been proposed by Settle(1) who suggests that the whole range of tool steels may be reduced to twelve essential tool materials. In this simplified classification the hot work steels are represented by three types, 381, 521 and 540 together with the addition of two others suitable for use as die casting dies. It is interesting to note that it is considered possible to reduce the vast number of tool materials to such a few and provide confirmation of a widely held opinion that many of the specifications and compositions so zealously held may be unjustifiable. On the other hand, the importance of hot die steels may be realised when it is considered that five of the twelve designated steels are for hot working operations.

The properties of hot work die steels are complex and no single parameter is sufficient to provide an index of suitability of a particular steel. The situation is further complicated by the fact that many of the required properties are mutually exclusive. In the most general terms, however, the criterion of suitability of a material for use as a hot work die steel will be the stability of its structure and its resistance to deformation and wear under the appropriate service conditions. Comprehensive reviews of property requirements have been given by Settle(1), Hopkins and Williams(2) and Bayliss(3) and these will only be briefly outlined here.

i) Thermal and Mechanical Stability

The alloy structure, which is a result of alloy composition and previous mechanical and thermal treatments, must be stable within the working temperature range. Heat treatment should produce a material that is strong enough to withstand the loads imposed in service. The normal strength parameters of yield stress and ultimate tensile strength at the usual working temperatures act as useful guides to mechanical stability and hot ductility is suitably manifested in elongation and especially reduction of area values. Kövesi(4) qualifies these mechanical test results by suggesting that reduction of area values less than 30% and elongation less than 8% indicates a susceptibility to brittle fracture in service. It is important that no significant deterioration in properties should occur during service since this will result in a change of die shape either by gross deformation or, more commonly, by surface erosion. Thermal stability is related to an alloys resistance to tempering which involves an appreciation of the kinetics of the nucleation and growth of carbide particles and precipitates.

ii) Toughness

Maximum toughness is usually demanded but, as this property bears an inverse relationship with hardness, it is at best a compromise value. The toughness of materials is usually determined using the standard Izod or Charpy impact tests which are no more than acceptance tests for metallurgical quality. These tests will be discussed in greater detail later and a more significant fracture toughness approach outlined.

iii) Abrasion and Wear Resistance

The relative movement between the forging stock and the dies establishes conditions of abrasion which leads to cumulative wear. Since, after hardening, hot work die steels usually show only small quantities (if any) of undissolved carbides in the structure, it is expected that the high temperature abrasion resistance will, in principle, run parallel with the high temperature strength and hardness properties. The hot forging stock will raise the temperature of the die surface and in extreme cases may lead to the formation of austenite. This will greatly increase the wear of the die due to the relatively poor mechanical properties of the austenite. At the die surface, therefore, the kinetics of the $\alpha \rightleftharpoons \gamma$ transformation become important.

iv) Resistance to Mechanical and Thermal Fatigue

During the forging process the dies are subjected to the effects of thermal cycling. The repeated heating and cooling of the dies by the hot forging stock creates thermal stresses which eventually lead to cracking known as thermal fatigue, craze cracking or heat checking. It has been shown(5), that factors important in controlling the occurrence of thermal fatigue are thermal conductivity and diffusivity, coefficient of thermal expansion, proof stress and temperature cycle range.

Cracking of the die by mechanical and thermal fatigue leads initially to the forging sticking in the die. This reduces production rates by increasing the time interval between each forging operation and by necessitating die removal for caulking or dressing of the cracks. Both these modes of cracking are predominantly surface phenomena and thus their occurrence will depend on surface condition as well as the design of the forging impression. The fatigue strength of these hot die steels, in common with other materials, falls with increasing temperature.

Other factors which must also be taken into account to varying degrees are :-

v) Hardenability, which governs the form of heat treatment employed.

vi) Distortion on heat treatment which is related to (v)

(vii) Ease of machining which is a combination of high rates of metal removal with good surface finish without undue tool wear.

viii) Ease of hot working if the alloy is to be forged.

ix) Resistance to oxidation.

The complexity of the property requirements for hot work die steels is illustrated in Figure 1 (page 7). Here the principle modes of die failure are indicated and also the positions in a die cavity where each type offailure is likely to occur. To demonstrate how these property requirements control the development of a commercial hot work die steel, the history of the basis steel used in this investigation may be outlined.

Early interest was aroused in the alpha molybdenum steels(6) of low carbon content containing 3% molybdenum because of their resistance to thermal fatigue and softening at elevated temperatures. During World War II, the Ford Motor Company of America developed this steel and it was put into commercial use as moulds for the centrifugal casting of aeroplane cylinders. Several blocks of this material were put into experimental service as hot working dies and it was apparent that impact properties were much lower than desired. Corbett et.al.(7) overcame this by the addition of 3% nickel which also gave the material a greatly increased depth of hardening enabling the die blocks to be air cooled to a fully martensitic structure. This base composition was further modified and 0.5% chromium added to improve oxidation resistance. Thus the alloy "Bestem"** was developed according to the specification:-

---

** Bestem is a Trade Name of Walter Somers Ltd.

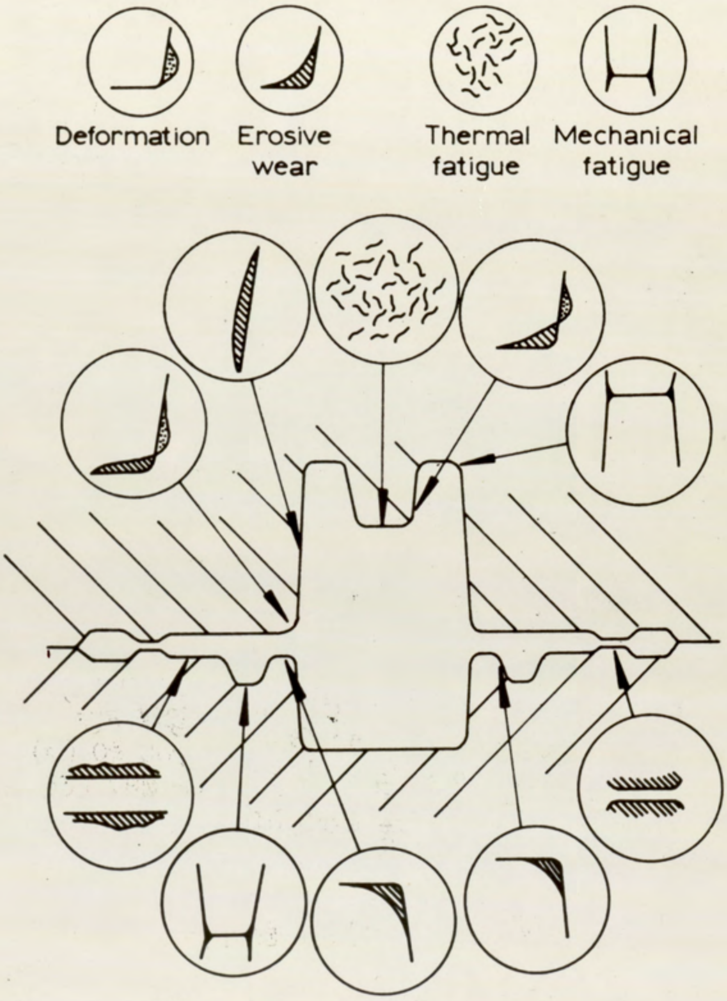

FIGURE 1

Modes of die failure

Carbon	0.25 - 0.30%	Manganese	0.65 - 0.70%
Silicon	0.35% max.	Nickel	3.0 - 3.5%
Sulphur	0.04% max.	Molybdenum	3.25-3.50%
Phosphorus	0.04% max.	Chromium	0.5 - 0.6%

It is this alloy (termed 3M steel in the following text) which forms the base composition in this investigation and an assessment is made as to its further development by alloying techniques.

An increase in hardness and hence, according to empirical relationships, an increase in wear resistance may be effected by raising the carbon and molybdenum contents of the steel to give a higher martensitic hardness and content of free carbides. However, increasing the carbon content would almost certainly reduce the toughness of the material and an uncontrolled increase in the molybdenum content could lead to difficulties during heat treatment due to its ferrite forming properties. The hardenability and toughness would appear "acceptable" at their present levels so it is considered that increasing the nickel content would not be economically justifiable. The problem therefore is how to increase the tempering resistance without increasing the carbon content and it is in this application that cobalt is of extreme importance.

Recently there have been several reviews published on the effect of cobalt in steels(8-11) and while it is not necessary to go over this ground in detail again, several features germane to this discussion may be mentioned.

The chemical and physical properties of cobalt and iron are similar since cobalt is found between iron and nickel in the Periodic Table. Iron and cobalt have an almost identical atomic size (Co - 2.506 Å and Fe - 2.481 Å), a common allotropic form and the same number of valency electrons and hence fulfil Hume - Rothery's conditions governing the formation of a wide solid solution. Moreover, the atomic properties of the two metals are not conduc~~t~~ive to the formation of intermetallic compounds. Consequently only slight improvement in the mechanical properties can be expected from the addition of cobalt alone. This is illustrated in Figure 2 (page 10), which is taken from work by Lacy and Gensamer(12) and Allen(13).

The effect of cobalt on the main property requirements of hot work steels will be outlined in the course of this thesis but its influence on several less critical requirements may be mentioned at this point. The term "less critical" is used advisedly here since the emphasis given to a particular property of a hot work steel will depend upon the application of the material.

Cobalt is an austenite stabliser and thus, unlike further molybdenum additions, would not lead to heat treatment problems. The rate of diffusion of carbon in steels is increased by cobalt(14-17) and this would imply an increase in the rate of decarburisation. Consequently, after heat treatment it may be necessary to remove a thicker layer of surface material from the cobalt steels and hence material losses and machining costs would be increased.

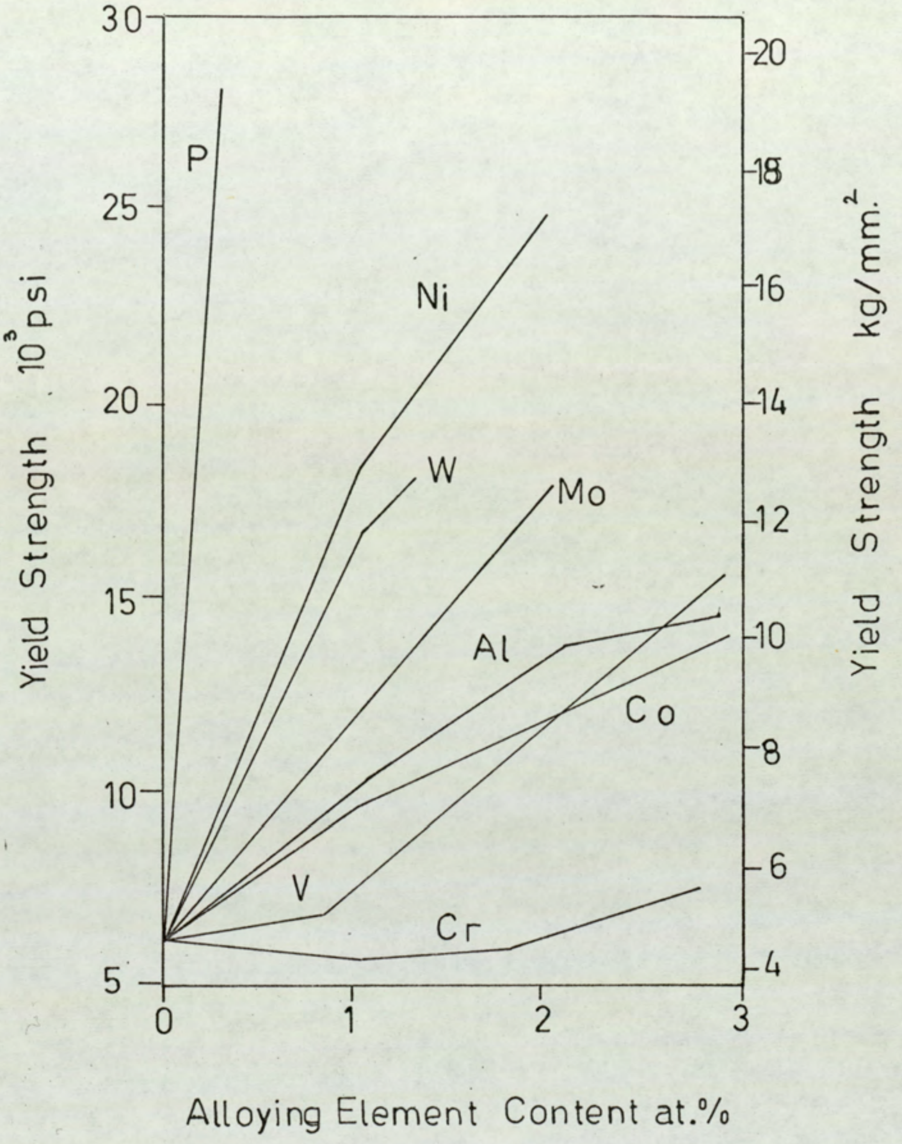

FIGURE 2

The effect of cobalt on the room temperature yield strength of iron (after Lacy and Gensamer (12) and Allen (13))

Evidence concerning the effect of cobalt on the hot-workability of steels is both fragmentory and contradictory. Investigations carried out by the Comité pour L'Etude du Fluage à Chaud des Metaux aux Temperatures Elevées indicate that the forgeability of a 9% chromium 3% molybdenum 0.1% carbon steel is improved by the addition of cobalt. A similar finding has also been reported(18) for a 14% chromium steel used in the manufacture of cutlery. These results suggest that the beneficial effect may be due to the austenite-forming nature of cobalt eliminating any δ-ferrite formed during heat-treatment. Michel(19), on the other hand, reports that cobalt reduces the hot workability of some tool steels. Generally it is difficult to appreciate how the addition of relatively small amounts of cobalt could affect the forgeability of steel apart from the effect it may have on grain boundary cohesion phenomena or surface energy of phases such as carbides and non-metallic inclusions.

The oxidation behaviour of both the die material and the forging stock is now recognised as yet another factor contributing to the complex wear parameter. Oxidation of the die material involves not only a loss of metal in the formation of the oxide, but the oxide becomes detached and acts as abrasive particles between the dies. Roos(20) has suggested that, as the ionic diameter of cobalt is smaller than that of iron, the diffusion coefficient of iron in iron oxide will be reduced and hence the rate of oxidation will be lessened. To define more accurately the influence of cobalt on the oxidation resistance of the 3M steel, a separate investigation was undertaken which entailed the plotting of oxidation curves directly from thermo - balance readings and examination of the distribution of the constituent elements by means of the electron probe microanalyser. The main details are given elsewhere(21) but the results indicated that cobalt did, in fact, reduce oxidation rates and was found to be distributed in the inner layer of the oxidised cross section with the nickel as discrete metallic particles. The role of cobalt in oxidation resistance would thus be similar to that of nickel, the metal particles interrupting the countercurrent diffusion of metal and oxygen ions through the oxide lattice thereby performing a function similar in principle to that of porosity. These results, however, must be viewed with some caution since they relate only to static oxidation resistance. During the forging process, the die surfaces are subjected to both mechanical shock and fluctuating temperatures so that the oxide is continuously being formed over a temperature range and removed at the forging stroke. It would be of morevalue, therefore, to determine the effect of cobalt on the adhesion of the oxide to the base steel, the mechanism of oxide repair and the nature of the scale formed.

Recent results at the University of Aston(22) and by Thomas(23) indicate that it is the quantity and nature of the scale formed on the incoming stock material that is the more important factor. Thomas investigated the effect of three stock materials, mild steel, En 24 and En 57, on the wear of three different die steels and found that by introducing a scale adhesion factor for the oxide on the stock material, good agreement could be found between the observed and predicted wear values. Lack of data on the oxidation behaviour of the die materials under mechanical and thermal shock loading restricts any attempt to separate the effects of the two oxidation behaviours but it would seem that the nature and formation of the oxide film on the die cannot be ignored completely.

The present investigation was thus undertaken with the aim of producing an economically attractive steel using cobalt additions. Steels containing up to 10% cobalt have been investigated to determine the effect of cobalt on retained austenite, tempering characteristics, fracture toughness, isothermal transformation, hardenability, and die wear properties and an attempt has been made to explain the observed effects of cobalt. The basis 3M composition was subsequently modified and molybdenum was replaced by cobalt on a cost equivalent basis. A series of ausformed alloys have also been prepared and a die wear test used as a criterion of performance for all steels. A cost analysis has been prepared for the steels so that any improvement in die wear could be related to the cost per unit forging produced.

2. PREPARATION OF MATERIALS

Six alloys were cast with cobalt contents of 0,1,3,5,7 and 10% respectively by remelting 3M steel scrap with the required additions of cobalt of commercial purity (99.9%). To compensate for melting losses and to counteract the dilution effect of the cobalt additions, nickel and molybdenum were added as commercially pure nickel (99.9%) and a 70% ferromolybdenum alloy. The charges were melted in a Birleco 50-Kg. capacity high frequency furnace using a zircon lining. The molten metal was superheated to 1560°C and held for 3 minutes and deoxidised with 80% ferromanganese and ferrosilicon alloys. The amounts of ferromanganese and ferrosilicon added were calculated to compensate for melting and dilution losses as well as deoxidising the molten charge. A small piece of broken glass was used as a flux for the slag which was removed as effectively as possible before pouring into a preheated cast iron mould approximately 2-ins. square and 10-ins. long. Several mould dressings were tried with varying success before a carbon deposit from a smoky oxy-acetylene flame was finally adopted. A refractory feeder was fitted to the top of the mould and, after pouring, this was covered with an exothermic powder to promote increased feeding.

After cooling, the feeder head was cropped from the ingot and analysis samples taken from the top and bottom of each ingot to determine the extent of macrosegregation. The ingots were subsequently reduced 50% in a one-squeeze operation on a 1200 ton press, at 1150°C. The resultant "pancakes" were air cooled and finally annealed for 1 hour at 760°C to render them readily machinable.

The chemical analysis results for this series of steels are given in Table 1 (page16), the values quoted being the average of the samples taken from the top and bottom of each respective ingot. Chemical analysis failed to show any significant macrosegregation but metallographic examination of the cast structures revealed a pronounced microsegregation, a typical structure being shown in Figure 3 (page 17). The as-cast structures of the 0 and 10% Co steels were examined on a Cambridge electron probe microanalyser and the results are summarised in Figure 4 (page 18). It was found that the inhomogenity was due in the main to segregation of molybdenum and, to a lesser extent, of nickel. Approximate point-analysis results for the 0% Co steel were :-

	% Mo	% Ni
Light-etching areas	3.6	3.5
Dark-etching areas	2.9	3.2

In the 10% Co steel, the cobalt was found to be distributed uniformly throughout the structure. The addition of cobalt to the steel in no way affected the overall segregation, point analysis values similar to those above being recorded. Using a Leitz micro-hardness tester (300 g.load), a hardness scan was made across the as-cast structures. The lighter etching regions were found to be some 100 VPN harder than the darker etching regions, typical values being shown inserted in Figure 3 (page 17). These results would indicate that the

TABLE 1

CHEMICAL ANALYSIS OF 3M ALLOY SERIES

Cast No.	Nominal % Co	%C	%Ni	%Mo	%Cr	%Mn	%Si	%Co
3M/0	0	0.27	3.3	3.3	0.56	0.69	0.24	<0.1
3M/1	1	0.25	3.3	3.3	0.55	0.69	0.25	1.0
3M/3	3	0.25	3.2	3.3	0.53	0.66	0.25	2.9
3M/5	5	0.25	3.2	3.3	0.53	0.63	0.24	4.6
3M/7	7	0.26	3.3	3.4	0.58	0.65	0.20	6.4
3M/10	10	0.25	3.4	3.3	0.58	0.65	0.25	9.7

All alloys contained less than 0.02% sulphur and phosphorus

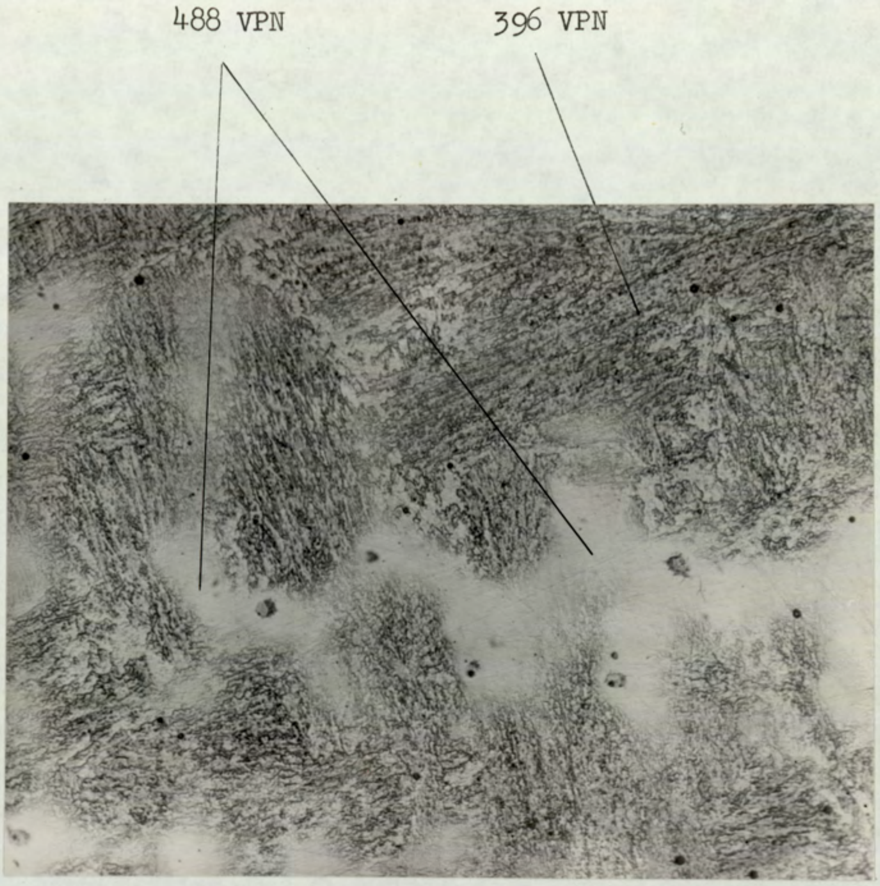

FIGURE 3

Typical as-cast structure.
Etched - 2% Nital x 250

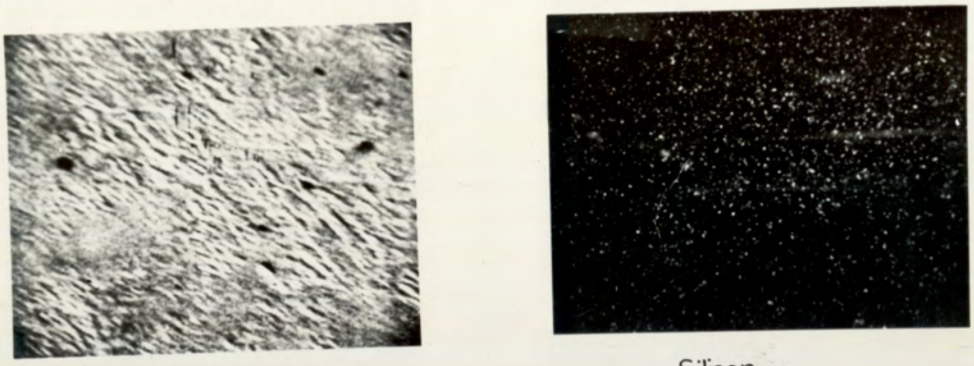

Electron Image
x500

Silicon

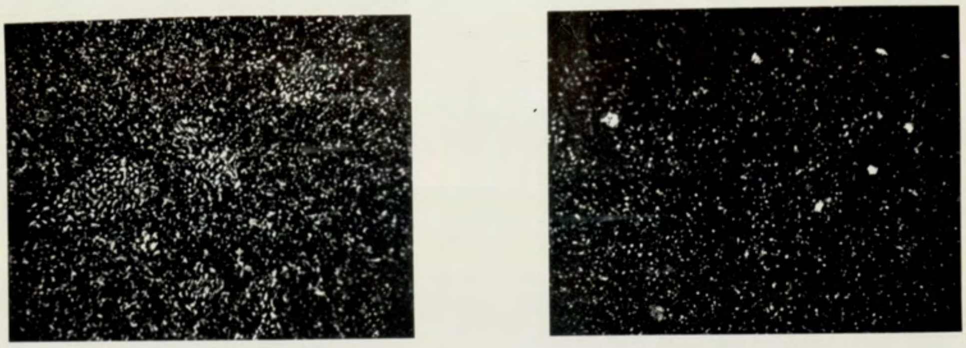

Molybdenum

Manganese

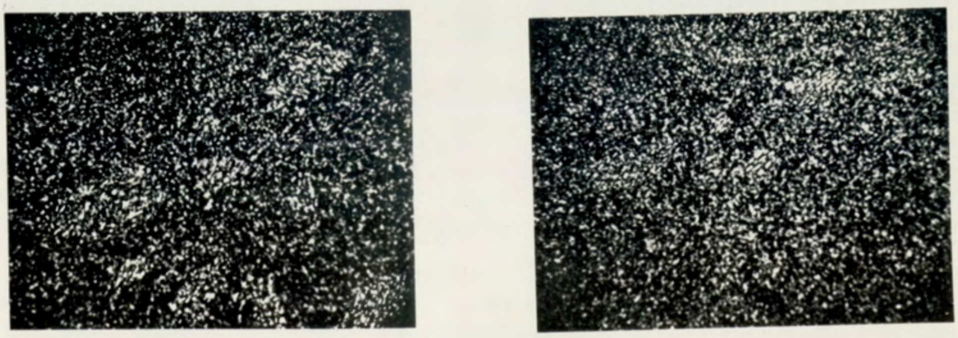

Nickel

Cobalt

FIGURE 4

As-cast microsegregation revealed by electron probe microanalyser structure is one of martensite (light areas) and bainite (dark areas).

The coarse as-cast structures were considerably refined by the hot working operation as can be seen illustrated in Figure 5 (page 20) but a certain degree of heterogeneity still appeared to be present. Examination of the forged structures on the electron probe microanalyser, however, revealed no distinct segregation. This finding is in agreement with work by Bayliss(24) who examined a similar as-forged banded structure in No.5 die steel and could detect no effective alloy segregation.

FIGURE 5

Typical as-forged structure
Etched - 2% Nital x 250

3. TEMPERING CHARACTERISTICS

3.1 Tempering - General

The breakdown of martensite in quenched steel during tempering has been the subject of numerous papers over the past years. The use of X-ray techniques has now defined the tempering process into three distinct stages in plain carbon steels:-

Stage I. During tempering in the range 100 - 150°C, the axial ratio of the tetragonal martensite lattice decreases with the precipitation of carbon from solid solution. The carbon is precipitated as a close packed hexagonal carbide of approximate composition $Fe_{2.4}C$ (25).

Stage II. In the temperature range 230 - 280°C, the austenite retained on quenching decomposes to give the same products as would be obtained from the transformation of primary austenite at the same temperature.

Stage III. Complete breakdown of the martensite occurs in the range 260 - 350°C. The transition carbide $Fe_{2.4}C$ and the remaining martensite decompose to form ferrite and cementite, Fe_3C.

Additions of the stronger carbide forming elements such as Cr, Mo, V, W, Ti and Nb will, if present in sufficient concentration, cause the replacement of cementite by an alloy carbide with quite different morphology and behaviour on tempering. These carbides, such as Cr_7C_3, Mo_2C and V_4C_3, have been discussed in detail by Goldschmidt(26, 27), Kuo(28) and Woodhead and Quarrell(29). Alloy carbide precipitation occurs in the temperature range 500-600°C and is termed Stage IV in the tempering process. A substantial increase in hardness is associated with the precipitation of these alloy carbides known as secondary hardening and it is this behaviour that is of paramount importance in tool and hot die steels.

Replacement of the cementite may occur in two ways:-

i) Transformation in situ. The appropriate alloying element diffuses into the cementite causing a gradual transformation to the alloy carbide.

ii) Separate nucleation. The cementite goes back into solution in the ferrite whilst the alloy carbides are freshly nucleated in the matrix.

Seal and Honeycombe(30) have proposed that separate nucleation is the major transformation mode. Their results showed that cementite went back into solution in the range 400 - 500°C and then the alloy carbides were nucleated in the matrix. This mechanism is supported by Woodhead and Quarrell(29). Raynor et.al.(31) have, however, produced evidence that in a 0.2% carbon 4% molybdenum steel transformation also occurred in situ. Using dark - field techniques, they were able to show that the secondary carbide could be nucleated not only at dislocations and grain boundaries but also at the interface between ferrite and cementite and that the carbide thus nucleated grew more rapidly than that nucleated within the matrix.

In the Fe - Mo - C system, the hexagonal carbide Mo_2C is generally responsible for secondary hardening and follows after Fe_3C. Mo_2C is acicular in form having the orientation relationship

$$(0001)\ Mo_2C \ // \ (011)\ \alpha$$
$$[1120]\ Mo_2C \ // \ [100]\ \alpha \text{ (}Mo_2C\text{ growth direction)}$$

as demonstrated by Dyson et. al.(32) Detailed crystallographic examination shows that there is only one direction of low indices in Mo_2C namely $[1120]$ which gives good lattice matching, 5% misfit with $[100]\ \alpha$. The misfit is 22% in the $[100]\ \alpha$ and $[001]\ \alpha$ directions so a needle habit is to be expected.

Although Mo_2C is the usual alloy carbide precipitated in molybdenum steels, Kuo(28) has shown that other carbides are observed if the Mo/C ratio of the steel falls below 1.5. With a Mo/C ratio of 1, the ultimate stable phase MoC forms directly after Fe_3C whereas the double carbide $M_{23}C_6$ appears between Fe_3C and MoC when the Mo/C ratio is reduced to 0.7.

The result of this change from Fe_3C, however, need not be the equilibrium carbide and often one or more transitional alloy carbides may form before eventual equilibrium is reached. The tempering process may be stopped at any point and steels are often put into service at a stage of tempering which is far from equilibrium.

Weak carbide forming elements such as Ni, Si, Mn and Co, when added to plain carbon steels do not alter the basic form of the precipitated carbides(33-35). The orthorhombic Fe_3C, however, can take into solution considerable amounts of other elements depending on the percentages of the elements in the steel and their partitioning between the carbide and the ferrite. The latter is usually expressed as the partition coefficient i.e. the ratio of the alloy content of the cementite to that of the ferrite with which it is in equilibrium. Cobalt dissolves to a considerable extent in the carbide (sometimes termed M_3C due to its variable metal atom content) as might be expected since it also forms a metastable orthorhombic carbide. On the other hand, it has no great affinity for carbon and thus partitions preferentially to the ferrite. The partition coefficient for cobalt at 700°C is reported as 0.2(36,37).

These elements can, however, influence to varying degrees the kinetics of tempering as demonstrated by Kenneford and Williams(38) for plain carbon steels and Irani and Honeycombe(39) for a 0.2% carbon 4% molybdenum steel which exhibited a secondary hardening peak. It is in this latter effect that cobalt is of considerable importance.

3.2 The Role of Cobalt in Tempering Reactions

The influence of cobalt on the tempering characteristics of plain carbon steels has been reported by Biswas and Seal(40), Irvine(41), Seal et. al.(42) and Loria(43). The general conclusion from these investigations is that, although cobalt increases the resistance to softening on tempering, its beneficial effect is hardly sufficient to justify the high cost of the cobalt additions. This is due almost entirely to the relative cheapness of the base material to which the cobalt additions were made. When added to the more expensive alloy steels containing carbide forming elements such as vanadium or molybdenum, cobalt may increase the secondary hardening behaviour to such an extent that the increased properties far outweigh the cost of the additions.

Why cobalt increases red hardness in alloy steels is still unresolved despite several attempts to elucidate the operative mechanism. Houdremont and Schrader(44), Geller and Novikova(45) and Kuo(46) have all shown that cobalt retards the precipitation of alloy carbides in tool steels. Houdremont asserted that the role of cobalt in this retardation was to reduce alloying element diffusion, but Irani and Honeycombe(39) have shown that cobalt additions did not affect the activation energy associated with peak hardness in a 4% molybdenum steel. This activation energy they found to be approximately 65 kcal/mole which agrees well with that for the diffusion of molybdenum in α - iron. Kuo postulated that the effect of cobalt was a direct consequence of the reduction of the rates of precipitation and agglomeration of alloy carbides in the presence of cobalt but did not expand this argument further. Other earlier work on this problem has attributed the increase in red hardness to the migration of cobalt to the M_6C carbide during tempering(27,46), formation of $(Co,W)_6C$(47), an equalisation of tungsten partitioning between carbide and matrix(48) and to the interaction of cobalt and vanadium(49). A recent report by Seal et.al.(42) accounted for the increased tempering resistance of cobalt containing steels by detecting the separate precipitation of Co_3C. Carbides of cobalt have been reported(50-56) but only prepared under laboratory conditions and are metastable. With a free energy of formation of some +1700 cal/mole(57) it seems extremely doubtful that this carbide would persist under tempering conditions even in relatively high concentrations of cobalt, and the results of Seal must be viewed with some reservation.

A more recent theory to account for the behaviour of cobalt containing steels has been proposed by Chandhok et.al.(58). In previous work(59) these same authors showed that cobalt increased the activity of carbon in austenite and ferrite, a result which was later confirmed by Smith(60) using Fe - C and Fe - Co - C alloys heated in CO - CO_2 atmospheres of fixed activities. During the tempering of a 0.2% carbon, 2.2% molybdenum steel containing up to 10% cobalt, they found that the cobalt containing steels had smaller and more numerous carbide particles than did the cobalt-free steel. They considered therefore that cobalt affected the nucleation rate, $\dot{N}$, and the growth rate, $\mathring{G}$, of the carbides and related these variables to the effect of cobalt on the activity of carbon.

The nucleation rate $\dot{N}$ is related to the bulk free energy change ΔF_V accompanying nucleation by the expression(61) -

$$\dot{N} \ \alpha \ \exp \left[-C\sigma^3 \ / \ R\,T\,(\Delta F_V + E)^2 \right] \ ......(1)$$

where C is a factor dependant on particle shape usually about 10, σ is the surface energy of the carbide/ferrite interface and E is the strain energy accompanying critical nucleus formation. The increase in carbon activity with cobalt additions causes an increase in the absolute value of ΔF_V which is negative by an amount

$$\delta \Delta F_V \left[(RT)/(V) \right] \left[X_c \ \ln. \ (\gamma c')/(\gamma c) \right] \ ......(2).$$

where V is the molar volume of carbide, X_c is the mole fraction of the carbon in the carbide, $\gamma_c{}'$ and γ_c are the activity coefficients of carbon in ferrite for cobalt containing and cobalt free steels respectively. It is argued that, since ΔF_V is increased, then from Equation (1), the value of $\dot{N}$ is also increased. The effect of cobalt on the surface energy of the carbide/ferrite interface and strain energy accompanying critical nucleus formation are ignored by Chandhok on the grounds that no absolute values can be alloted to them. The validity of their argument may be questioned since they ignore two variables which must change when cobalt is added to the steel. The phenomenon of secondary hardening is a precipitation hardening process and the precipitates are initially coherent with the matrix. The coherency stresses reach a maximum just before the formation of incoherent interfaces and, since cobalt partitions preferentially to the ferrite, it alters the coherency stresses and interfacial free energy between the matrix and coherent cluster. Further the interfacial and strain energy terms are raised to the powers 3 and 2 respectively so that any small change in these values could have a marked effect on the nucleation rate determined from Equation (1).

The effect of cobalt on γ_c was also related to $\dot{G}$ by Chandhok who proposed an "interface control" model previously described by Heckel and Paxton(62) and Darken(63) to account for the action of silicon in Fe - Si - C alloys. Cobalt partitions preferentially to the ferrite and, since cobalt and silicon increase the carbon activity coefficient in ferrite, these authors postulate that the activity gradient for carbon diffusion into the carbide is reduced. This is represented diagrammatically in Figure 6 (page 28). The growth rate of carbides in cobalt containing steels should be reduced, therefore, by this interface control mechanism. The

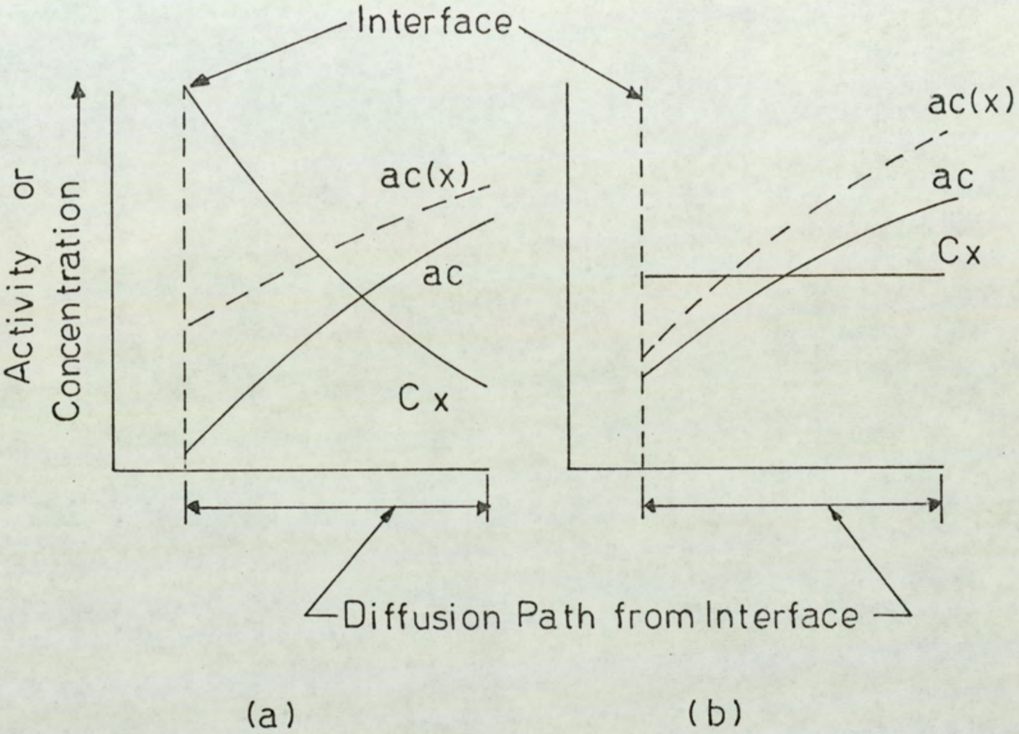

FIGURE 6

Interface control model showing the effect of partitioning of cobalt on carbide growth rate.

a_c and $a_c(x)$ are the activities of carbon respectively with and without the addition of cobalt

C_x is the concentration profile for cobalt

Case (a) corresponds to partitioning of the alloying element ahead of the interface
Case (b) corresponds to no partitioning of the alloying element ahead of the interface

thermodynamic arguments which form the basis of this theory are above reproach and indeed this may be a contributing factor to the observed reduction in growth rate. To determine the effect of cobalt on activity coefficients, Chandhok measured the carbon profile across the faces of diffusion couples. Dividing the activity by the atom fraction of carbon at the interface for each side of the couple, the activity coefficient of carbon for both the high and low cobalt sides was calculated. The results showed that at 1038°C, a 0.23% carbon steel and a 0.27% carbon plus 10% Co steel gave a ratio

$$\frac{\gamma_C \text{ on high Co side}}{\gamma_C \text{ on low Co side}} = 1.15$$

These results show only a slight effect of cobalt and indeed Smoluchowski$^{(14)}$ performed similar experiments on welded specimens containing 0 and 4% Co, both with 0.8% carbon, and found no change in the carbon distribution at the weld. It is thought, therefore, that interface control is insufficient in itself to fully explain the action of cobalt in tempering conditions.

The most recent theory on the action of cobalt on nucleation and growth processes has come from research into its effect in maraging steels. Banerjee and Hauser$^{(64)}$ and Pellissier$^{(65)}$ consider that the effect of cobalt is to produce a more dense distribution of dislocations in the matrix which act as nucleation sites for precipitation. Banerjee expands this theory and accounts for the higher dislocation density by the lowering of the stacking fault energy of the base steel by cobalt additions. The stacking fault energy of cobalt is about 20 ergs/cm^2 $^{(66, 67)}$ so it is assumed that it lowers the stacking fault energy of the base material. Examples are given of reverted austenite in an iron - 18% nickel alloy which show only dislocation tangles but exhibit stacking fault energy contrast of substantial width when 8% cobalt is added. The presence or absence of stacking faults in the f.c.c. structure, however, does not mean that a corresponding effect on the fault energy must persist in the b.c.c. phase. Banerjee therefore observed parameters in the b.c.c. phase which significantly depend upon the stacking fault energy. His results showed that cobalt retards dislocation cell development in quenched and cold worked martensitic structures producing a more uniform dislocation density throughout the structure, and both the number of twins per mm^2 and twins per martensite lath in cold worked materials were increased by cobalt. The interpretation of these results is that, since cobalt lowers the stacking fault energy, twin deformation is encouraged in the martensite and cross slip becomes more difficult which impedes the development of cell structure. Cross slip requires the two partials of a dissociated dislocation to recombine hence the energy for cross slip increases with a decrease in stacking fault energy making cross slip more difficult; the resulting cell size becomes smaller and the average dislocation density increases. Results similar to those presented by Banerjee have been reported by Stoloff et.al.(68) who showed that cobalt additions to iron reduced the tendency for dislocation tangles and cell formation at concentrations above 5%.

The theory of Banerjee involves the whole question of the occurrence and geometrical nature of dislocations in b.c.c. materials. From work on the observation of slip lines, it has been stated that the slip plane in α - iron is predominantly $\{110\}$ but that other planes ($\{112\}$ or $\{123\}$ or even more complex ones) could be operative. There is only one slip direction, however, the $\langle 111 \rangle$. Further study has shown that the Burgers vectors of the dislocations may differ from those predicted from the slip line observations. Dislocations with Burgers vectors of $\frac{1}{2}a \langle 111 \rangle$, $a \langle 100 \rangle$, and $a \langle 110 \rangle$ have been found and these were present in the ratio of 94 : 5 : 1 over a wide range of deformation rates, strain and temperatures. Stacking faults have been reported to form in niobium, tungsten, vanadium and chromium predominantly on the $\{112\}$ planes.(69-71) The results obtained in both these experiments and those of Banerjee can all be criticised on the grounds that the observed electron optical contrast may be due to precipitate formation or very high concentrations of solute at the stacking faults. However, there is clear evidence that the addition of silicon tends to confine the dislocations to the $\{110\}$ planes(72) and thus, by hindering cross slip, would lead to stacking faults of substantial width. In this context the proposal by Ohr and Beshers(73) that the observed effects of cobalt on cell formation and dislocation density are good evidence for a restriction in the proportion of dislocations moving on secondary slip systems seems valid. The relationship between the energy of these faults in b.c.c. materials and the occurrence of deformation twinning is as yet uncertain.

In general, the proposal and supporting evidence offered by Banerjee of cobalt increasing the dislocation density in the steel is open to considerable question. In the absence of further work on this subject, several results have been cited and these, in particular the effect of silicon in restricting effective cross slip, offer indirect support for the Banerjee hypothesis.

3.3 Tempering Programme

Since quenching and tempering form the basis of the hardening mechanisms and property control in these steels, the general tempering characteristics must first be investigated. Retained austenite in the qeunched samples would cause erroneous results on subsequent tempering and thus the first part of this programme is concerned with the evaluation of retained austenite after quenching and refrigerating, and air cooling. Samples measuring $^1/_4$ - in. by 1-in. square were austenitised for 1 hour at 1020°C in a controlled atmosphere furnace and one series air cooled whilst a second series were oil-quenched and refrigerated in liquid nitrogen for 30 minutes.

The effect of cobalt on tempering parameters was investigated by quenching and refrigerating a number of 1-in. by $^1/_2$-in.square samples of each steel as described above. To minimise excessive scatter in the tempered results, the hardness of all the quenched samples were checked and only samples falling within a standard deviation of ± 1 VPN from a norm determined statistically for each alloy were used. These

These samples were tempered for 1 hour in salt baths controlled to within ± 2°C of the required temperature and subsequently oil quenched. The tempered samples were carefully slit to give two $\frac{1}{2}$-in. cubes and one half mounted and polished for metallographic examination. Direct carbon extraction replicas were prepared from these specimens by coating the pre-etched surface with carbon and etching off the carbon film with Nital. The other halves of the tempered samples were retained for further investigation into the tempering process by electrolytic carbide extraction and line breadth measurements.

3.4 Determination of Retained Austenite

The percentage of retained austenite was determined by comparing the integrated intensities of selected (h,k,l) planes of ferrite and austenite. The integrated intensities, I, is given by the expression -

$$I\,(h,k,l) = n^2\,V\,m\,(LP)\,e^{-2m}\,(F,\,f)^2 \quad \ldots\ldots\ldots\ldots\ldots(3)$$

where n is the number of cells in one cm^3, V is the volume exposed to the X-ray beam, LP the Lorentz Polarisation factor, m the multiplicity of (h, k,l), e^{-2m} the Debye - Waller temperature factor, F the structure factor, and f the atomic factor. In place of n^2V the term V/v^2 can be substituted v being the volume of the unit cell. If the ratio of intensities of the α to γ lines is P then Equation (3) can be written as

$$P = \frac{\text{I martensite } (\alpha)}{\text{I austenite } (\gamma)} = \frac{V\alpha \quad v\gamma \ m\alpha \ (LP)\alpha \ e^{-2m}{}_{\alpha} \ (F\alpha, f\alpha)^2}{V\gamma \ v\alpha \ m\gamma \ (LP)\gamma \ e^{-2m}{}_{\gamma} \ (F\gamma, f\gamma)^2} \ldots (4)$$

The respective values in Equation (4) can be obtained from various tables depending on the reflections used and reduced to a constant G which is a factor determined for each combination of α and γ peaks. Equation (4) thus reduces to -

$$P = \frac{V\alpha}{V\gamma} \quad x \quad 1/G \ \ldots\ldots\ldots\ldots\ldots\ldots\ldots\ldots (5)$$

and if only martensite and austenite are present (i.e. there are no undissolved carbides) then the final equation form is simply

$$V\gamma = 1 \,/\, (1 + GP) \ldots\ldots\ldots\ldots\ldots\ldots\ldots\ldots (6)$$

The two strongest lines, $(110)\alpha$ and $(111)\gamma$ cannot be used in this comparison due to the closeness of their Bragg angles, θ, 26.2° and 25.5° respectively for Co Kα radiation. It is necessary therefore to compare the relative intensities of the higher order planes, the $(200)\alpha$, $(211)\alpha$, $(200)\gamma$, $(220)\gamma$ and $(311)\gamma$ being selected on the basis of the separation of their respective Bragg angles. From these five lines it is possible to achieve six different permutations of $I\alpha/I\gamma$ and this helped to counteract any extraneous results that might be introduced by, for example, textures, if only two lines were studied. The constants for each peak have been calculated and are shown in Table 2 (page 35) and also used to compute the values of the constant, G, shown in Table 3 (page 36).

TABLE 2

CALCULATED CONSTANTS FOR THE VARIOUS α AND γ PEAKS USING CoKα RADIATION

	(200)α	(211)α	(200)γ	(220)γ	(311)γ
Bragg angle, θ^o	38.67	49.89	29.99	34.92	55.85
Multiplicity m	6	24	6	12	24
Lorentz Polarisation factor (LP)	3.44	2.73	5.79	2.83	2.96
Debye-Waller temperature factor e^{-2m}	0.908	0.869	0.941	0.889	0.852
Atomic factor, fo	10.78	9.14	12.69	9.84	8.60
Structural factor F	2	2	4	4	4
$1/V^2$ where V = vol of cell unit	1.79×10^{-3} kx units		4.68×10^{-4} kx units		

TABLE 3

CALCULATED VALUES OF G FOR VARIOUS α/γ COMBINATIONS

α/γ Combination	G
$(200)\alpha/(200)\gamma$	2.52
$(200)\alpha/(220)\gamma$	1.40
$(200)\alpha/(311)\gamma$	2.15
$(211)\alpha/(200)\gamma$	1.09
$(211)\alpha/(220)\gamma$	0.61
$(211)\alpha/(311)\gamma$	0.93

The samples were carefully ground and the surface prepared by a polish - etch technique prior to mounting in a specimen holder on a Siemens X-ray unit. The equipment incorporated a wide - angle goniometer, proportional counter and a 6 volt channel pulse height discriminator used in place of a single crystal monochromator. The specimens were irradiated with Co Kα radiation using an iron filter and the angles step - scanned at $^1/_{20}$ ° intervals to determine the integrated intensities of the lines.

The results from the air cooled and quenched and refrigerated samples for all α/γ combinations are shown in Table 4 (page 38). As might be anticipated, the amount of retained austenite in the air cooled samples is slightly greater than detected in the quenched and refrigerated specimens although all samples show far less than 1.5% retained austenite for each α/γ combination. The effect of cobalt on the retention of austenite is seen to be essentially neutral, certainly no clear trend emerging from the present results. The importance of comparing several α/γ combinations can be seen in Table 4 (page 38), where, if only the (200)α and (200)γ lines were studied, it might be inferred that cobalt increased the amount of retained austenite whilst comparison of the (200)α and (311)γ lines would indicate a reverse trend. The average of all six α/γ peaks however summarises the overall observed action of cobalt on austenite retention. The values determined for each α/γ combination show little scatter which would imply that the

TABLE 4

RESULTS OF RETAINED AUSTENITE DETERMINATIONS

(a) Quenched and Refrigerated Specimens

Alloy	Nominal Co %	Retained Austenite for Given α-γ Peaks %						Av. % RET AUS
		(200)α (200)γ	(200)α (220)γ	(200)α (311)γ	(211)α (200)γ	(211)α (220)γ	(211)α (311)γ	
3M/0	0	0.7	0.5	0.8	0.5	0.7	0.7	0.65
3M/1	1	0.6	0.8	0.8	0.6	0.5	0.5	0.65
3M/3	3	0.7	0.6	0.6	0.6	0.8	0.7	0.65
3M/5	5	0.8	0.7	0.7	0.7	0.6	0.5	0.65
3M/7	7	0.8	0.8	0.5	0.4	0.6	0.6	0.60
3M/10	10	0.8	0.4	0.6	0.7	0.7	0.6	0.60

(b) Air Cooled Specimens

3M/0	0	0.9	1.0	0.9	0.8	0.8	0.9	0.88
3M/1	1	0.8	1.1	1.0	0.9	0.9	0.7	0.90
3M/3	3	0.8	0.8	0.7	1.0	1.1	0.8	0.87
3M/5	5	1.0	0.9	0.9	1.1	0.9	0.9	0.95
3M/7	7	0.9	0.8	1.0	0.7	0.8	0.8	0.83
3M/10	10	1.1	0.8	0.8	0.9	0.9	0.8	0.87

structures were quite homogenous and retained very little texture that might have been developed during the working process.

3.5 Tempering Results and Structures

The isochronal tempering behaviour of the steels is shown in Figure 7 (page 40). All the alloys yielded a similar pattern of gradually increasing hardness to a tempering temperature of 400°C followed by a sharp increase in hardness reaching a maximum at 550°C then falling rapidly as the tempering temperature is increased. Cobalt additions are seen to increase the peak hardness in quite a regular manner but the tempering temperature associated with peak hardness is unaltered. In the as-quenched condition, cobalt raises the hardness by just over 1 VPN/wt.% Co but at peak hardness this increases to 6 VPN/wt.% Co.

Direct carbon extraction replicas were taken from the tempered samples and examined on a Phil~~l~~ips 200 electron microscope. The as-quenched structures, Figure 8 (page 41), show that the addition of cobalt to the steel leads to the formation of a finer martensite. This observation would tend to support the hypothesis that cobalt increases the dislocation density of the parent austenite and creates a more heavily faulted martensite.

The tempered structures are found in Figures 9 to 18 (pages 42 to 51), shown only for the 0 and 10% cobalt steels for convenience. At low tempering temperatures all

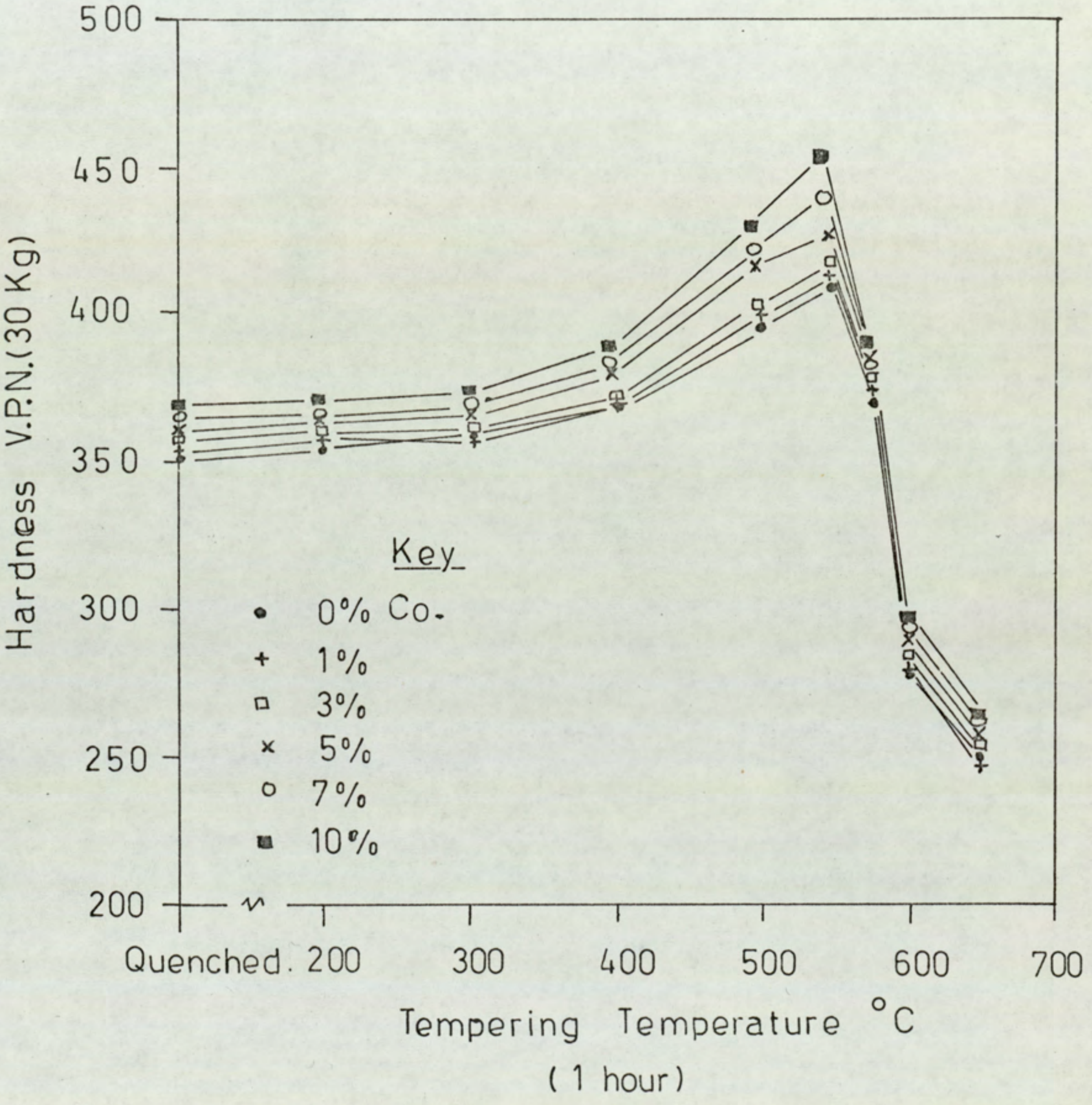

FIGURE 7

Isochronal tempering results for 3M steels containing up to 10% cobalt

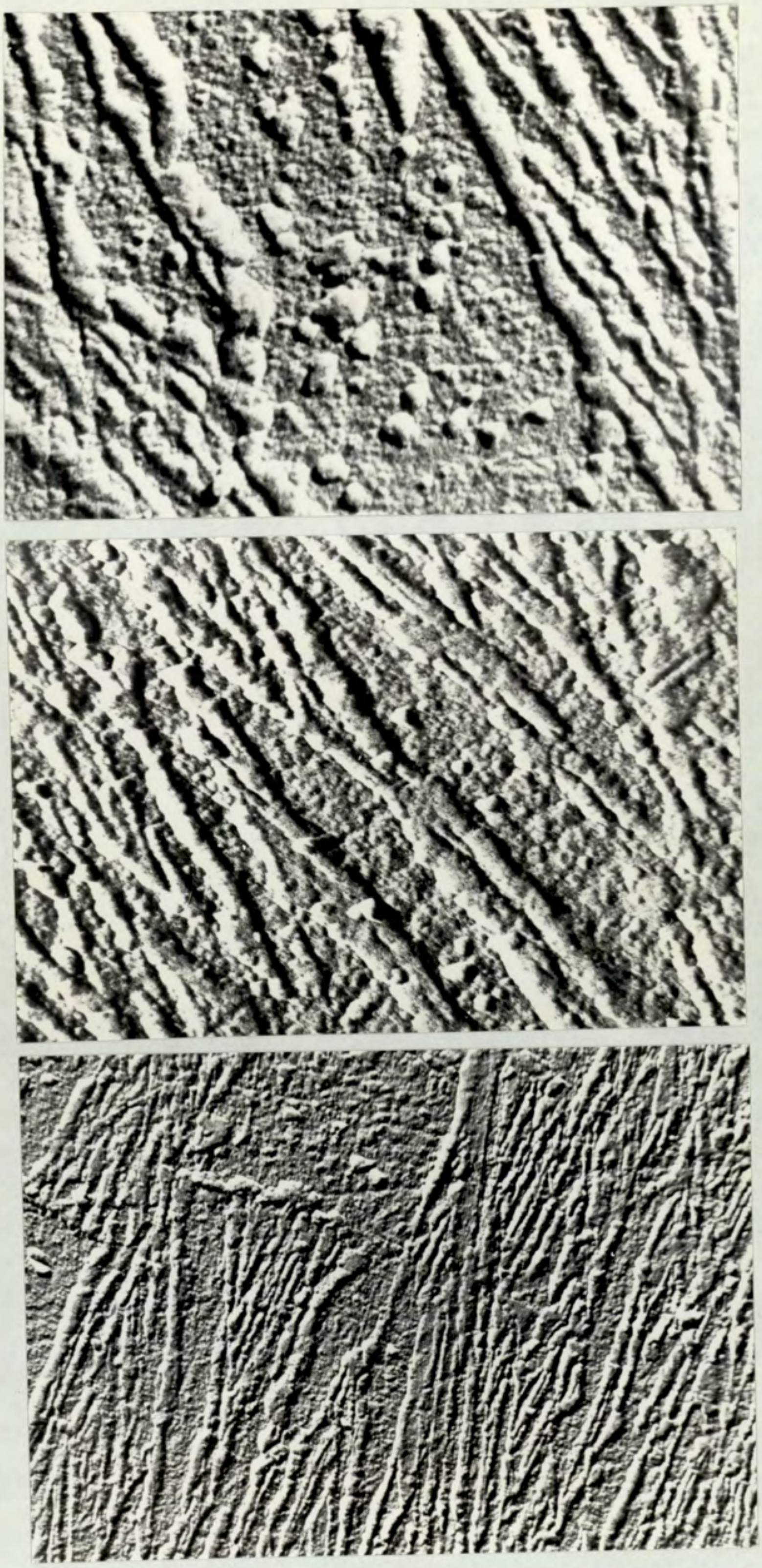

0% Co

5% Co

10% Co

FIGURE 8

Effect of cobalt on as-quenched structure

Au/Pd shadowed carbon replicas x 3500

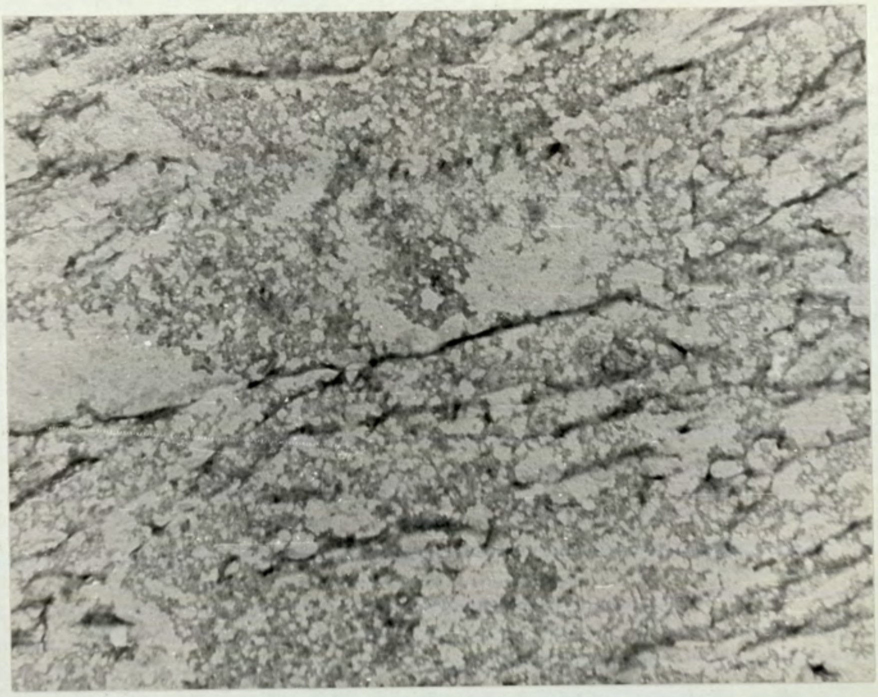

0% Co

10% Co

FIGURE 9

Steels tempered for 1 hour at 200°C

Direct carbon extraction replicas x 3500

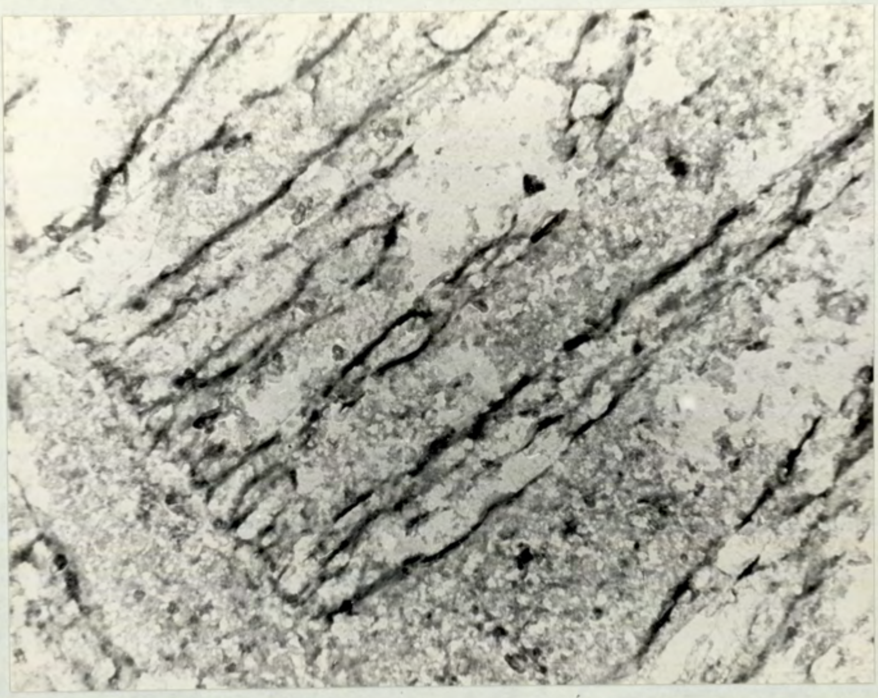

0% Co

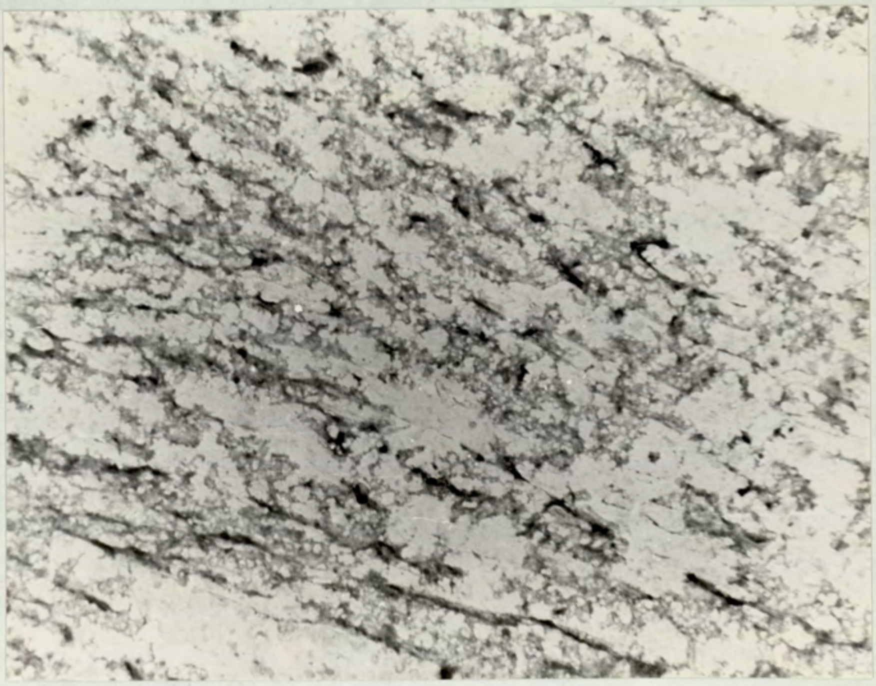

10% Co

FIGURE 10

Steels tempered for 1 hour at 300°C

Direct carbon extraction replicas x 3500

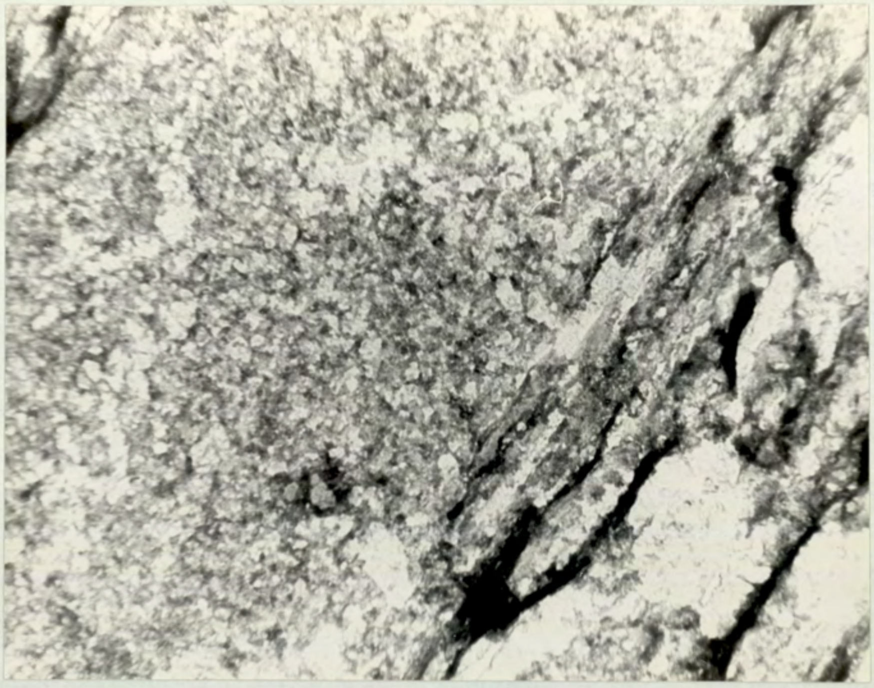

0% Co

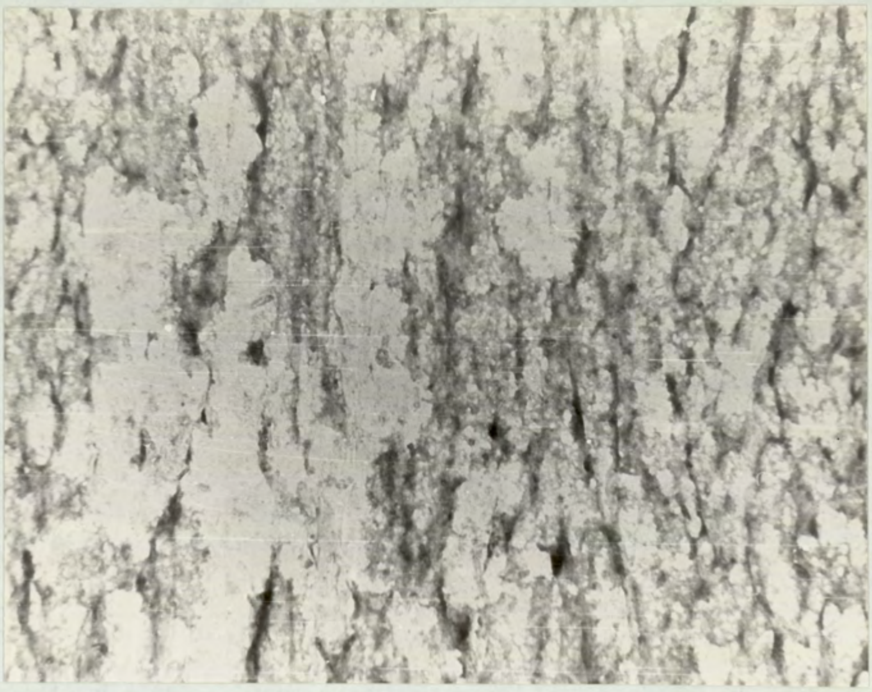

10% Co

FIGURE 11

Steels tempered for 1 hour at 400°C

Direct carbon extraction replicas x 3500

0% Co

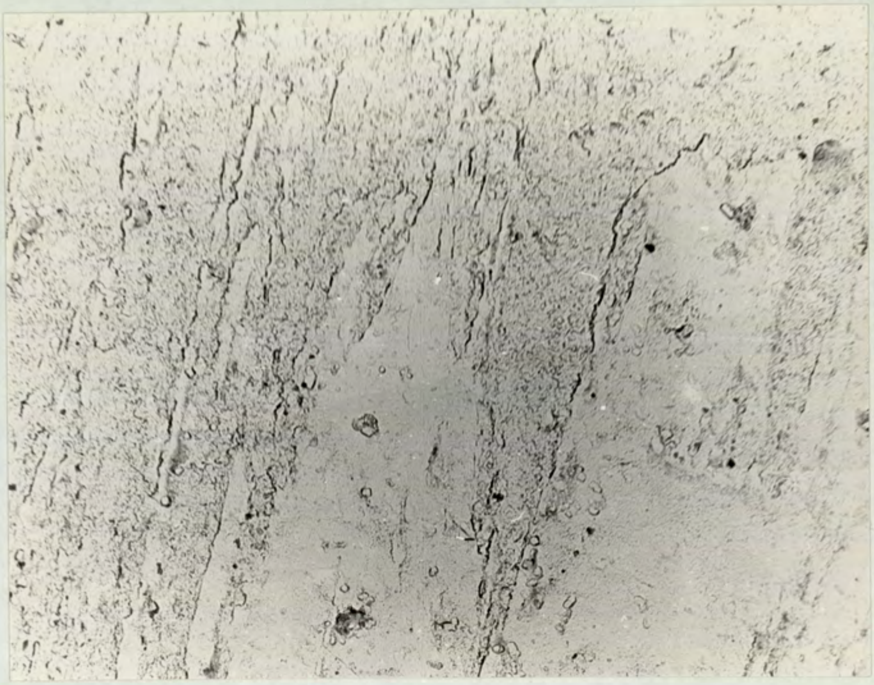

10% Co

FIGURE 12

Steels tempered for 1 hour at 500°C

Direct carbon extraction replicas x 3500

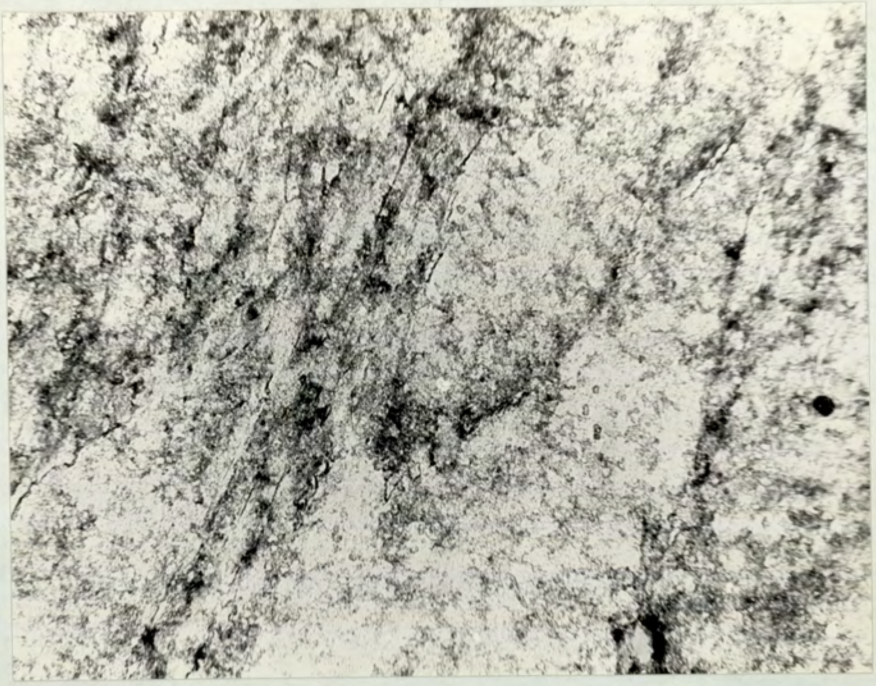

0% Co

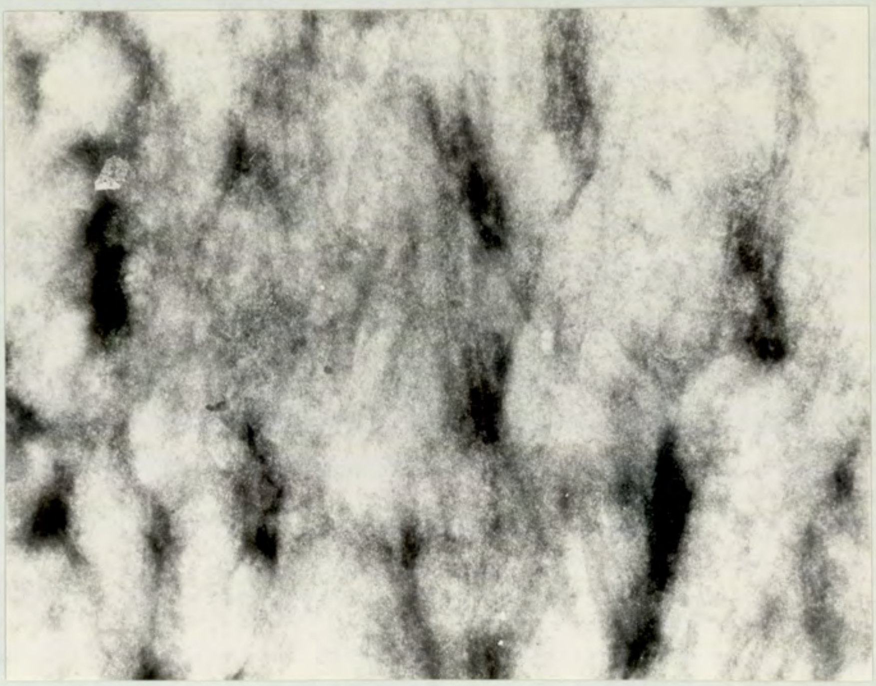

10% Co

FIGURE 13

Steels tempered for 1 hour at 550°C

Direct carbon extraction replicas x 3500

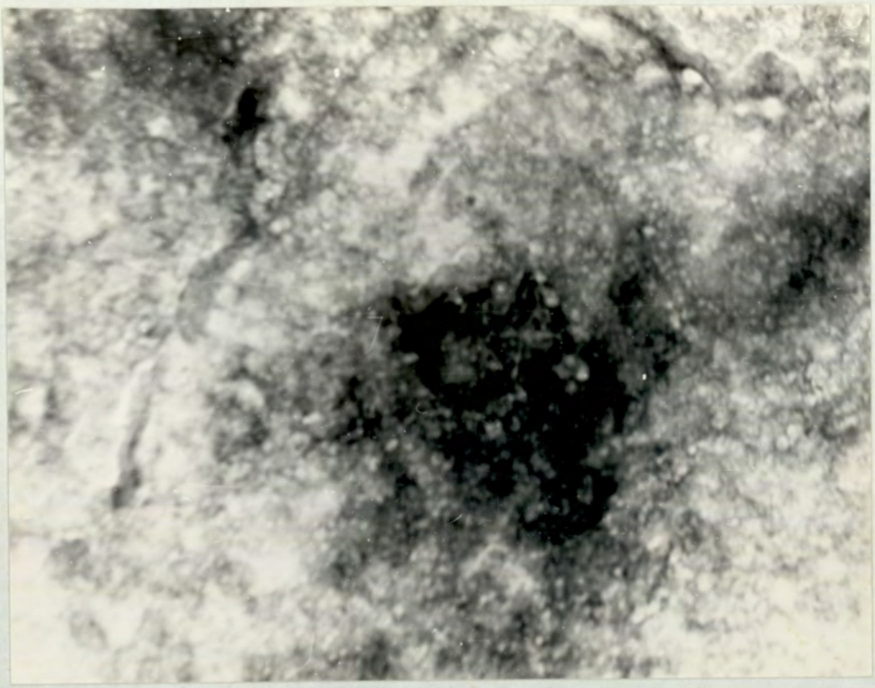

0% Co

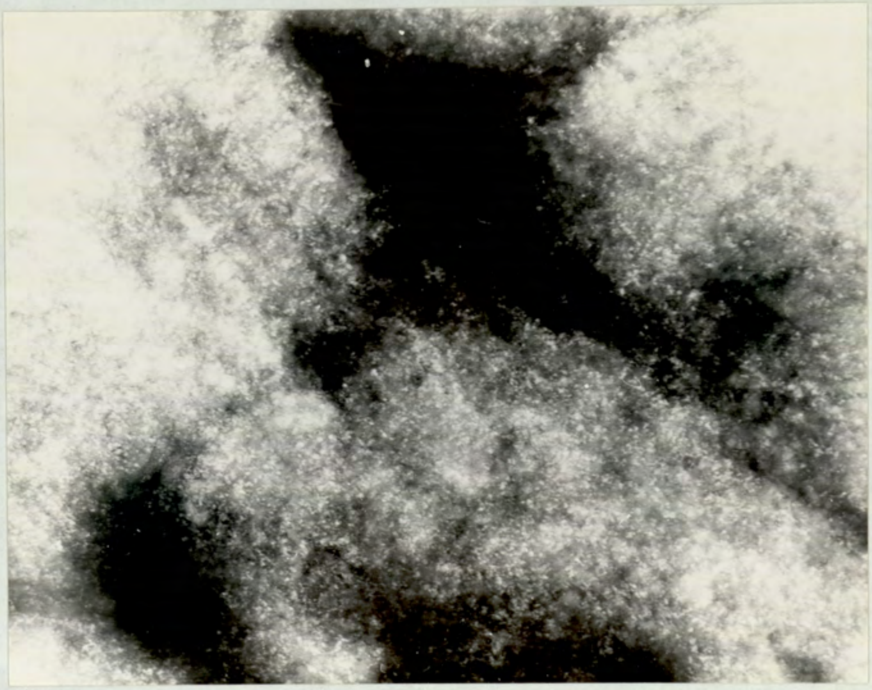

10% Co

FIGURE 14

Steels tempered for 1 hour at 550°C

Direct carbon extraction replicas x 27500

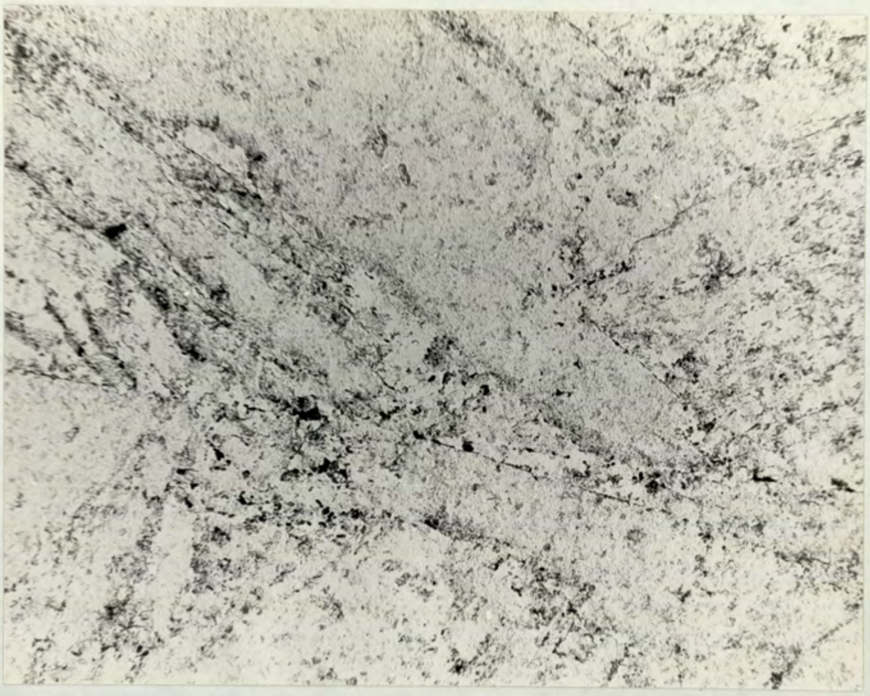

0% Co

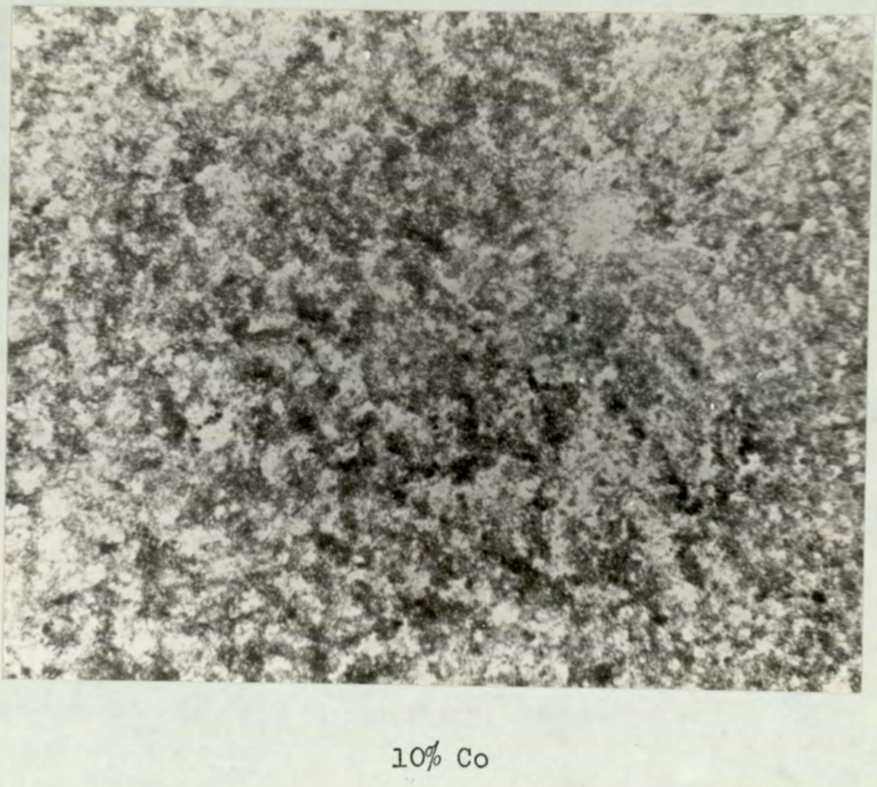

10% Co

FIGURE 15

Steels tempered for 1 hour at 575°C

Direct carbon extraction replicas x 3500

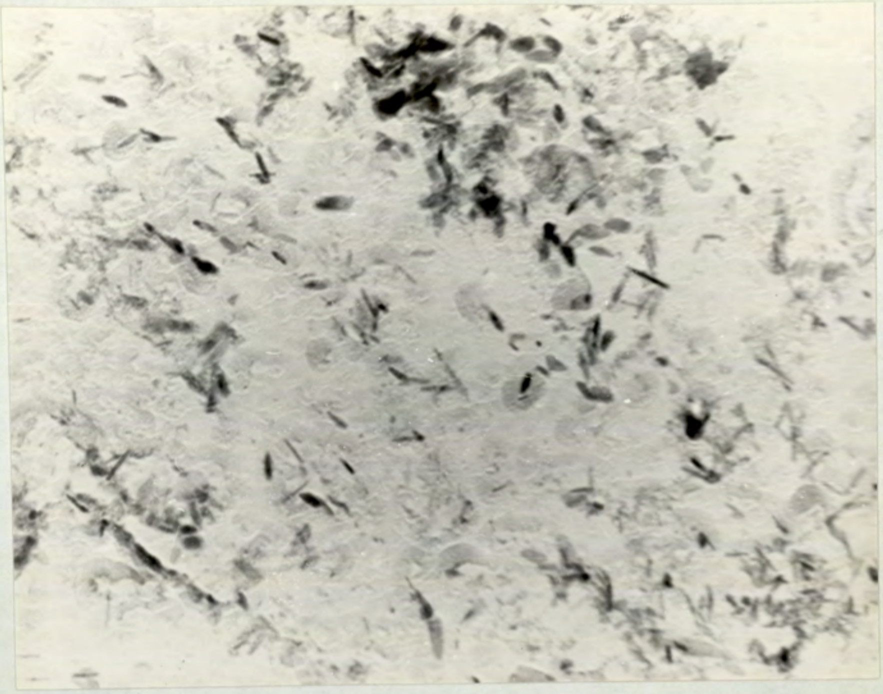

0% Co

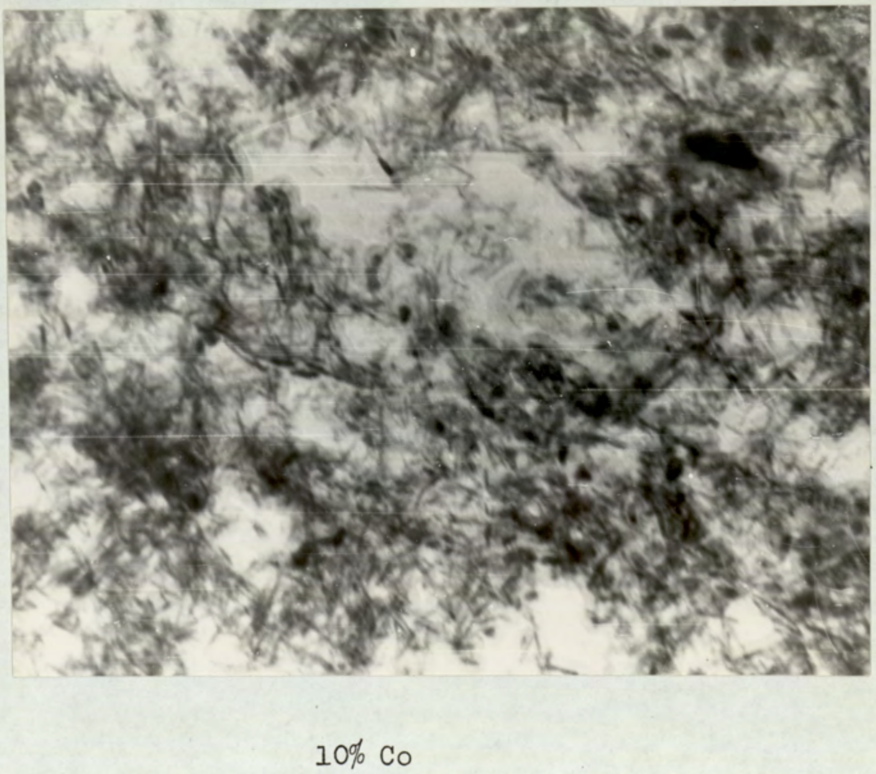

10% Co

FIGURE 16

Steels tempered for 1 hour at 575 °C

Direct carbon extraction replicas x 27500

0% Co

10% Co

FIGURE 17

Steels tempered for 1 hour at 600°C

Direct carbon extraction replicas x 27500

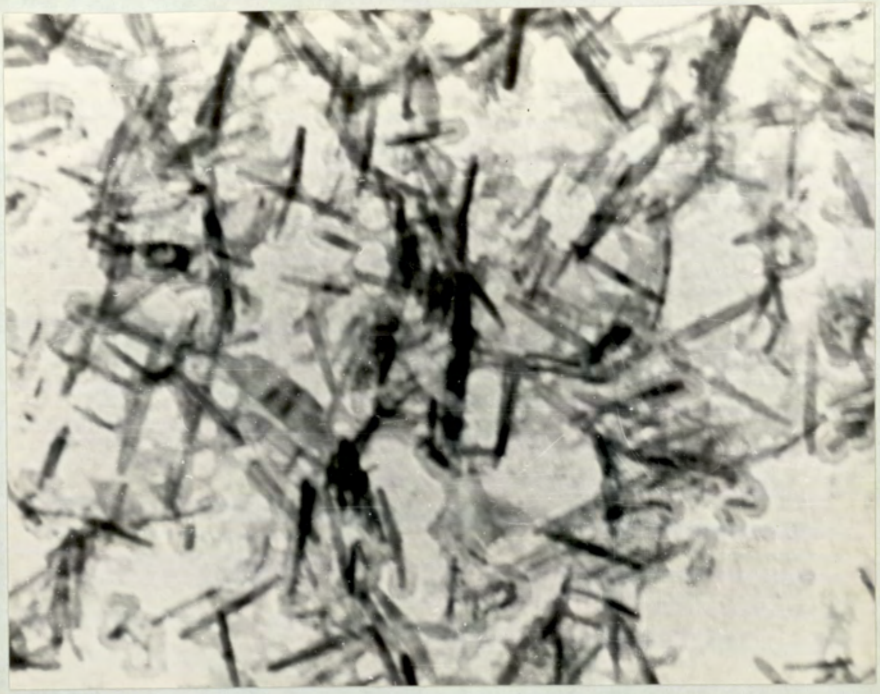

0% Co

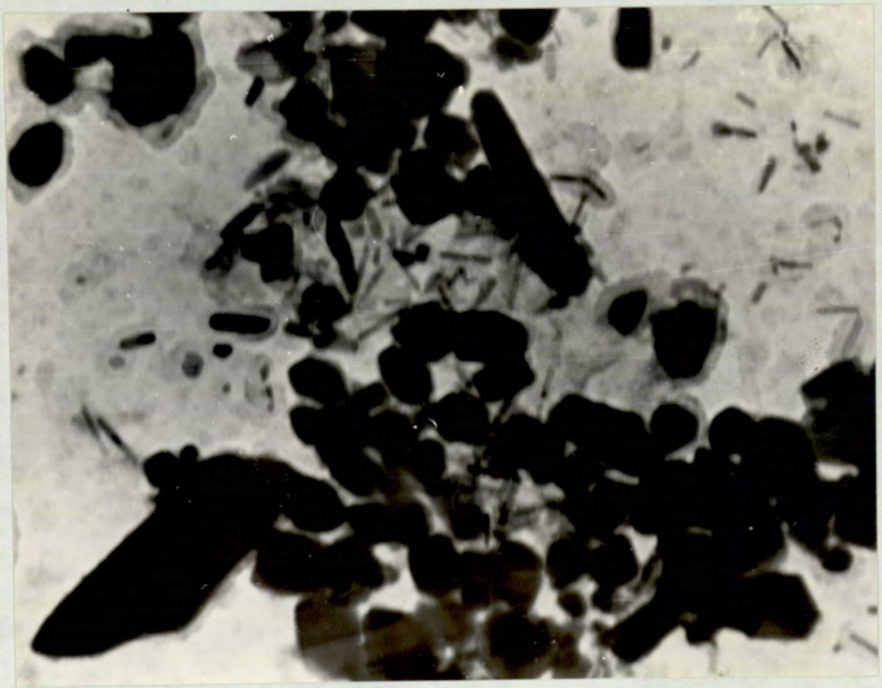

10% Co

FIGURE 18

Steels tempered for 1 hour at 650°C

Direct carbon extraction replicas x 27500

steels precipitate Fe_3C initially at the martensite plate boundaries. As the temperature of tempering is raised, the Fe_3C thickens and is precipitated within the plates, but for the cobalt containing steels these reactions become increasingly slower. Thus after tempering at 400°C, which is approximately the point of maximum Fe_3C precipitation, the basis steel shows a dense precipitation of Fe_3C both at plate boundaries and within the plates. In the cobalt steels, on the other hand, carbide formation is still associated mainly with the plate boundaries, the degree of precipitation within the plates reducing with the cobalt content of the steel. Above 400°C re-solution of the Fe_3C occurs, a process which is more complete in the cobalt steels after tempering at 500°C presumably due to its reduced Fe_3C precipitation previously. Peak hardness occurs for all steels after tempering at 550°C at which point a highly strained structure is observed which could not be clearly resolved even at a magnification of x 27,500.

The first signs of the secondary carbide were detected after tempering at 575°C when the acicular Mo_2C formed as in Figures 15 and 16 (pages 48 and 49). It is immediately seen that the carbides in the cobalt steel are far more numerous than those in the basis steel although the respective sizes of the carbide particles at this stage are approximately equal. Tempering above 575°C increases the size of the Mo_2C needles but their rate of growth in the cobalt-containing steels is considerably slower than in the cobalt-free steel (Figure 17 page 50). The rate of agglomeration of the carbides is increased by the presence of cobalt after tempering at 650°C as shown in Figure 18 (page 51).

The secondary hardening process may be followed by examination of the diffraction patterns obtained from the extraction replicas and shown in Figure 19 (page 54). No precipitate could be detected at peak hardness but at 575°C a distinct pattern is seen although it is rather "spotty" showing no well-formed rings. This is due to the highly preferred orientation of the Mo_2C needles especially in the early stages of formation when growth is essentially two-dimensional. At higher tempering temperatures the Mo_2C needles take on a more three dimensional growth and produce a well defined diffraction pattern as observed in Figure 19(c) (page 54).

3.6 Carbide Extraction

One half of the tempered samples of the 0 and 10% cobalt steels were carefully slit to give two specimens $\frac{1}{4}$-in. by $\frac{1}{2}$-in. square. One sample was retained for the (310)α line breadth measurements outlined in the next section and the other used in these experiments.

To follow the carbide reactions during tempering, the carbides were electrolytically extracted from the tempered samples by making the sample the anode in an electrolytic cell described in Figure 20 (page 55). In early trials with this cell a 5% HCl electrolyte was used but a great deal of difficulty was encountered on the subsequent analysis of the

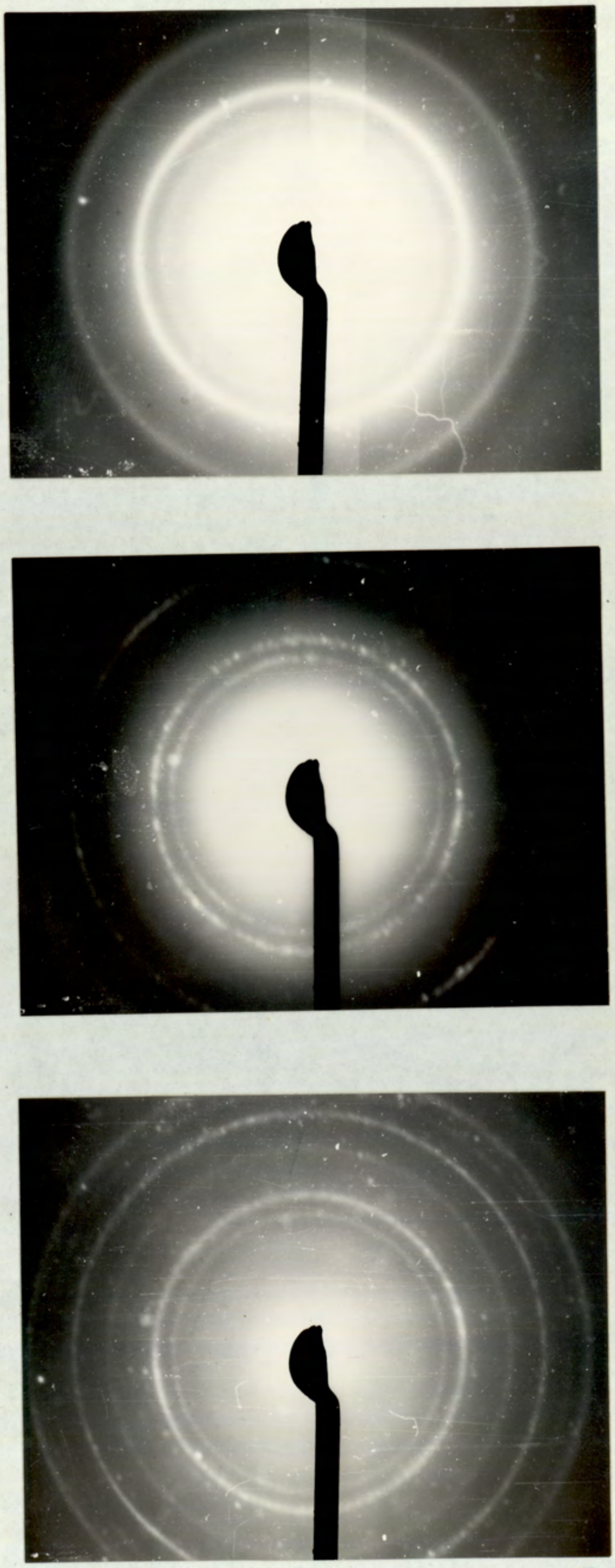

550°C

575°C

600°C

FIGURE 19

Diffraction patterns from extraction replicas for steels tempered for 1 hour at temperatures shown

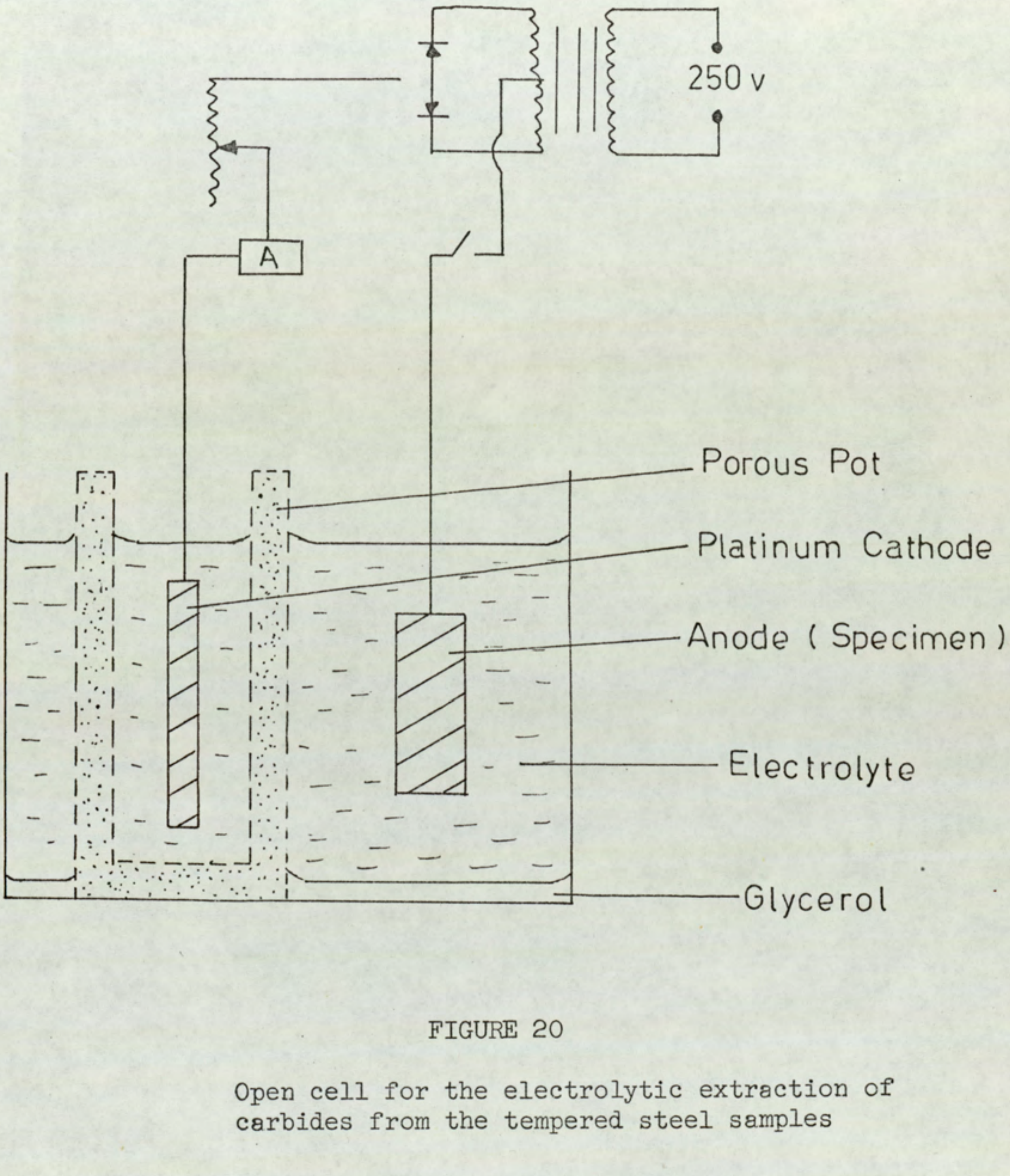

FIGURE 20

Open cell for the electrolytic extraction of carbides from the tempered steel samples residue due to oxidation of much of the iron carbide and interference by the oxide diffraction rings on the film pattern. Finally a solution of 15% sodium citrate and 1% potassium thiocyanate was adopted as the electrolyte, this being a neutral solution and reduced much of the oxide contamination. The cell was further improved by incorporating a layer of glycerol at the bottom of the container into which the carbides fell and became completely isolated from the action of the electrolyte. The specimens were ground to remove all traces of scale formed during heat treatment, placed in the cell and subjected to a current density of 0.05 - 0.1 amps per sq.cm. for approximately 8 hours.

At the end of each extraction, the solution was carefully filtered through a series of fine filter papers, washed with distilled water and iso-propyl alcohol and dried. The residue was ground and packed into a Lindemann capillary tube which is a thin walled tube made of lithium borate glass, a weakly absorbing substance. The packed tube was placed in a Debye-Scherrer camera and irradiated with Fe - filtered Co Kα radiation for between 2 and 3 hours.

The resultant film patterns from the tempered samples are shown in Figures 21 and 22 (pages 57 and 59), and the observed "d" values of the carbides recorded in Tables 5 and 6 (pages 58 and 60). Although oxide contamination was considerably reduced by incorporating a layer of glycerol at the bottom of the cell, several interference lines still

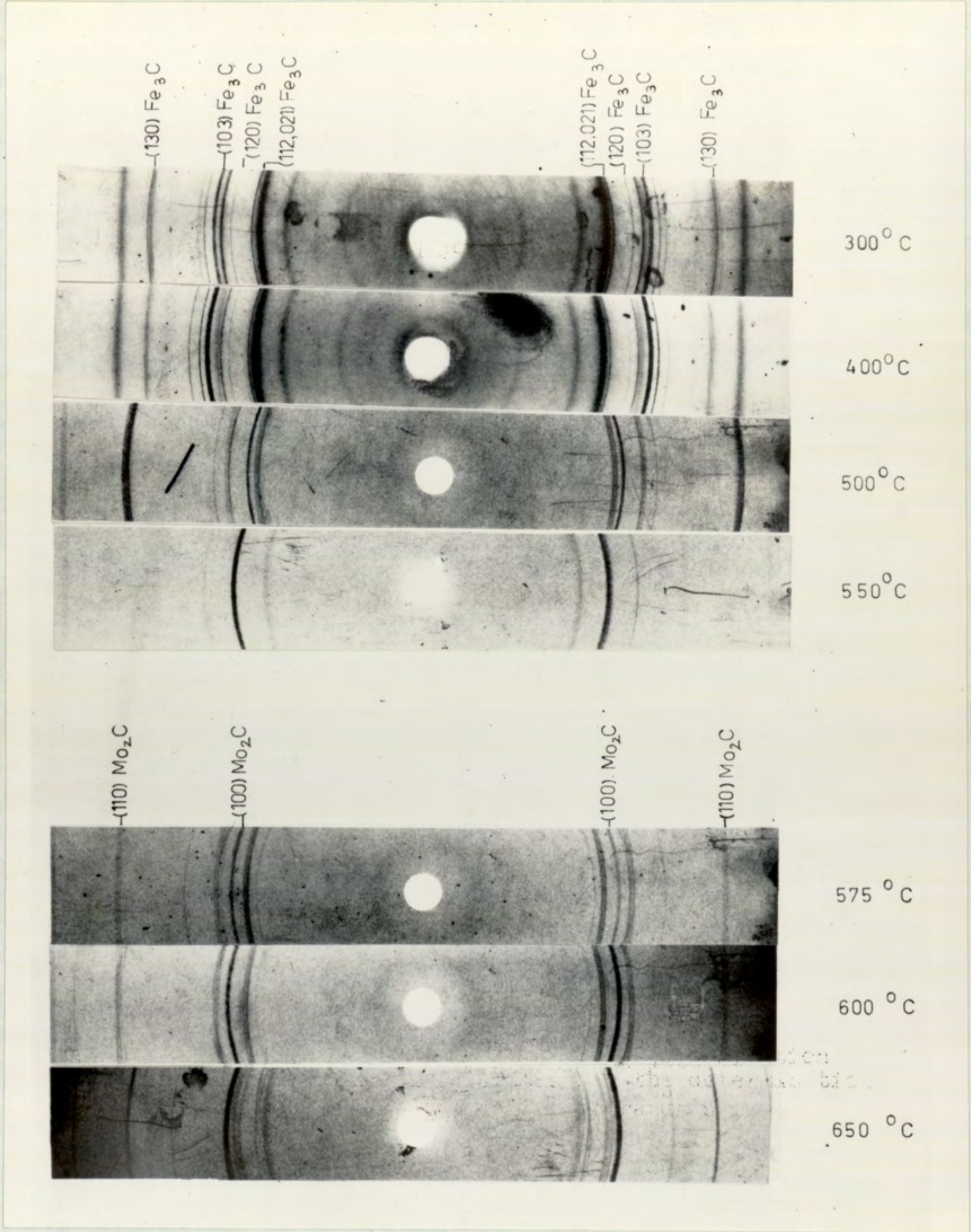

FIGURE 21

Powder camera diffraction patterns for carbides electrolytically extracted from steel 3M/0 after tempering for 1 hour at temperatures shown.

TABLE 5

OBSERVED "d" VALUES OF CARBIDES ELECTROLYTICALLY EXTRACTED FROM STEEL 3M/O TEMPERED BETWEEN 300 AND 650°C FOR 1 HOUR

Standard "d" Values Å for Carbides*		Observed "d" Values, Å, for Steel 3M/O Tempered for 1 hour at						
Fe_3C	Mo_2C	300°C	400°C	500°C	550°C	575°C	600°C	650°C
-	2.60 (20						2.61	2.60
2.38(65)	-	2.39	2.38	2.38				
-	2.37(30)						[2.37]	2.36
-	2.28(100)					2.27	2.28	2.27
2.26(25)	-							
2.20(25)	-	2.19	2.21					
2.10(60)	-	2.09	2.09	2.10				
2.06(70)	-		2.07					
2.02(60)	-							
2.01(100)	-	2.00	2.01	2.01				
1.97(55)	-	1.95	1.97					
1.87(30)	-	1.86						
1.85 (40)	-		1.83	[1.84]				
-	1.75(16)							1.76
1.68(15)	-		1.67					
1.58(20)	-	1.60	1.59					
-	1.503(12)						[1.50]	[1.50]
-	1.35(18)						1.36	1.37
-	1.269(16)							1.27

* A.S.T.M. Powder Data File, 1961. Numbers in round brackets are relative intensities.
Square brackets indicate very weak lines.

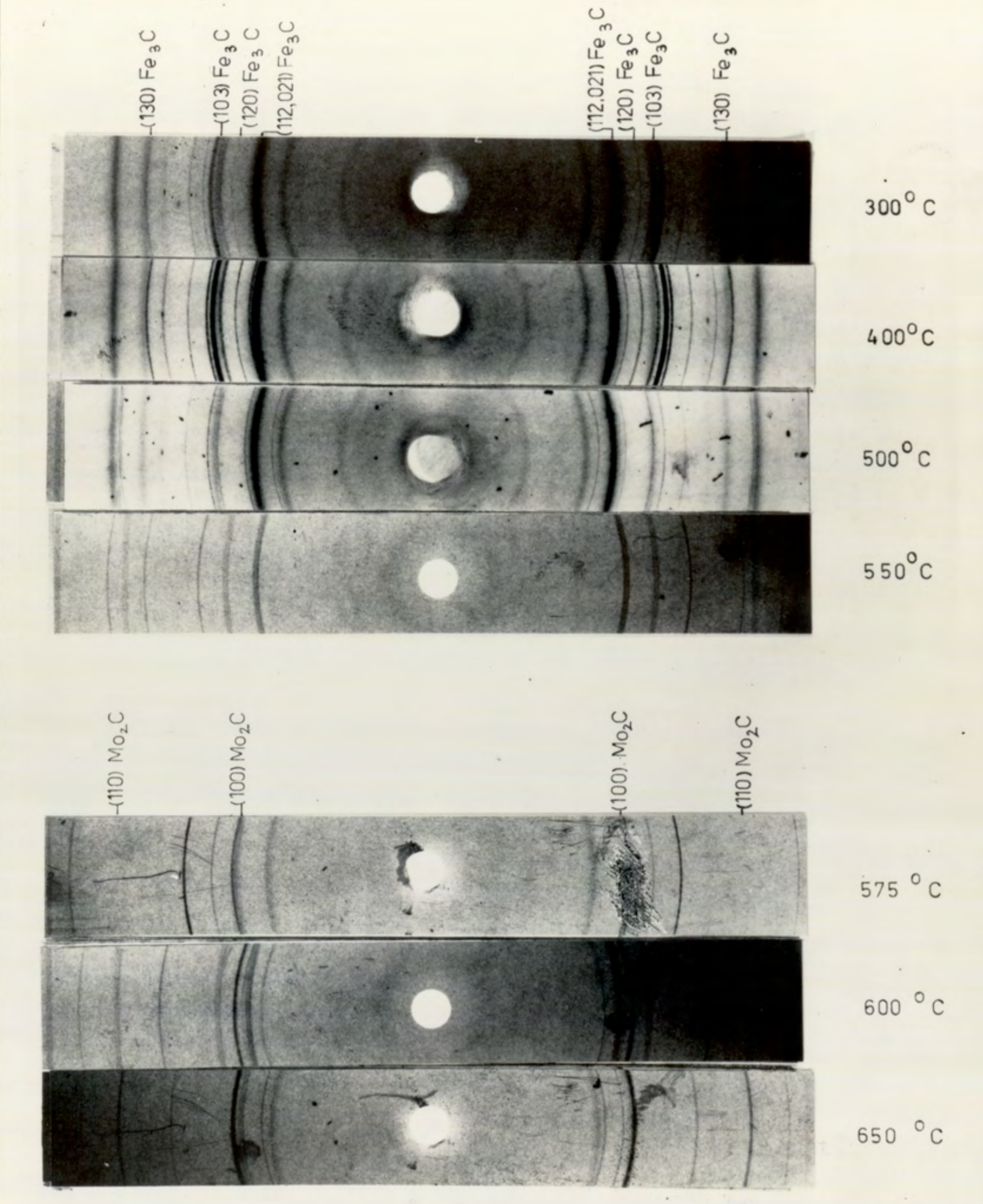

FIGURE 22

Powder camera diffraction patterns for carbides electrolytically extracted from steel 3M/10 after tempering for 1 hour at temperatures shown.

TABLE 6

OBSERVED "d" VALUES OF CARBIDES ELECTROLYTICALLY EXTRACTED FROM STEEL 3M/10 TEMPERED BETWEEN 300 AND 650°C FOR 1 HOUR

Standard "d" Values Å for Carbides*		Observed "d" Values, Å, for Steel 3M/0 Tempered for 1 hour at						
Fe_3C	Mo_2C	300°C	400°C	500°C	550°C	575°C	600°C	650°C
-	2.60(20)					[2.59]	2.63	2.61
2.38(65)	-	2.41	2.39					
-	2.37(30)						2.37	2.38
-	2.28(100)					2.27	2.26	2.26
2.26(25)	-							
2.20(25)	-	2.17	[2.18]					
2.10(60)	-	2.08	2.11	[2.12]				
2.06(70)	-							
2.02(60)	-							
2.01(100)	-	2.03	2.00	[2.00]				
1.97(55)	-	1.94	1.99					
1.87(30)	-	1.87	[1.86]					
1.85(40)								
-	1.75(16)							1.77
1.68(15)	-							
1.58(20)	-	1.57						
-	1.503(12)						[1.51]	[1.52]
-	1.35(18)						1.32	1.35
-	1.269(16)							1.25

* A.S.T.M. Powder Data File, 1961. Numbers in round brackets are relative intensities.

Square brackets indicate very weak lines.

persisted on the films. Both steels exhibited almost identical carbide reactions, the only differences being in the number and strength of the lines. Tempering up to 400°C gave only Fe_3C diffraction lines, the "d" values of which were very close to the standard values obtained from the A.S.T.M. Powder Data File. The lines calculated for the carbides extracted from the basis steel were generally stronger and more numerous than those for the 10% Co steel. Very weak Fe_3C lines were recorded after tempering at 500°C and no carbide lines whatsoever were detected at 550°C, the peak hardness temperature. The first sign of the Mo_2C carbide was from the samples tempered at 575°C and the higher tempered specimens increased the number and intensity of the diffracted lines. At no stage in the tempering process was the M_6C carbide detected.

The analysed "d" values for the carbides extracted from both steels were very close to the standard "d" values for the respective carbide Fe_3C or Mo_2C. Certainly no distinct and consistent distortion of the carbide lattice could be found in the 10% Co steel and it would thus appear that very little partitioning of cobalt occurred to the carbide phase.

3.7 (310)α Line Breadth Measurement

In addition to the carbide reactions during tempering, it is also instructive to follow the strain in the ferrite matrix and relate this to tempering processes. The strain in the ferrite matrix can be related to the broadening effect it has on a diffraction line from a specific ferrite plane, usually the (310)α, determined at half - height of the line. The component factors that contribute to the line broadening effect are complex and cannot be related to strain alone. However since no absolute value of strain is required, the values of the line breadth can be used on a comparative basis.

The samples, taken from the tempered specimens as described in the previous section, were polished and heavily etched to remove all traces of working from the surface and placed in a specimen holder on a Siem~~a~~ens X-ray unit. The wide angle goniometer was aligned to near the (310)α Bragg angle and the sample irradiated with Co Kα radiation. A continuous scan was made through the Bragg angle at a rate of $1^{\circ}/\text{min.}$ and the diffracted radiation graphed on a continuous chart recorder. The half height position of each line was calculated and the breadth measured with a sliding micrometer scale.

Results from the line breadth determinations are represented in Figure 23 (page 63). The strain in the ferrite is seen to gradually decrease as the samples were tempered up to 400°C and this corresponds to the relaxation of matrix distortion as carbon is precipitated from the supersaturated

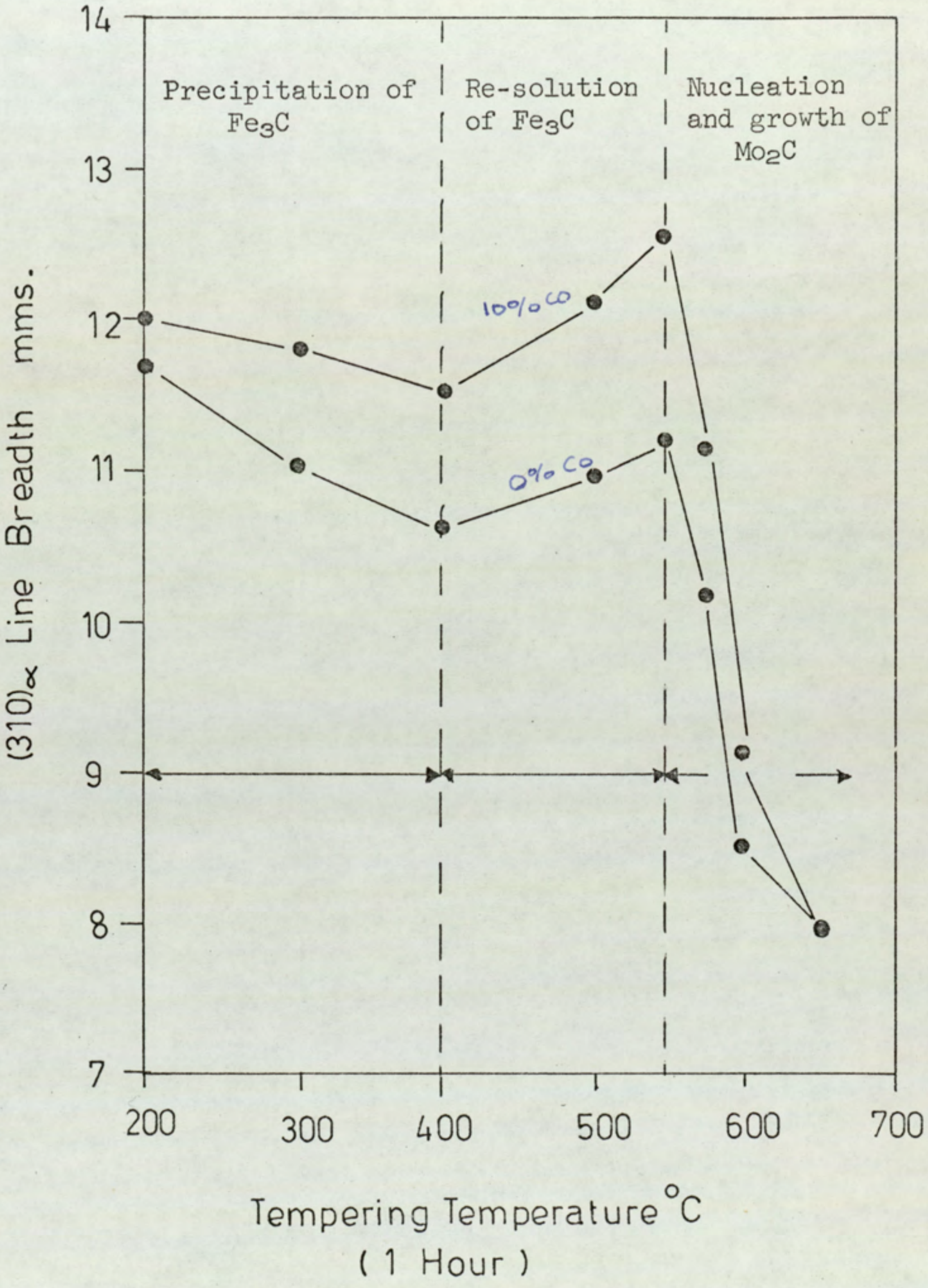

FIGURE 23

Variation in the matrix strain of the 0 and 10% cobalt steels after tempering between 200 and 650°C for 1 hour solid solution as Fe_3C. Over this tempering range, the strain in the 10% Co matrix of the 10% Co steel remains higher than that in the basis steel. This behaviour would seem to be due to the decreased Fe_3C precipitation in the cobalt steel as observed previously in Figures 9 to 11. Tempering above 400°C increases the strain the matrices of both steels reaching a maximum at 550°C, the peak hardening temperature. The temperature range 400 - 550°C has been shown to be associated with the re - solution of the Fe_3C and the development of a highly strained structure at peak hardness. The increase in matrix strain of the cobalt steel over this tempering range is considerably greater than that found for the cobalt-free steel. If this were due solely to the re-solution of Fe3C then it would be expected that the steels would exhibit a similar strain relationship at 500°C as was found in the quenched samples. In fact the 10% cobalt material shows a substantial increase above this and the strain in the matrix at peak hardness is much higher than in the basis steel. On tempering above 550°C a sharp decrease in line breadth was recorded and this has been shown to be associated with the nucleation growth and agglomeration of the secondary carbide Mo_2C. After 600 and 650°C tempering for both steels the matrix strain is reduced to very low levels.

4. MECHANICAL PROPERTIES

4.1 Fracture Toughness

The energy absorbed by fracturing a notched specimen using an impact test is a familiar quantity through which the brittleness or toughness of a material can be envisaged. Values of energy are obtained over a range of temperatures and steels may be graded in terms of their transition temperature. Thus a steel with a low transition temperature is regarded as "better" than a steel with a higher transition temperature. Such a test is a valuable production control technique since it is extremely cheap and easy to perform, and if a material of a certain impact energy has previously withstood certain service conditions, then this value can be used as an acceptance level. Additionally, if high toughness is required, it may be possible to work above a ductile-brittle transition temperature which can be controlled by metallurgical techniques. There is some merit in the use of a specific value of impact energy at some particular temperature to designate toughness; for example the N.D.1 acceptance standard of 20 ft.lbs. at 0°C. Here again, however, the values only become meaningful when substantial background data on a steel ~~has~~ have been acquired. For a newly developed steel, there is no established correlation between energy and service performance and such values are therefore of little value. The question as to what such values of energy do represent is still obscure and much research into this is being undertaken through instrumented Charpy tests.

The limitations of these tests have become increasingly apparent as the need for more realistic data has arisen and materials of increased strength have required a more critical appraisal. To take an example, if a material of increased tensile strength is accepted with the same energy absorption value as that of a lower strength material, then the former may have a much greater liability to fracture in service because its ductility prior to fracture may be much reduced. Lack of appreciation of this aspect has led to a number of catastrophic failures.

A further major consideration is the effect of specimen size. It is now recognised that the testing of samples of small size may indicate relatively high fracture strength whereas larger pieces may break at much lower stress levels. This size factor effect is of particular importance to the die-steel metallurgist since the behaviour of small impact samples must be related to the service performance of large die blocks sometimes weighing many tons.

The shortcomings of this qualitative evaluation of fracture toughness has given rise to a new approach in appreciating factors of importance in the satisfactory application of materials. Many of the problems associated with fracture toughness measurement were due in the main to an inadequate definition of toughness. In the field of fracture mechanics this is defined as the resistance of a material to the rapid propagation of a crack and the present approach is therefore to assume that all materials contain flaws of some magnitude. Here again the limitations of the standard impact tests are brought into focus. The stress analysis at the root of the machined notch is a very complex function and the energy absorbed represents not only that required to propagate a crack but also that to initiate the crack at the root of the notch.

The development of fracture mechanics has expanded rapidly since the fracture process was first characterised by Griffith(74) in 1921 in terms of the area-specific energy required to propagate a crack. Recent papers by Barnby(75), May and Walker(76) and Greenwood(77) have covered in great detail the basic theory leading to the present concept of fracture. In summary, precracked specimens are tested under predominantly plain strain conditions and toughness can be then quantitatively measured in terms of the critical stress intensification factor, K_{Ic} , which specifies the resistance of the material to the propagation of sharp, natural cracks in the material. Provided that the specimen is thick enough to minimise the constraint - relieving influence of the free faces and impose a triaxial stress system over most of the thickness, then K_{Ic} may be regarded as a material constant in the same way as are tensile strength and yield stress.

K_{Ic} is given in terms of the specimen thickness, B, width, W, crack length, a, and the load P for crack propagation by an expression of the form -

$$K_{Ic} = Y \frac{Pa^{1/2}}{BW} \quad \text{.........................(7)}$$

Here Y is a geometrical constant depending on the shape of the test piece or cracked component. The application of fracture mechanics allows the behaviour of cracks to be studied on a laboratory scale. In the fracture toughness test, the samples are machine notched as with the conventional Charpy or Izod specimens and the sharp cracks simulated by fatigue cracking from the root of this notch. The nucleation and growth characteristics of these fatigue cracks are subject to stringent conditions which are outlined in B.I.S.R.A. publication MG/EB/312/67 "Recommended A.S.T.M. Practice for Plain-Strain Fracture Toughness Testing of High Strength Metallic Materials Using a Fatigue Cracked Bend Specimen" and which also details the method used for determining the respective K_{Ic} values.

Localised cracks invariably form, by fatigue stressing or thermal fatigue, on the surfaces of hot working dies during their normal working life. These cracks may be so small, or the local stresses so low, that they do not propagate and are therefore harmless. In contrast, working conditions may be such as to propagate these cracks, particularly from regions of stress concentration such as corners, leading to a reduction in working life of the dies. Resinking of the die impression may be possible, but the depth of resinking necessary is determined by the depth of crack penetration. Quantitative information on the cracking characteristics of die tool steels is therefore of commercial value.

4.1.1 Development of a Fracture Toughness Specimen and Testing Procedure

Many techniques have been proposed to determine fracture toughness parameters and a comprehensive range of specimen forms are available(76, 78, 79) that enable tests to be performed either in tension or bending. The most important dimensions in a fracture toughness specimen are its thickness and the length of the crack. The lower limit of thickness for reliable K_{IC} measurements cannot be predicted from theoretical considerations alone, but a tentative basis has been established that specimen thickness should not be less than a factor, β, where

$$\beta = 2.5\ (K_{IC} / \sigma_{YS})^2 \ \ldots\ldots\ldots\ldots\ldots\ldots\ldots (8)$$

A similar criterion can be used for the crack length.

A series of experimental test specimens were made from 3M steel scrap and the final specimen form adopted is shown in Figure 24 (page 70) tested under a 3-point bend stress system. Blanks were machined from the forged stock, austenitised for 1 hour at 1020°C, oil quenched, tempered for 1 hour at the respective temperatures in salt baths and finally oil quenched. To avoid any extraneous results that might occur

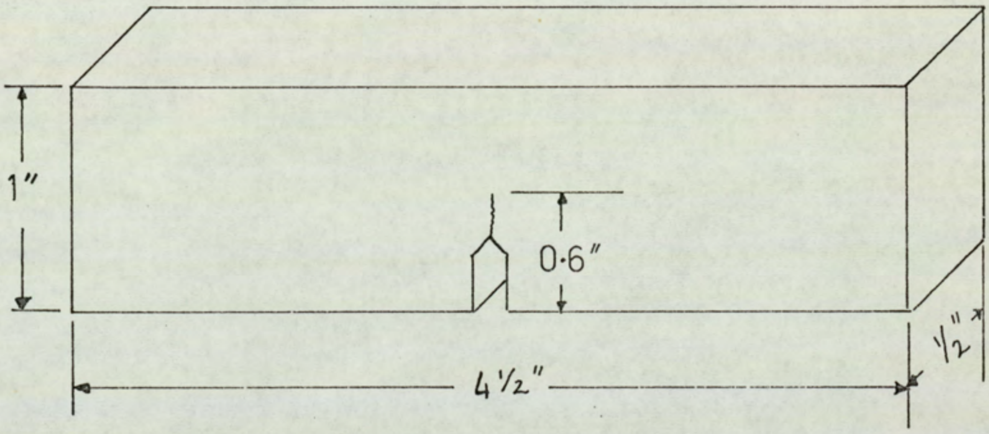

FIGURE 24

Dimensions of the 3 - point bend fracture toughness specimen from different orientations to the forging direction, the samples were machined so that the direction of cracking was always normal to the original forging direction. After final machining and notching, the samples were fatigue cracked in a 2-ton Amsler Vibrophore under an alternating 3-point bending stress. The requirements for the nucleation of the cracks were generally met using a mean ~~stress~~ load of 0.4 tons and a ~~stress~~ load range of ± 0.3 tons. The ~~stress~~ load range was reduced to around ± 0.15 tons after nucleation to conform with the required growth characteristics.

The specimens were tested on a 5000 Kg capacity Instron testing machine at a strain rate of 0.02 cm/min. crosshead movement. On the moving platform of the Instron was positioned a bend test fixture which consisted of two hardened silver steel, 1-in. diameter rolls seated in a base of a similar material. To minimise friction between the specimen and support rolls, the assembly was designed to permit both rotational and lateral movement of the rolls and thereby maintain rolling contact during the test. The central loading beam was suspended from a load-sensing transducer mounted in the middle of the overhead cross beam of the Instron frame.

To perform a test, two machined knife-edges were clamped to the test piece either side of the notch with set screws. A double cantilever displacement gauge was clipped between the knife-edges and the specimen placed on the bend test fixture with the notched edge in contact with the rolls. During the careful positioning of the bar, the rolls were positively positioned

4 inches apart against stops using low tension springs which were removed before the test began. The platform was raised until the top face of the specimen just made contact with the central loading beam and the test continued at the predetermined strain rate. The test record consisted of an autographic plot on an X-Y recorder of the output from the displacement gauge (X-axis) and the load-sensing transducer (Y-axis). From these graphs were calculated the respective K_{IC} values as outlined in the B.I.S.R.A. publication referred to previously.

After testing the fracture faces were coated with Formvar to protect the surfaces whilst cutting samples from the bars for examination on the scanning electron microscope. The Formvar was later removed by immersing the samples in chloroform. One half of the broken bars were retained for tensile test specimens and from the other half were machined small Izod samples, the dimensions of which are shown in Figure 25 (page 73).

4.1.2 Results

The results from the 3-point bend tests are given in Table 7 (page 74) and represented diagrammatically in Figure 26 (page 75). The basic 3M steel shows an increasing toughness on tempering, reaching a maximum value of 71.7 ksi $\sqrt{in.}$ (78.8 hb $\sqrt{cm}$) after tempering for 1 hour at 400°C. Above this temperature, tempering reduces toughness

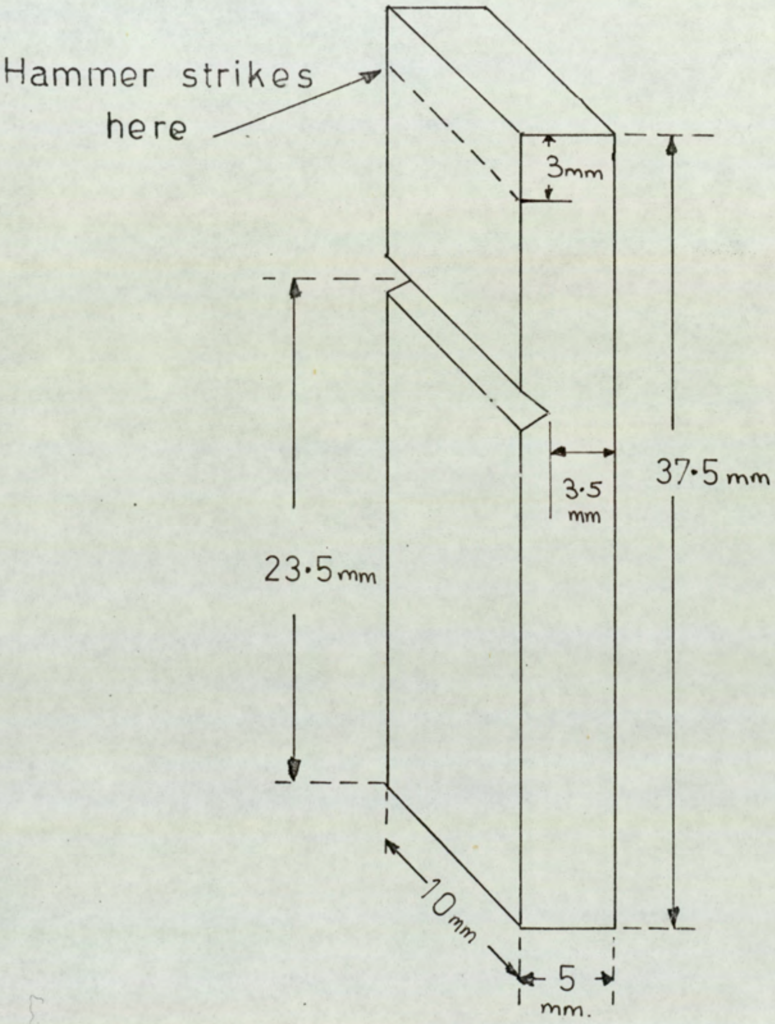

FIGURE 25

Dimensions of the small Izod impact specimen

TABLE 7

FRACTURE TOUGHNESS RESULTS OF 3M ALLOYS

Melt	Nominal % Co	Treatment	Hardness VPN	K_{Ic} ksi/$\sqrt{in}$	K_{Ic} hb/$\sqrt{cm}$	β in
3M/0	0	As quenched	352	55.6	61.1	0.136
		Tempered 200°C	354	64.1	70.4	0.200
		" 300°C	356	67.5	74.2	0.286
		" 400°C	361	71.7	78.8	0.345
		" 500°C	386	68.5	75.3	0.292
		" 550°C	403	55.9	61.4	0.185
		" 600°C	284	44.2	48.6	0.09
3M/1	1	As quenched	355	57.3	63.0	0.137
		Tempered 200°C	356	65.6	72.1	0.202
		" 400°C	369	70.0	76.9	0.310
		" 500°C	400	68.1	74.8	0.258
		" 550°C	411	51.9	57.0	0.161
		" 600°C	289	45.0	49.4	0.09
3M/3	3	As quenched	355	58.1	63.8	0.142
		Tempered 200°C	360	68.8	75.6	0.174
		" 400°C	379	63.7	70.0	0.238
		" 500°C	405	62.0	68.1	0.196
		" 550°C	419	52.2	57.4	0.122
		" 600°C	290	38.4	42.2	0.066
3M/5	5	As quenched	360	62.0	68.1	0.147
		Tempered 200°C	359	66.9	73.5	0.206
		" 400°C	382	58.1	63.8	0.182
		" 500°C	417	54.4	59.8	0.131
		" 550°C	431	42.9	47.1	0.081
		" 600°C	294	28.3	31.1	0.035
3M/7	7	As quenched	361	60.2	66.1	0.156
		Tempered 200°C	361	68.1	74.8	0.208
		" 400°C	390	53.0	58.2	0.135
		" 500°C	431	49.1	54.0	0.099
		" 550°C	447	33.9	37.2	0.049
		" 600°C	291	21.3	23.4	0.015
3M/10	10	As quenched	364	64.2	70.5	0.156
		Tempered 200°C	369	70.8	77.8	0.212
		" 400°C	392	36.2	39.8	0.056
		" 500°C	446	33.1	36.4	0.036
		" 550°C	463	20.8	22.9	0.014

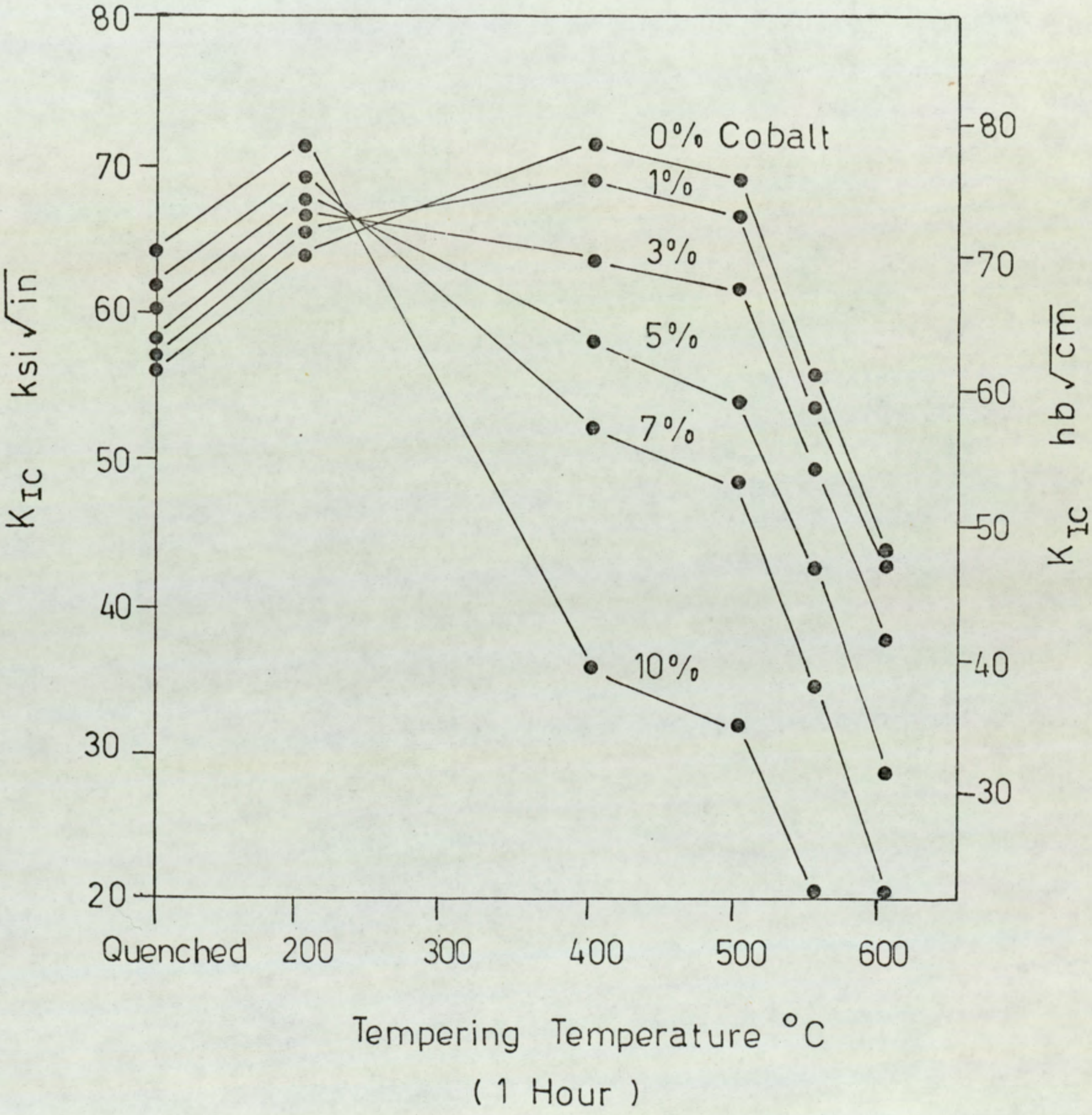

FIGURE 26

The influence of cobalt on the room temperature fracture toughness values for steels tempered at different temperatures until at 600°C the K_{IC} value has fallen to 44.2 ksi $\sqrt{in}$ (48.6 hb $\sqrt{cm}$). The effect of cobalt may be seen to essentially affect two tempering ranges differently. In the as-quenched and tempered 200°C conditions, increasing the cobalt content of the steel leads to a general increase in K_{IC}. Values for the basis steel in these two conditions are 55.6 ksi $\sqrt{in}$ (61.1 hb $\sqrt{cm}$) and 64.1 ksi $\sqrt{in}$ (70.4 hb $\sqrt{cm}$) respectively whilst the corresponding values for the 10% Co steel have increased to 64.2 ksi $\sqrt{in}$ (70.5 hb $\sqrt{cm}$) and 70.8 ksi $\sqrt{in}$ (77.8 hb $\sqrt{cm}$). After tempering above 200°C, however, cobalt is seen to drastically reduce toughness to extremely low values. At all cobalt contents, K_{IC} values are below those for the basis steel after tempering above 200°C, the greatest difference being at 400°C where values for the 0 and 10% Co steels are 71.7 ksi $\sqrt{in}$ (78.8 hb $\sqrt{cm}$) and 36.2 ksi $\sqrt{in}$ (39.8 hb $\sqrt{cm}$). respectively - a 50% reduction. To aid in the interpretation of these results, it may be noted that K_{IC} values for grey cast iron and maraging steel are typically 18 ksi $\sqrt{in}$ (19.8 hb $\sqrt{cm}$) and 90 ksi $\sqrt{in}$ (98.9 hb $\sqrt{cm}$).

The results from the Izod tests are shown in Figure 27 (page 77). Although these results show a considerable scatter, it is observed that a similar pattern of behaviour emerges. The addition of cobalt increases the fracture energy of the as-quenched and tempered 200°C samples but the higher tempered samples show a reducing fracture energy with

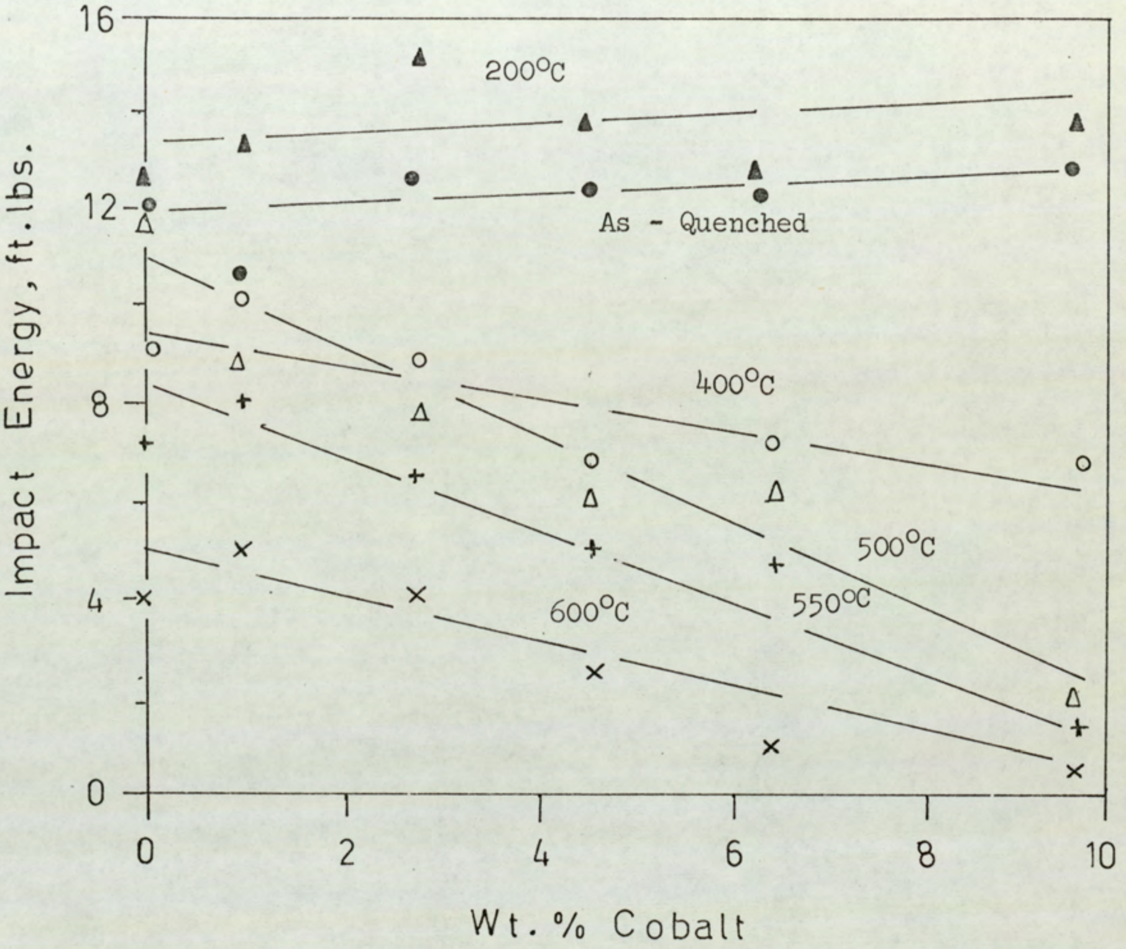

FIGURE 27

Effect of cobalt on impact fracture energy after tempering for 1 hour at the temperatures indicated progressive additions of cobalt. The lines of best fit for these points were determined using linear regression analysis and the respective correlation coefficients were found as follows:-

Test Condition	Correlation Coefficient r
As-quenched	0.112
Tempered 200°C	0.618
400°C	-0.838
500°C	-0.945
550°C	-0.936
600°C	-0.924

Fractographs from the scanning electron microscope are shown in Figures 28 to 33 (pages 79 to 84). Here again for convenience only the 0 and 10% Co containing steels are shown although a general overall pattern of behaviour of all steels will be described and discussed later in detail.

The 0% Co steel shows a honeycombed-type structure on fracture in the as-quenched and tempered 200°C and 400°C conditions. This type of plastic fracture is very common in metals and has been termed a "ductile fracture" or more commonly "dimple fracture". In most of the ductile tensile failures the reduction of area does not reach 100% although the overall deformation before fracture may be extensive. This is due to the fact that there is formation and coalescence of microvoids in the necked region of the test specimen. In the

0% Co

10% Co

FIGURE 28

Fracture surfaces of as-quenched steels

x 1600

0% Co

10% Co

FIGURE 29

Fracture surfaces of steels tempered for 1 hour at 200°C

x 1600

0% Co

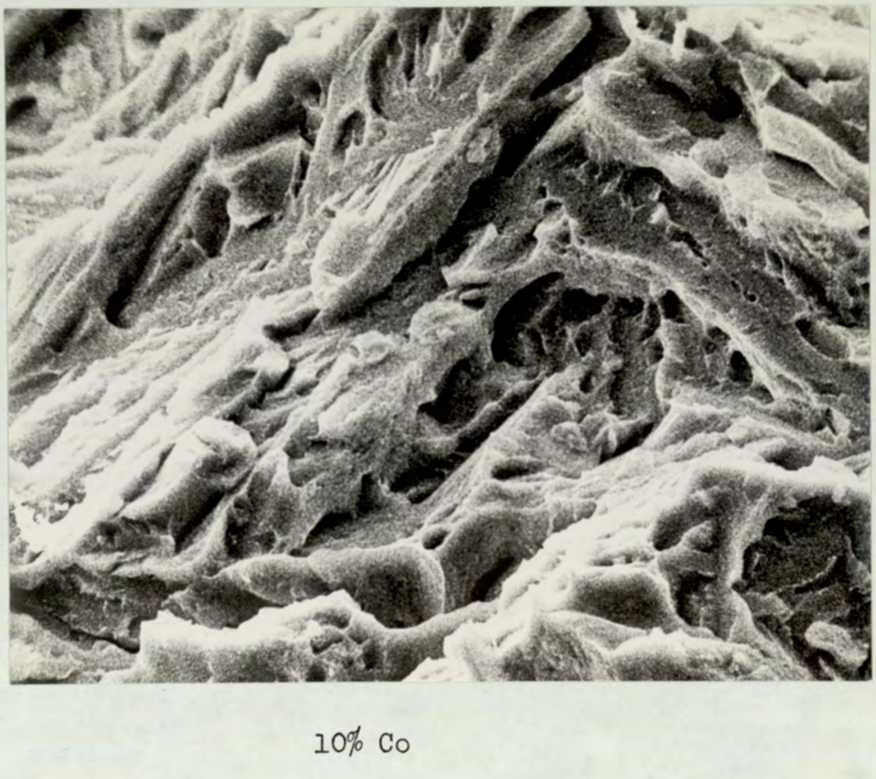

10% Co

FIGURE 30

Fracture surfaces of steels tempered for 1 hour at 400°C

x 1600

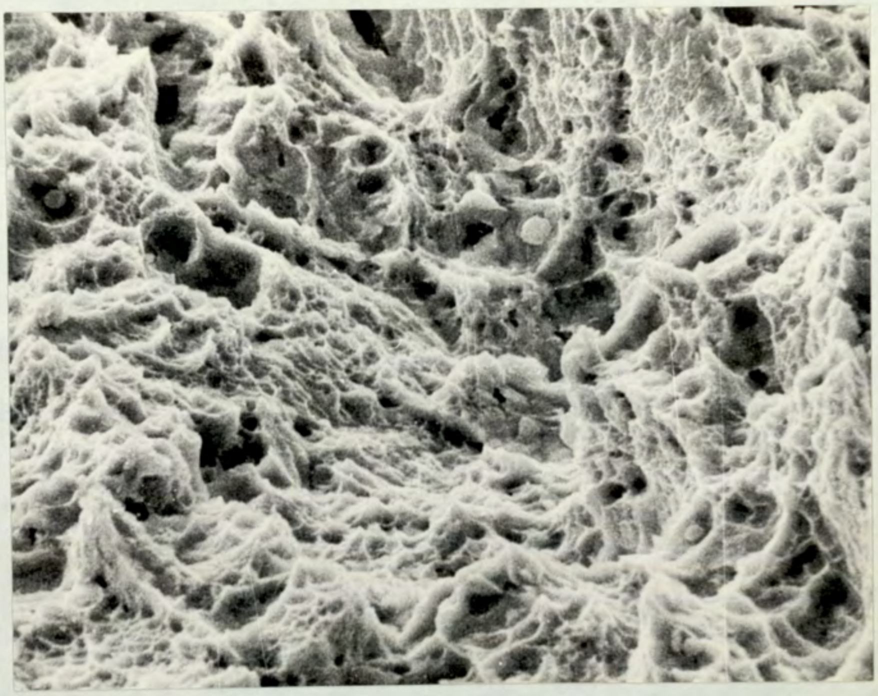

0% Co

10% Co

FIGURE 31

Fracture surfaces of steels tempered for 1 hour at 500°C

x 1600

0% Co

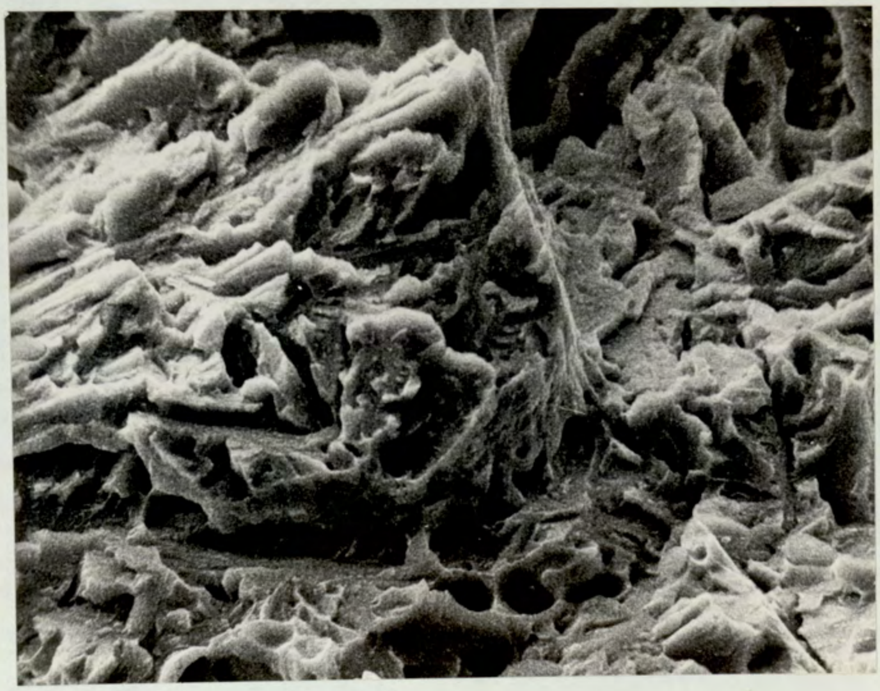

10% Co

FIGURE 32

Fracture surfaces of steels tempered for 1 hour at 550°C

x 1600

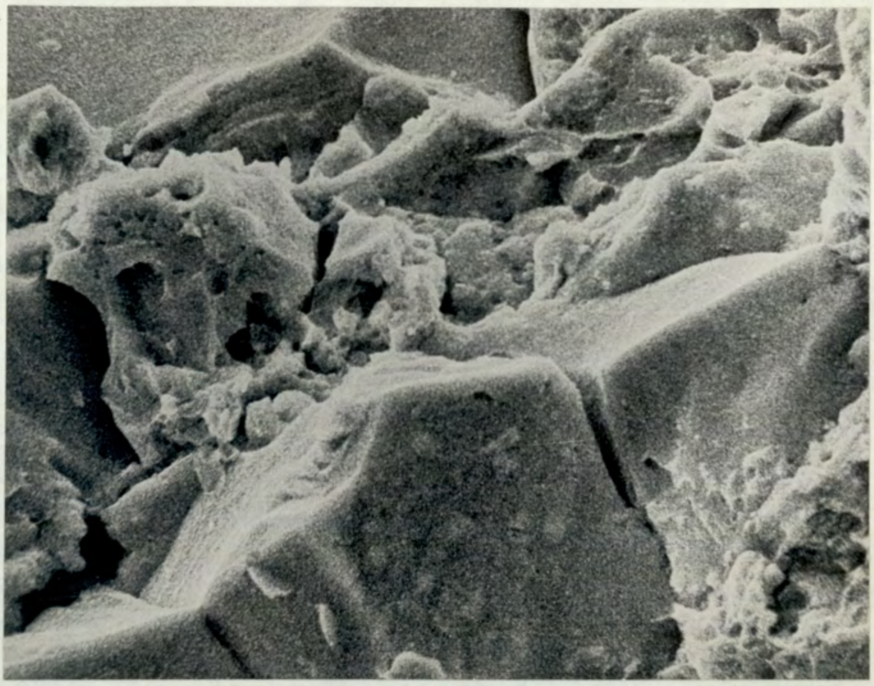

0% Co

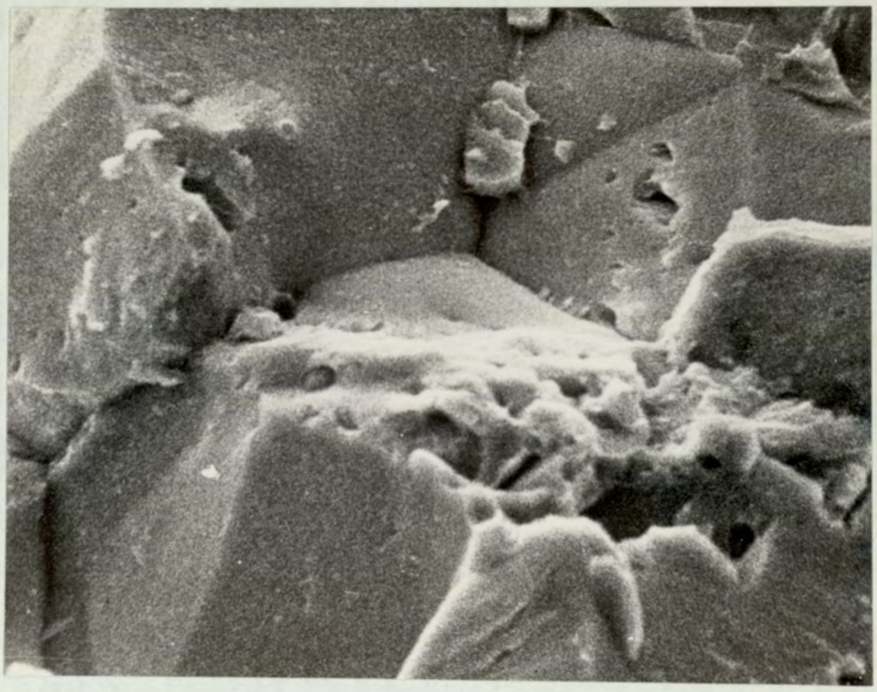

7% Co

FIGURE 33

Fracture surfaces of steels tempered for 1 hour at 600°C

x 1600

In the fracture toughness test the region ahead of the advancing crack is a small area subjected to a tensile stress and final fracture is thus a result of the formation and coalescence of microvoids. During deformation, the microcracks are nucleated at grain boundaries or, as a result of differences in elastic and plastic properties, at inclusions or precipitates ahead of the main crack. The coalescence of the voids takes place by a process of internal and localised necking and it is these voids that produce the numerous concave depressions observed on the opposite faces of the fracture. The fracture mechanism producing a dimpled surface is shown schematically in Figure 34 (page 86). The dimples are characterised by their shape and their average sizes. In general, the shape seems to depend essentially on the conditions of fracture while the size is more a function of the microstructure of the material. Since the stresses in the 3-point bend test are essentially tensile in nature, the shape of the dimples are seen to be approximately equiaxed, certainly not the parabolic form associated with shear mechanisms.

Tempering the basis 3M steel at 500°C and 550°C produces a fracture that, although still showing signs of a dimple fracture, is far less clearly defined and takes on an increasingly fibrous appearance until at 600°C the fracture is predominantly intergranular. Intergranular fracture is a separation of the crystals from each other along the grain boundaries and this fracture appearance is likened to a three dimensional model of a

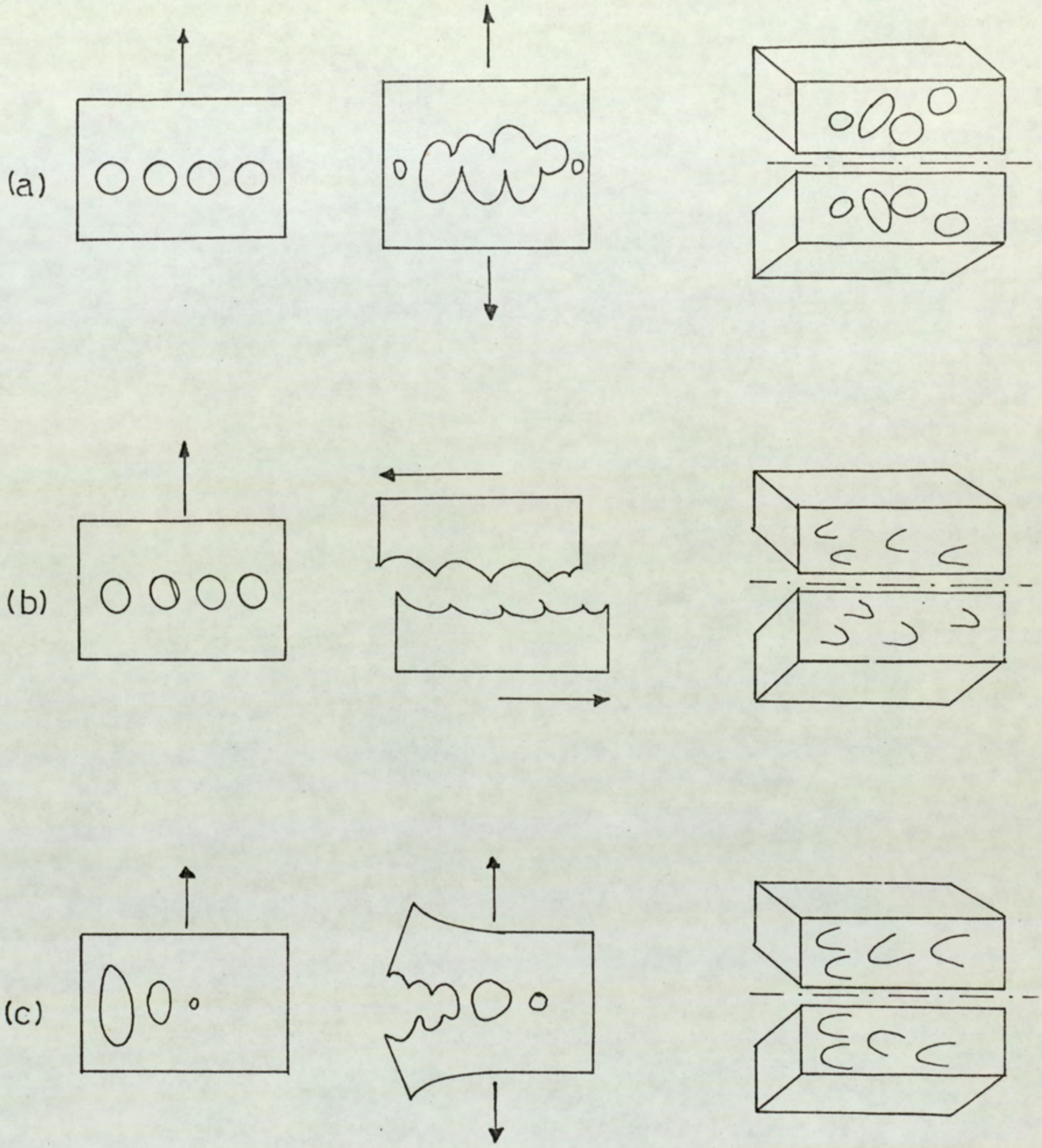

FIGURE 34

Plastic Fracture

(a) Normal plastic. Formation of round dimples

(b) Shear plastic. Formation of elongated dimples pointing in the direction of shear on each fracture surface

(c) Tear plastic. Formation of elongated dimples pointing in the opposite direction to the direction of each propogation stack of tetrakaidecahedrons. In the fractographs shown in Figure 33 (page 84) each facet of the grains is not straight but slightly curved which shows that the conditions for metastable equilibrium of the grain boundary network were satisfied during the austenitising treatment. This form of fracture is usually termed "brittle intergranular fracture", the term brittle referring to the total lack of deformation associated with the final separation of the grains. It is observed at room temperature in materials where the grain boundaries have been embrittled by a film of a brittle phase or by the segregation of an impurity without the appearance of a second phase. The exact mechanism of crack propagation associated with the intergranular fracture is so far uncertain.

The 10% Co steel shows a very similar dimpled fracture in the as-quenched and tempered 200°C conditions, although a somewhat larger process zone size is observed. After tempering at 400°C however a completely different fracture is observed as illustrated in Figure 30 (b) (page81) where the ductile necking fracture has been almost entirely replaced by a tearing mode of fracture which has occurred along specific directions. This fracture mode is also observed after tempering at 500°C and 550°C until, as with the basis steel, a brittle intergranular fracture is observed after tempering at 600°C. It will be noted that Figure 33(b) (page 84) shows the fracture surface from the 7%Co steel. Several attempts were made to grow a fatigue crack in the 10% Co steel tempered at 600°C but the material was so brittle that once the fatigue crack nucleated it propagated too quickly to permit the load and alternating stress to be reduced.

4.2 Tensile Properties

One half of each broken test bar was sectioned and a series of standard Houndsfield Number 11 tensile test specimens machined. Tensile properties were determined both at room and elevated temperatures using a conventional Houndsfield tensometer fitted with a double reduction gear. The room temperature properties illustrated the effect of cobalt and tempering temperature whilst the elevated temperature tests were performed on samples tempered to maximum hardness, viz. 1 hour at 550°C, tested at different temperatures. In the latter series of tests a small tube furnace was used for heating the specimens which fitted between the rails of the Houndsfield tensometer.

The effect of cobalt at the various levels of tempering on tensile strength, elongation and reduction of area is shown in Figures 35 and 36 (pages 89,90), all points representing the average of at least two tests. Cobalt is seen to increase the tensile strength of the steel after all heat treatments although this effect is much more pronounced at the higher tempering temperatures. In the as-quenched and tempered 200°C conditions the addition of cobalt increases the UTS of the steel in essentially a linear manner by 0.6 tons/sq.in./wt.% Co (0.93 hb./wt.% Co) and 0.9 tons/sq.in./wt.% Co (1.4 hb./wt.%Co) respectively. After tempering at 400°C this increase, although still essentially linear, has risen to just over 2 tons/sq.in./wt.% Co (3.1 hb./wt.% Co). Above

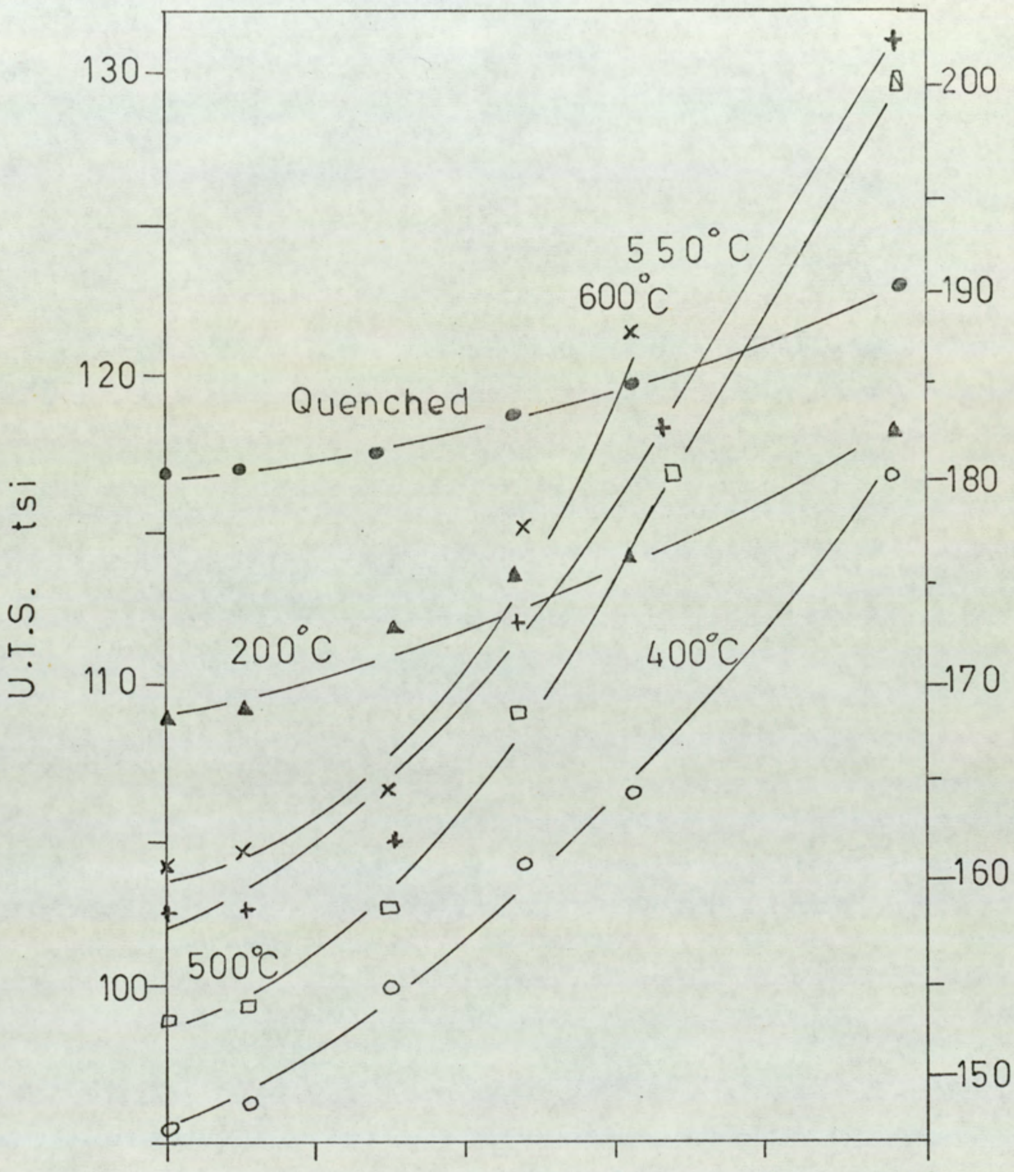

FIGURE 35

Effect of cobalt and tempering temperature on the tensile strength of the 3M steel

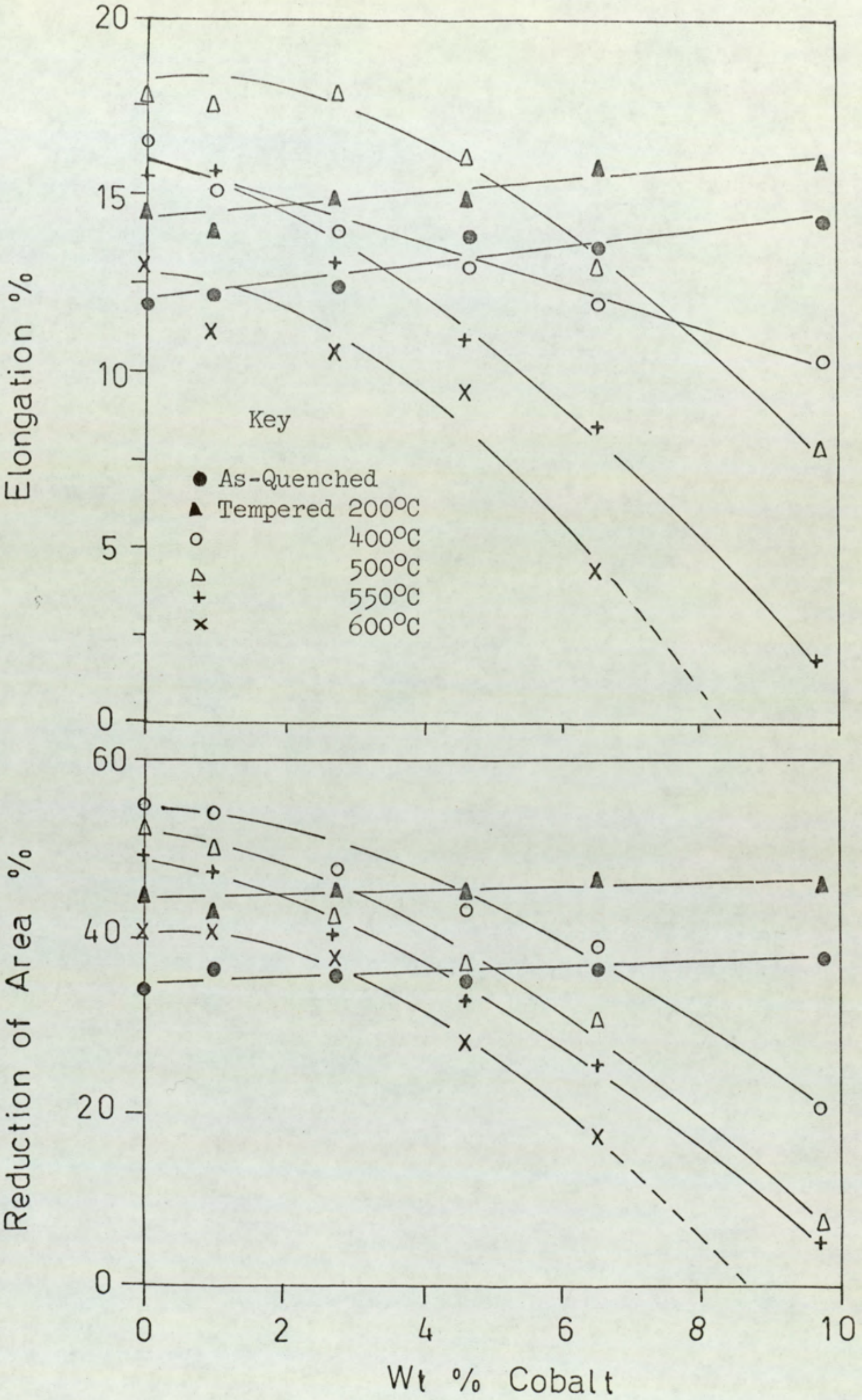

FIGURE 36

Variation of elongation and reduction of area values with tempering temperature and cobalt content

400°C the effect of cobalt loses its linearity and shows a marked increase above 3% cobalt. Tempering at 600°C greatly embrittled the higher cobalt containing steels such that the 10% Co steel specimens constantly broke at the shoulders of the test pieces. This behaviour persisted even after machining a larger fillet radius at the shoulder of the specimens.

Variation of elongation and reduction of area with cobalt content and heat treatment are shown in Figure 36(page 90). The effect of cobalt on these two parameters is, as might be expected, very similar. As-quenched and tempered 200°C, cobalt slightly increases both elongation and reduction of area values but above 200°C both of these parameters are reduced by cobalt additions. As was observed with the values of UTS, the effect of cobalt becomes more pronounced above the 3% level.

The tensile strength of the steels at elevated temperatures after tempering to maximum hardness is shown in Figure 37 (page 92). At all temperatures up to 500°C the same basic form of curve is observed showing cobalt to substantially increase UTS values, the effect of temperature being merely to reduce the level of strength. The elongation and reduction of area values were determined but showed a considerable degree of scatter, so much so that no definite pattern of behaviour could be deduced. The divergency of these results can be attributed to the relatively small size of the test samples.

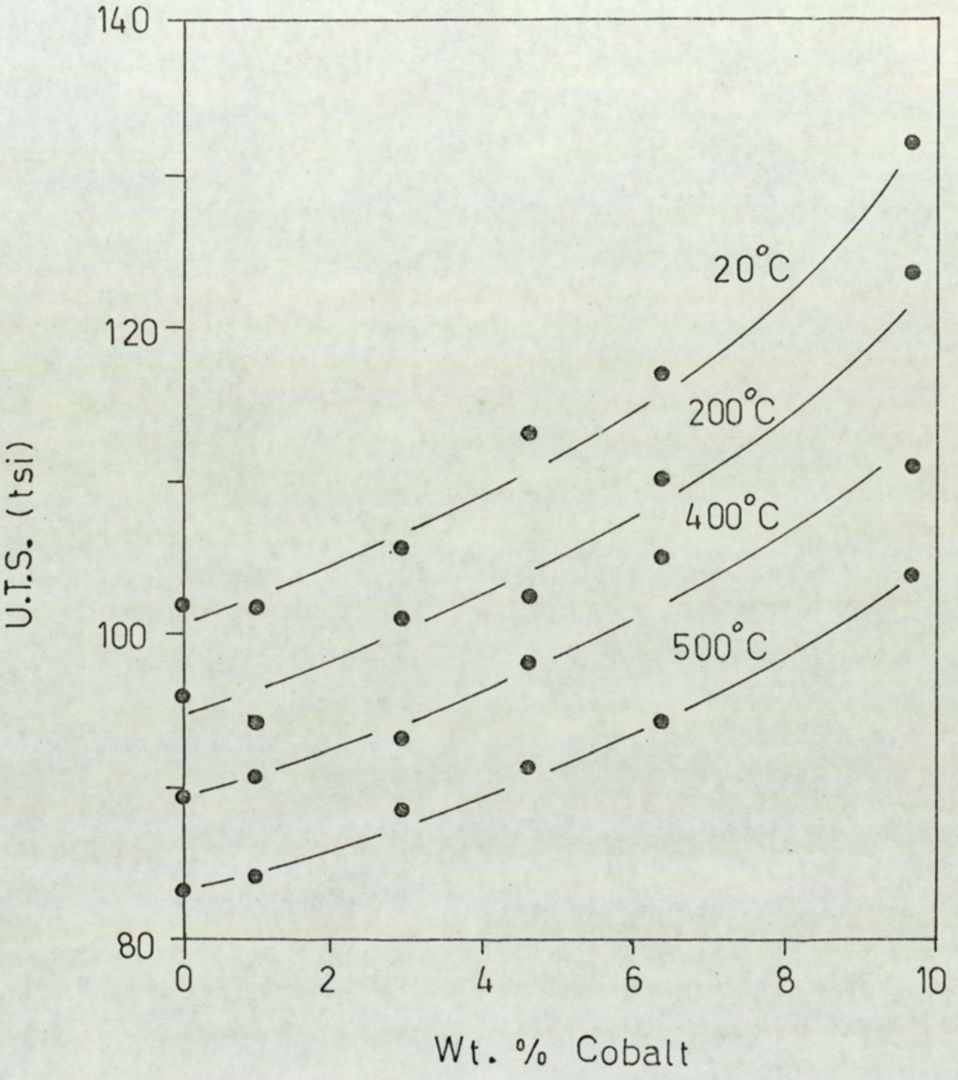

FIGURE 37

Effect of cobalt and temperature on the tensile strength of the 3M steel tempered to maximum hardness i.e. 1 hour at 550°C

5. TRANSFORMATION CHARACTERISTICS

5.1 Transformation Temperatures

5.1.1 Effect of Cobalt on Critical Points

The manner in which alloying elements affect the transformation temperatures M_s, A_1 and A_3 is of considerable importance. The maximum tempering temperature which can be used is governed by the A_1 and thus partly dictates the limiting operating temperature. The M_s is important because it can affect the resultant mechanical properties due to variations in the amount of retained austenite, and the volume expansion during the martensite transformation can influence the warpage in component parts and the risk of cracking during heat treatment. Since the effect of any additional alloying element on these transformation temperatures varies with the base composition, the figures quoted in the literature can only be taken as a guide. The general conclusion from these results(80-89) however indicates that cobalt, unlike most elements, increases the M_s and A_1 temperatures. Most of this work was performed on plain carbon or low-alloy steels and the opposite effect has been reported by Hammond(90) using a 0.03% carbon, 12% chromium, 4% nickel steel. He has recorded reductions in the M_s in the order of 3°C per 1% cobalt, this depression becoming even more pronounced in stainless steels. Clearly the effect of cobalt on the critical temperatures cannot be rationalised per se without first having some knowledge of the interaction mechanisms between the constituent elements.

5.1.2 Determination of Critical Points

In this work, the A_1, A_3 and M_s temperatures were determined dilatometrically using rod specimens, 1/8 - in. diameter and 1-in. long. A hole was drilled longitudinally along the specimen axis to half length to accommodate a thermocouple. This method of temperature recording was considered to be more accurate than merely attaching the thermocouple to the surface of the specimen. The specimen was enclosed in a silica sheath and dilation was recorded through a silica push rod and a specially designed dilatometer incorporating a Taylor-Hobson Magnagauge. The assembly is shown in Figure 38 (page 95) and a more detailed view of the dilatometer head represented diagrammatically in Figure 39 (page 96). The Magnagauge had as its sensing head an inductive displacement transducer mounted in a tubular clamp. The Magnagauge is normally used by reading a calibrated scale on the instrument but for these experiments a voltage output was applied to the Y-axis terminal of an X-Y plotter. Linear movements of the transducer (initiated by the expansion or contraction of the specimen) resulted in proportional voltage inputs to the Y-axis. Temperature measurements were by Pt-Pt/13%Rh thermocouples using very fine wires to reduce heat conduction from the sample. The thermocouple was attached to the X - axis of the X-Y plotter.

For M_s determinations, the specimens were austenitised for 1 hour at 1020°C and forced-air cooled. The cooling was facilitated by ultrasonically drilling a small hole in the side wall near the base of the silica sheath. When determining the

FIGURE 38

General apparatus for the determination of M_s A_1 and A_3 temperatures

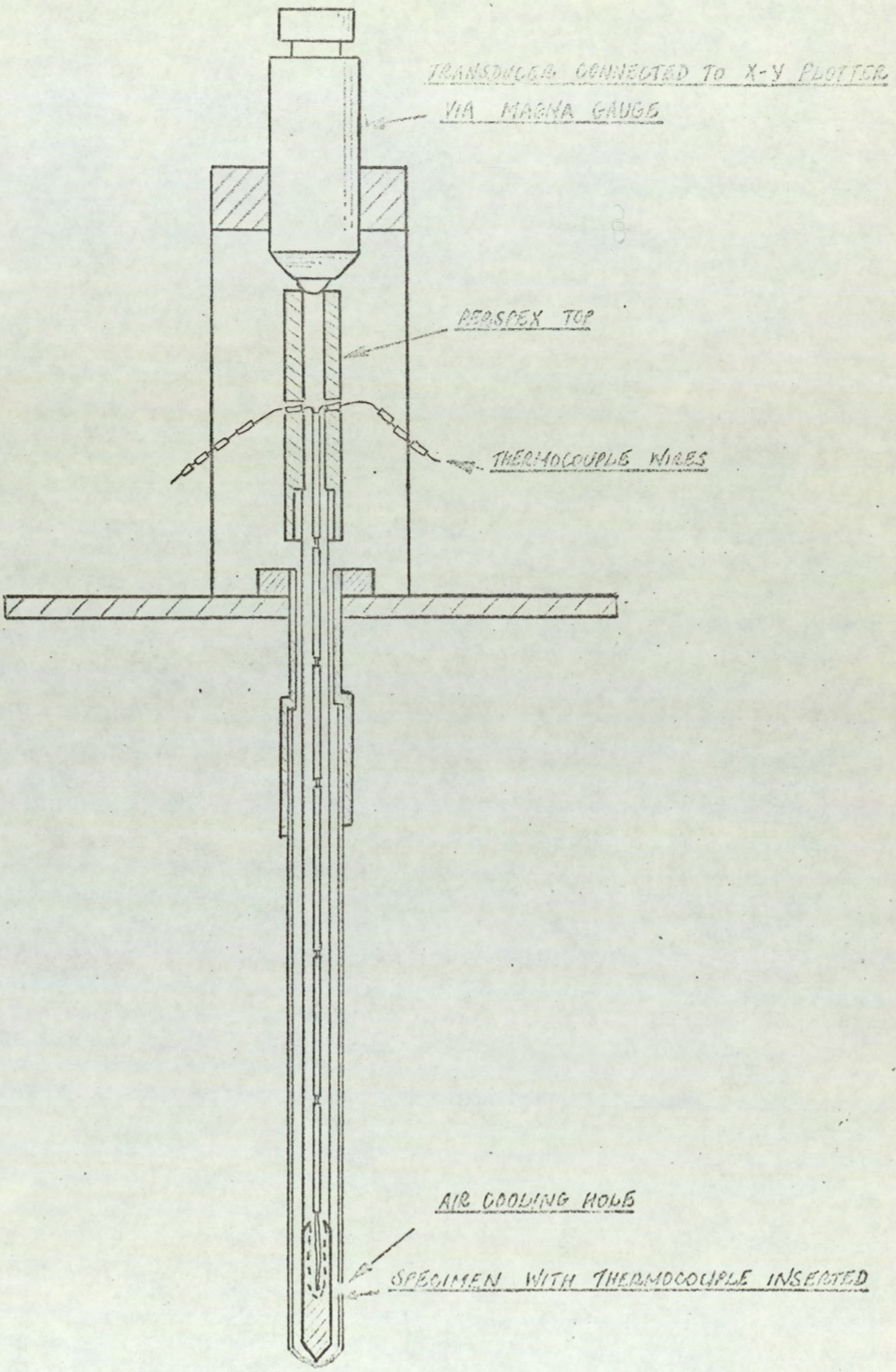

FIGURE 39

Dilatometer assembly for the determination of M_s

A_1 and A_3 temperatures, the samples were placed in a furnace at 600°C, allowed to stabilise for 30 minutes then heated at approximately 20°C/hour using a programmed controller. These results were checked using the more conventional form of dilatometry measurement when the transducer was replaced by a dial gauge and expansion-temperature curves plotted. Forall these tests, the specimens were coated with "Berkatekt", a proprietary lacquer, to reduce oxidation.

5.1.3 Results

The effect of cobalt on the A_1, A_3 and M_s temperatures is shown in Figure 40 (page 98) from which it can be seen that these critical points are raised quite linearly with increasing cobalt additions. The lines of best fit for the experimentally determined points were calculated by linear regression analysis. All the lines gave a close fit, the correlation coefficients being as follows:-

	M_s	A_1	A_3
Correlation coefficient, r	0.925	0.912	0.909

The A_1 and A_3 temperatures are raised by approximately 6.5°C per wt.% Co whilst the M_s increases at over twice this rate, 13.5°C per wt.% Co.

Figure 41 (page 99) illustrates the effect of cobalt on the volume changes associated with the martensite and α-γ transformations. Cobalt is seen to increase both transformation volume changes, the rate of expansion or

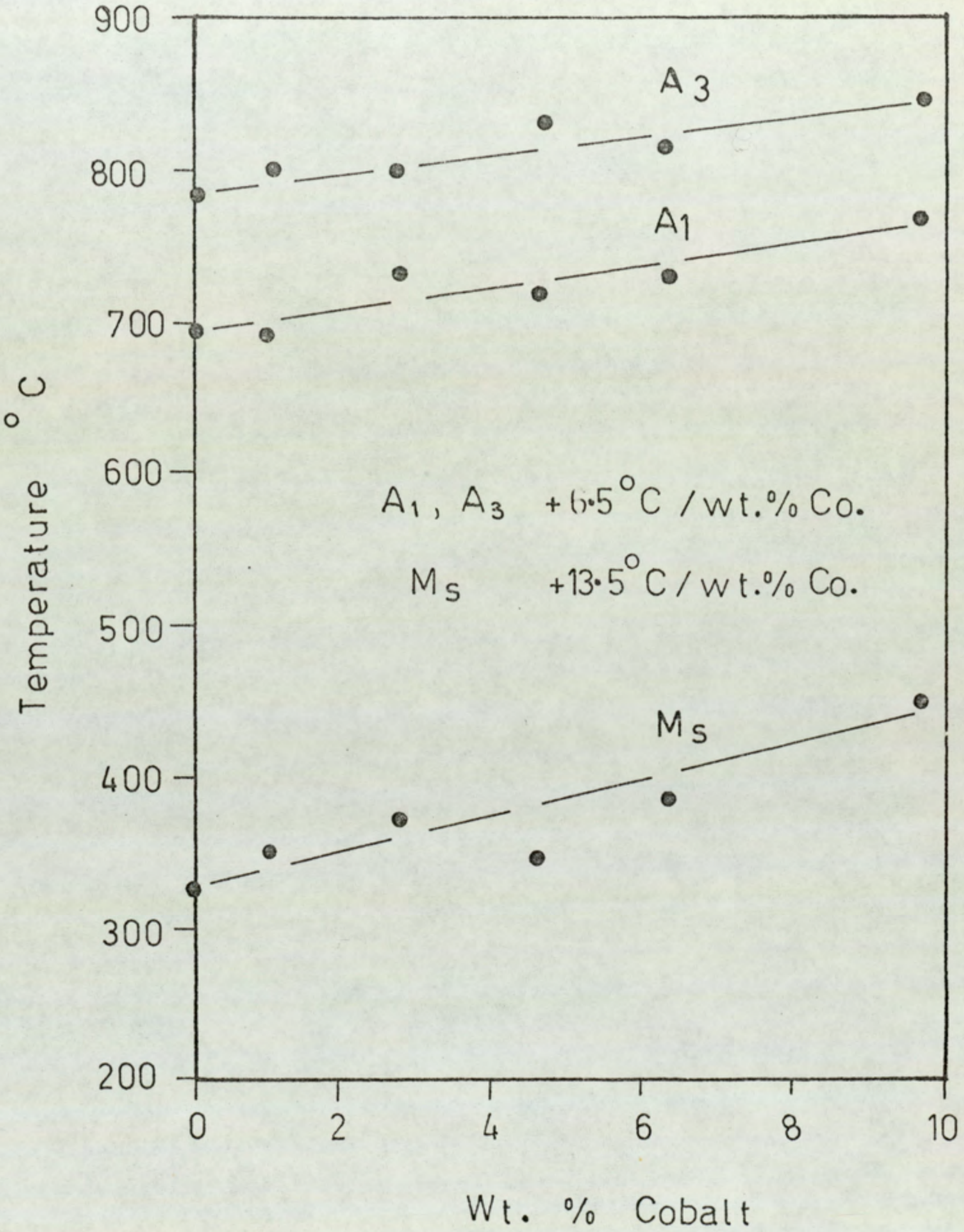

FIGURE 40

Effect of cobalt on the M_s A_1 and A_3 temperatures

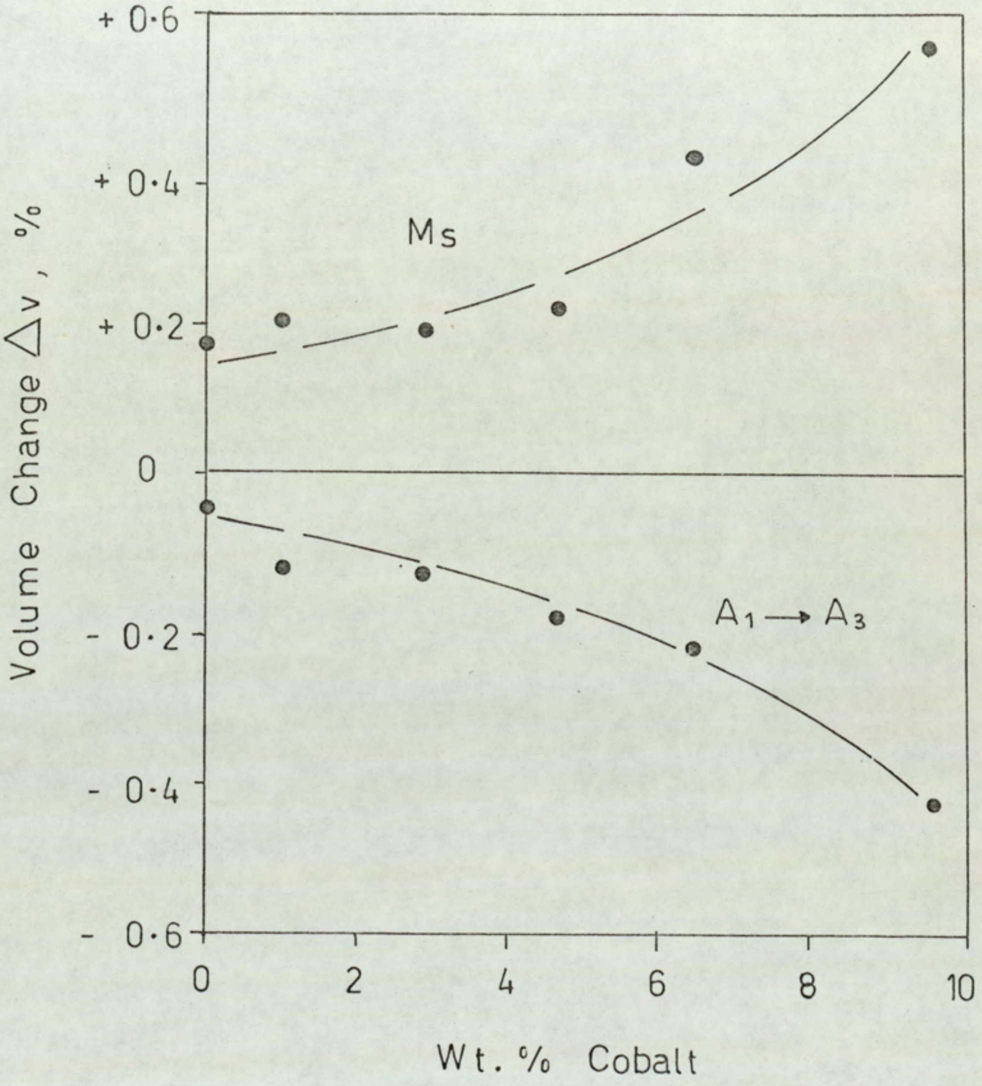

FIGURE 41

Effect of cobalt on the austenite and martensite transformation volumes contraction increasing sharply in the higher cobalt containing steels. From the autographic plots of temperature vs. displacement obtained for each test, the change in length of the specimen, Δ x, was determined and a factor of three was used to convert these readings into the reported volume changes, Δ v. This simple conversion assumed that the expansion or contraction was isotropic and that the value of Δ x was small enough to neglect all factors of Δx^2 and higher powers. Such a calculation may not be entirely justified though it is considered that the method is suitable for purposes of comparison.

5.2 Effect of Cobalt on Isothermal Transformation and Hardenability

The effect of cobalt on the isothermal decomposition of austenite and related hardenability problems has been the subject of numerous investigations over the past years. As early as 1927, both Allison(91) and Scherer (92) made brief reference to the effect of cobalt on the hardenability of carbon steels but it was left to Houdremont and Schrader(93) to make the first careful study of the problem. Their results, together with similar findings reported by Esser et. al.(94) and Davenport(95), laid the foundations for the now widely-held belief that cobalt is the only element to reduce the incubation time for the isothermal transformation of austenite and adversely affect hardenability. More recently, Hagel et.al.(96) and Kramer and Pound(97) have shown calorimetrically that the free energy change of the austenite - pearlite transformation was increased by cobalt additions. At 1000°K they found that the free energy change, ΔG, of the austenite- pearlite transformation was increased by 0.20 ± 0.02 cal.per.g. by the addition of 2% cobalt to a eutectoid steel.

Aaronson, Domain and Pound(98) have attempted to explain the effect of cobalt on the basis of a "no-partition temperature" which is a modified A_3 temperature below which no partition of the alloying elements occurs. Most elements lower this no- partition temperature and increase the hardenability whereas cobalt, silicon and aluminium raise the no - partition temperature above the A_3 and reduce the hardenability. This theory does not satisfy the effect of the carbide forming elements such as molybdenum, however, which should also reduce the hardenability on the basis of no - partition temperature.

A further explanation has been put forward by Chandhok et. al.(59) on the basis of their findings that cobalt increases the activity of carbon in steels. Considering the rate controlling mechanism to be carbon diffusion in austenite, if their were little partitioning of cobalt to austenite at the pearlite - austenite interface, cobalt would increase the activity coefficient and decrease the equilibrium carbon concentration in the austenite at the interface. The resultant increased carbon concentration gradient together with the slight enhancement of carbon diffusivity by cobalt would increase the local carbon diffusion flux and hence would increase the growth rate. Silicon is also known to increase the activity of carbon and increase the incubation period prior to the isothermal decomposition of austenite. This is explained by Chandhok on the basis that silicon, unlike cobalt, does partition to the austenite at the interface and hence decrease the local diffusion flux at the interface.

A rather curious anomaly is thus presented by these authors. Their results on the effect of cobalt on the pearlite reaction were interpreted on the basis that little partitioning of cobalt took place during the pearlite reaction yet they have interpreted subsequent results on the action of cobalt on tempering of steel(58) on the supposition that cobalt partitioned preferentially to the ferrite and exerted an interface control outlined in Section 3.2.

One possible explanation for this contradiction has been based on a consideration of the time available for partitioning between ferrite, austenite and carbide during pearlite formation at elevated temperatures since partitioning of cobalt will depend on the diffusion of cobalt atoms in the various phases present. During tempering, the ferrite-carbide structure is held at 400 to 650°C for several hours so that cobalt diffusion may be appreciable. On the other hand during the pearlite reaction particularly near the knee of the T.T.T. curve, the ferrite-carbide aggregate that forms from the austenite is at 400 to 650°C for only a short time so that cobalt diffusion will be significantly less. This explanation has several limitations however. Firstly, it deals mainly with the growth of pearlite rather than the actual incubation period.

If during austenite decomposition the carbide phase is the nucleant then to determine the effect of cobalt it is the austenite-carbide interface that is of predominant importance and thus the diffusion rate of cobalt in austenite must be considered and not that in ferrite. Secondly, it is assumed that the incubation period for transformation is a matter of minutes or even seconds and that tempering is for several hours. For the higher alloy steels the incubation period prior to the pearlite transformation may be several hours and so cobalt diffusion may be appreciable, especially in the austenite phase.

5.2.1 Isothermal Transformation

The incubation periods for the steels prior to the onset of the isothermal decomposition of austenite were determined dilatometrically using the inductive displacement transducer assembly previously described for use in the evaluation of critical points, Figure 39 (page 96). In these experiments however the voltage output from the Magnagauge was fed to a Kent recorder and the volume changes were automatically recorded on a continuous chart. Because the voltage output from the Magnagauge was small, extra resistors were incorporated into the Kent feed - in circuit to lower the voltage and increase the sensitivity. At the lower temperatures in the bainite transformation range, the incubation periods were too short for accurate determination by this method so the transducer was replaced by a dial gauge and the transformation times determined by conventional techniques.

The dilatometer tube containing the specimen (1 - in. long and 1/8 - in. diamter) was heated for 30 minutes at 1020°C, cooled to the required transformation temperature and quickly transferred to a constant temperature furnace. Temperature fluctuations of the furnace were reduced to a minimum using a specially designed controller. Time between the removal of the specimen from the austenitising furnace to the transformation furnace was as short as possible, generally less than 10 seconds.

To avoid overcomplication, only the results from the 0, 3 and 10% cobalt steels are shown in Figure 42 (page 105). Both bainitic and pearlitic incubation periods are seen to be reduced by the progressive additions of cobalt but the temperature of the pearlite "noses" of the curves remains unaltered. The curve for the basis steel agrees well with that determined by Corbett et. al.(7) for a steel of very similar composition. The pearlite nose for the steels occurs at 650°C where an incubation time of approximately 6.8 hours was recorded for the basis 3M steel. Cobalt reduces this incubation period in quite a regular and linear manner by approximately 13.5 min./wt.% Co until at a cobalt content of 10% the austenite begins to decompose after only 4.6 hours.

To study the effect of cobalt on the structures and transformation rates, a series of samples were isothermally transformed for periods up to 10 days. The specimens, 1/2 - in. long and 1/4 - in. square were austenitised for one hour at 1020°C and placed in furnaces controlled to within

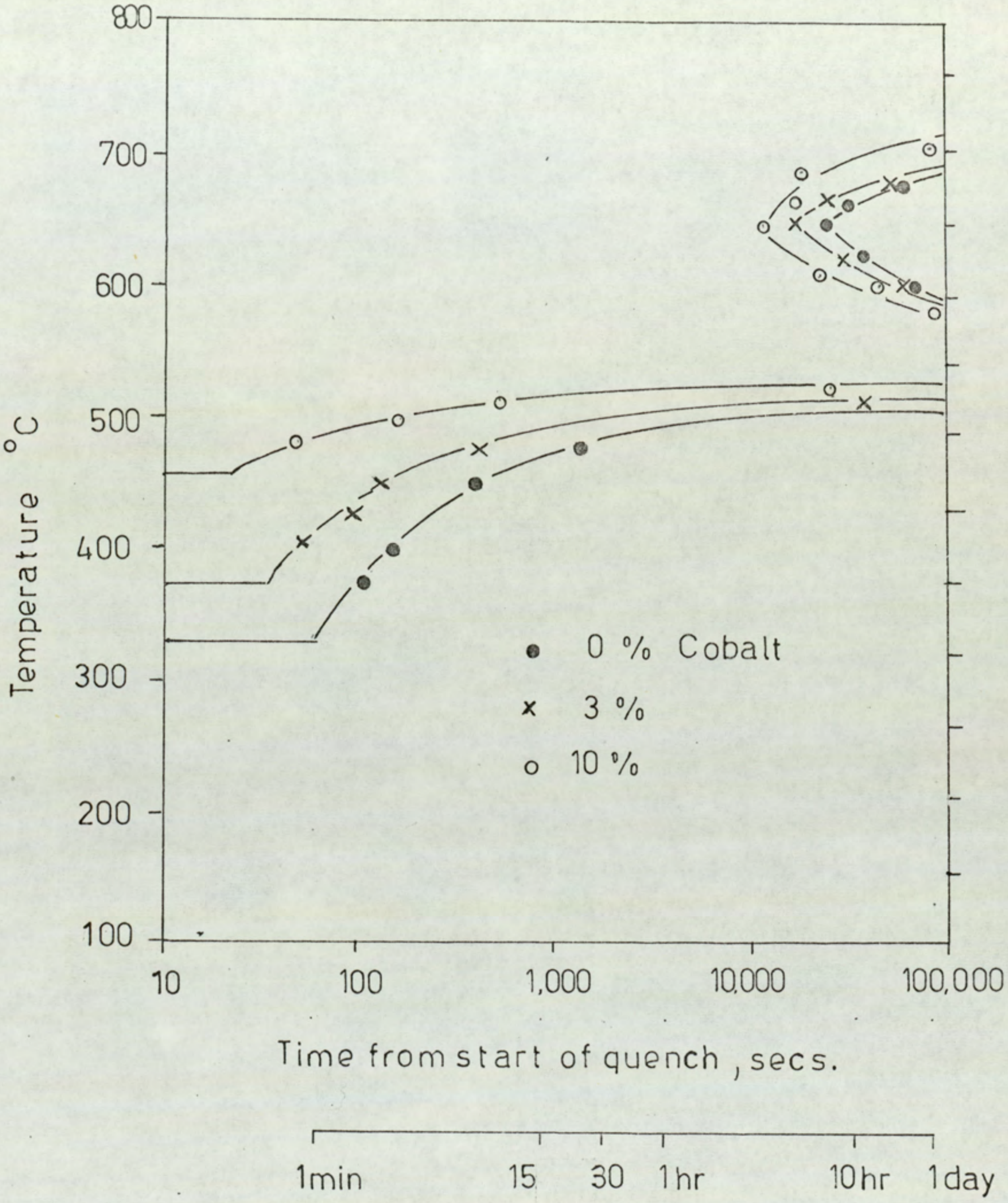

FIGURE 42

Incubation times for the isothermal decomposition of austenite for the 3M steel with additions of 3 and 10% cobalt

± 2°C of the required transformation temperature. At certain time intervals a sample of each steel at each temperature was taken from the furnace, water quenched and polished for metallographic examination. The general structures and hardness values are shown in Figure 43 (a) to (n) (pages 107 to 110) where again only the 0 and 10% cobalt steels are illustrated.

700°C All steels showed a partial transformation to pearlite, the rate of austenite decomposition increasing with the cobalt content of the steel. Even after 10 days no steel showed a complete transformation to pearlite being a maximum of approximately 70% in the 10% cobalt steel.

650°C This is the temperature of the pearlite nose for all the steels and the influence of cobalt on the transformation rate of austenite to pearlite is most clearly seen at this temperature. After 10 days the transformation is complete in the 10% cobalt steel but the percentage pearlite formed in this period falls with the cobalt content until in the basis steel only 50% pearlite is observed. Examination of Figure 43 (c) (page 107) illustrates the effect of austenite grain boundaries in nucleating the transformation with the subsequent growth of pearlite into the grains.

600°C The structures observed after transformation at 600°C are similar to those found after 650°C but as expected the pearlite is much finer and not resolvable. Again the higher cobalt steels showed a more complete transformation.

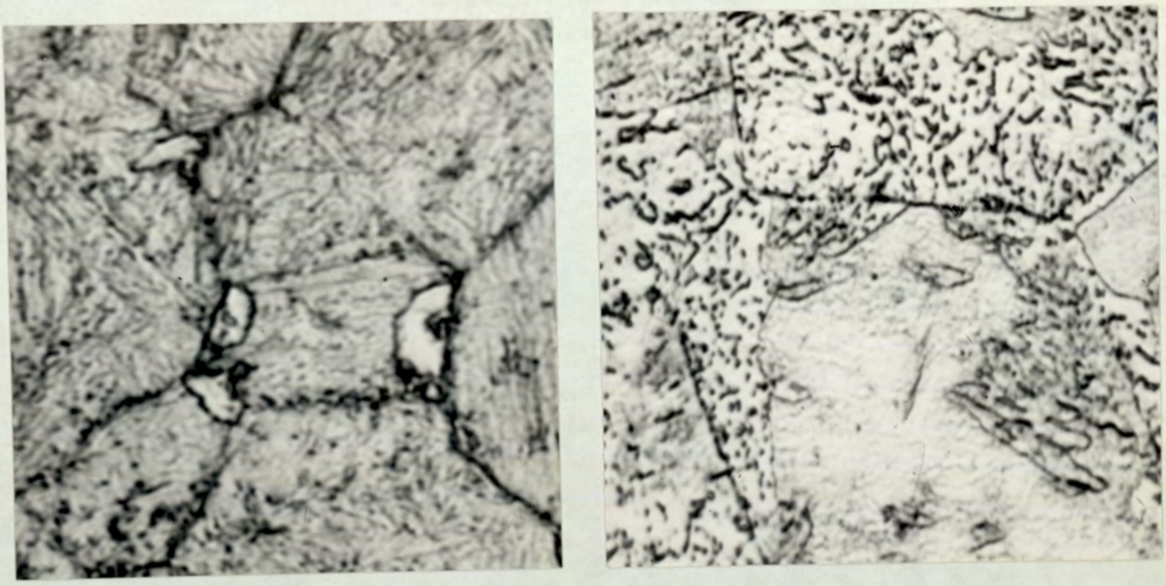

(a) 0% Co
327 VPN

(b) 10% Co
294 VPN

10 days at 700°C

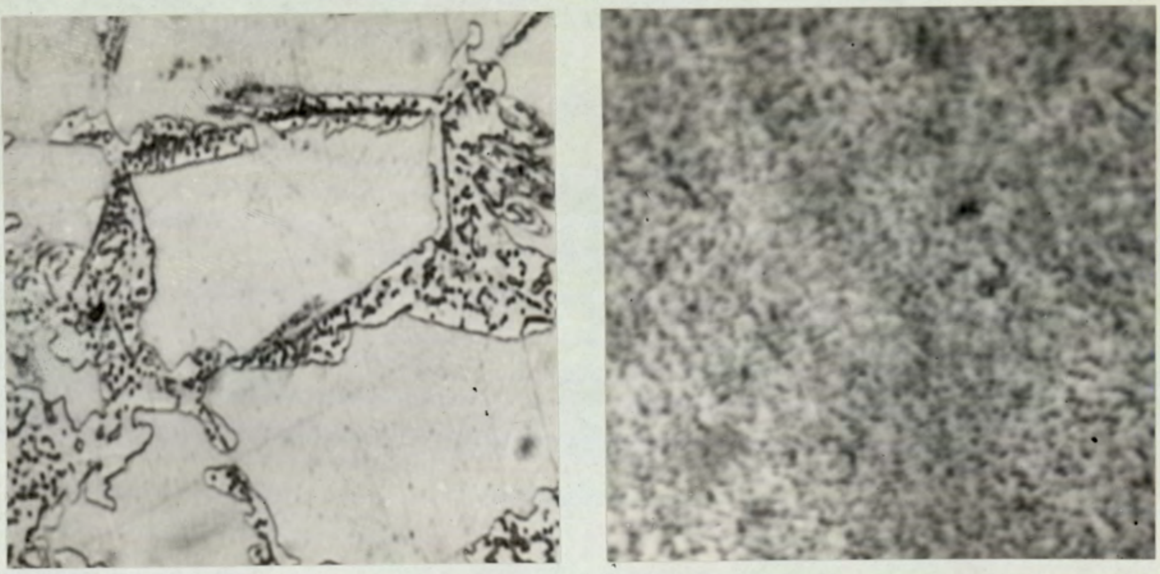

(c) 0% Co
306 VPN

(d) 10% Co
268 VPN

10 days at 650°C

FIGURE 43

Isothermally transformed structures at time and temperatures indicated
All samples etched 2% Nital x 1000

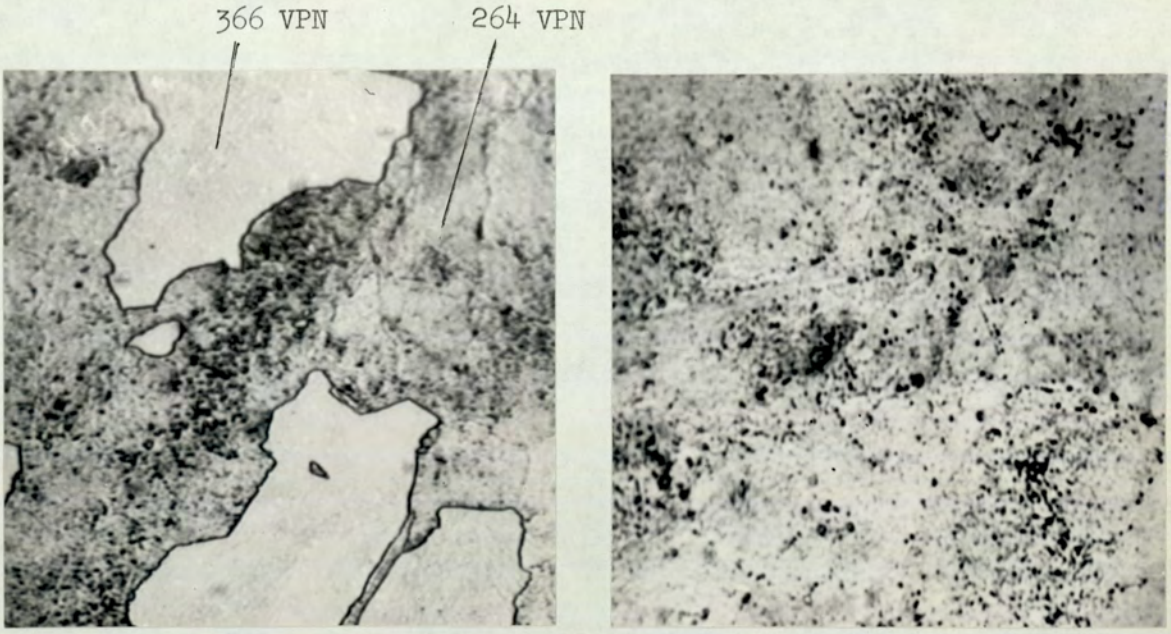

(e) 0% Co
303 VPN

(f) 10% Co
273 VPN

10 days at 600°C

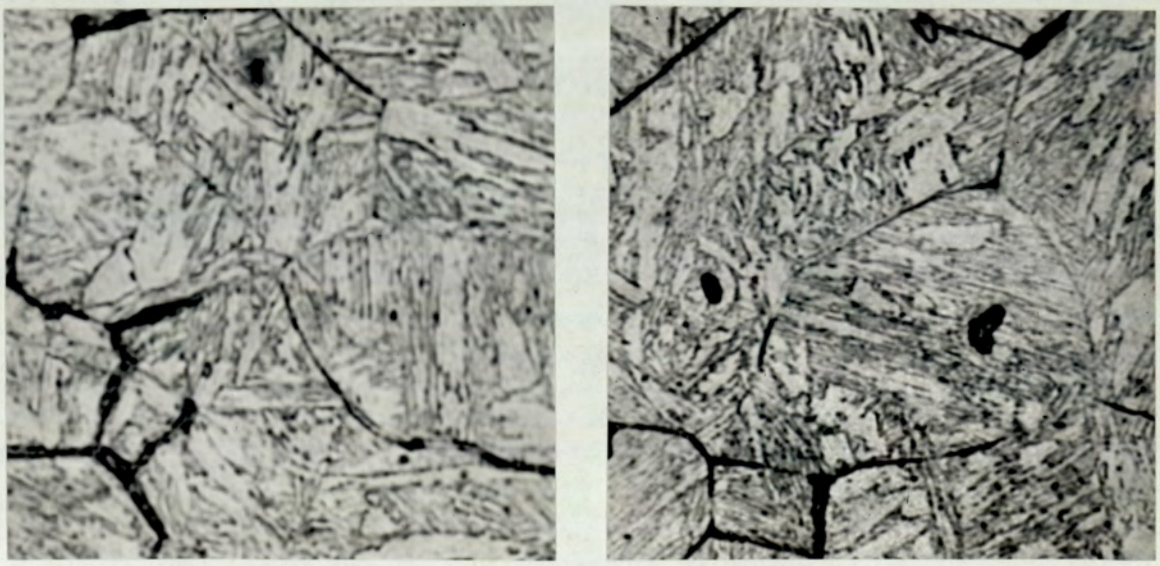

(g) 0% Co
348 VPN

(h) 10% Co
361 VPN

10 days at 550°C

FIGURE 43 (continued)

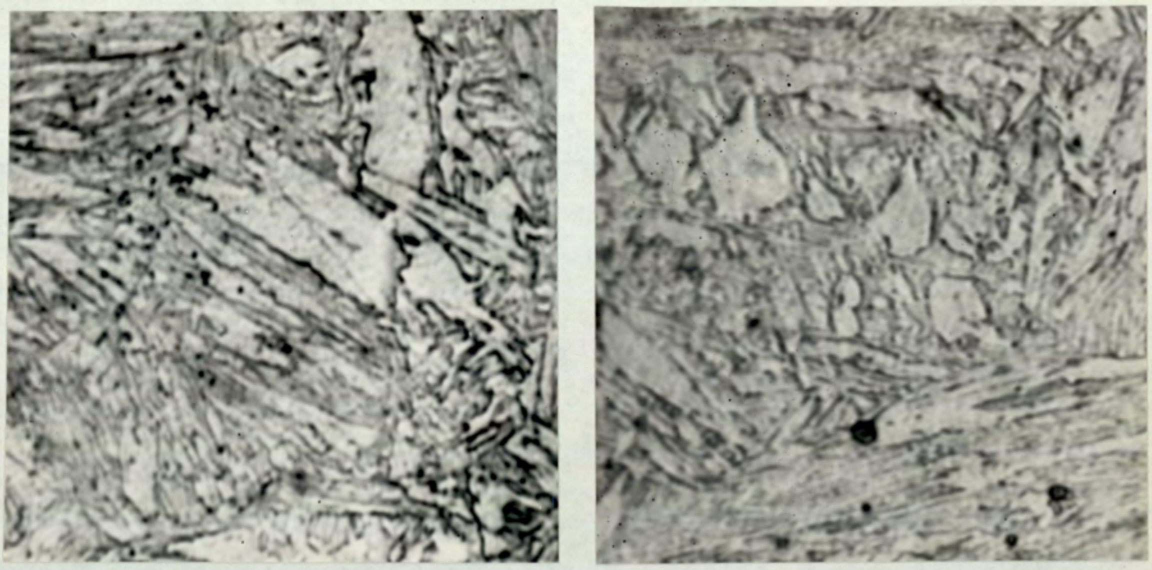

(i) 0% Co
314 VPN

(j) 10% Co
322 VPN

10 days at 500°C

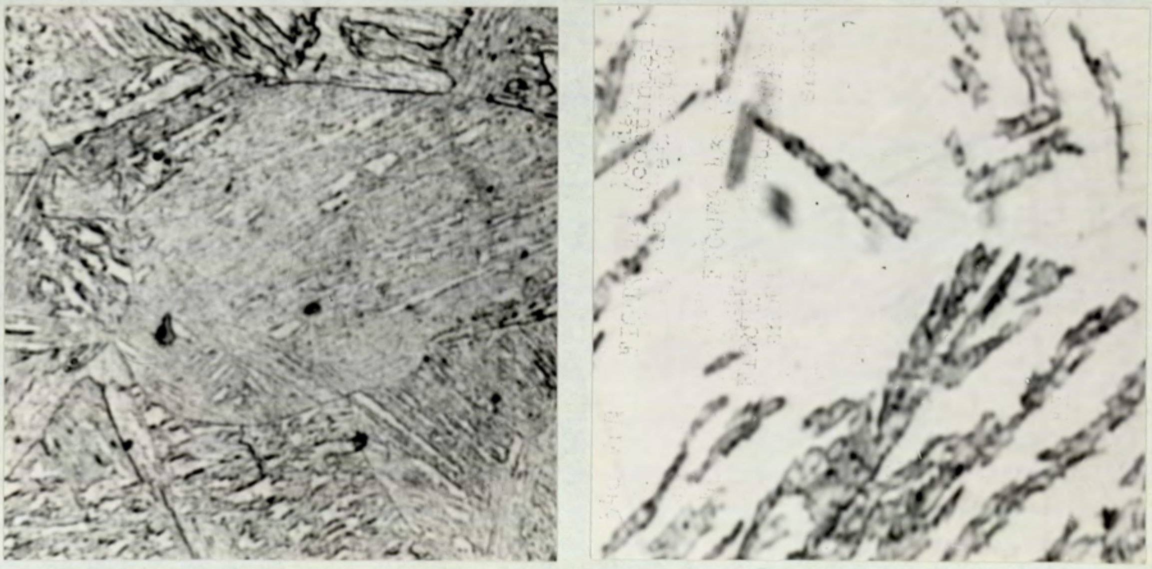

(k) 0% Co
328 VPN

(l) 10% Co
367 VPN

10 days at 450°C

FIGURE 43 (continued)

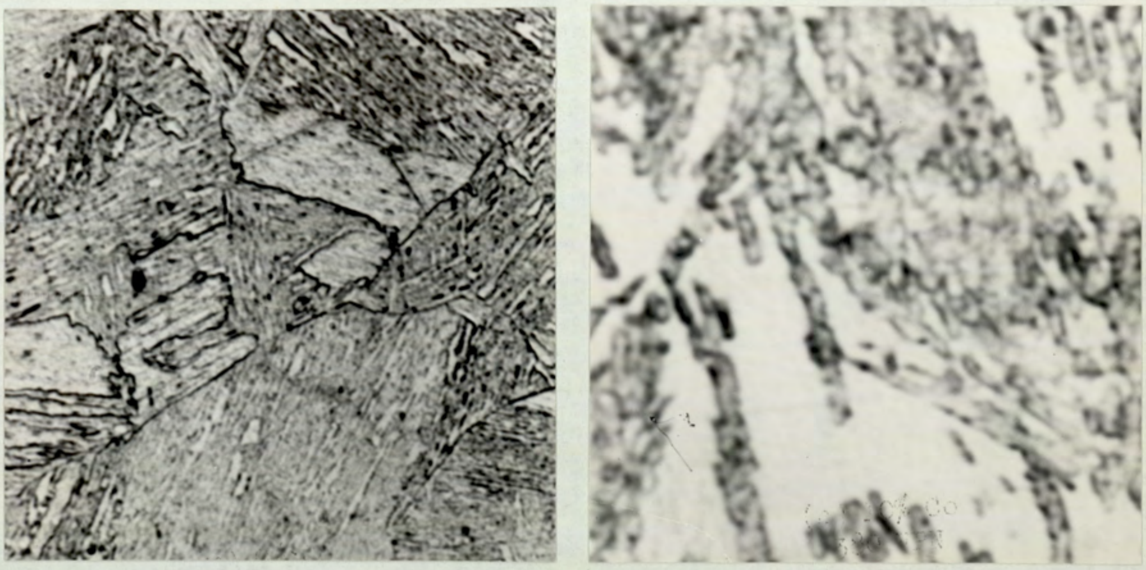

(m) 0% Co
333 VPN

(n) 10% Co
380 VPN

10 days at 400°C

FIGURE 43 (continued)

To identify the massive white constituent shown in Figure 43(e) (page 108), a microhardness scan was made on these samples and typical values obtained are inserted in Figure 42 (e). The white constituent was found to be some 100 VPN harder than the remainder of the structure and it seems that this is in fact martensite formed on quenching the untransformed austenite.

<u>550°C</u> This temperature is the mid - point of the metastable austenite bay previously determined on the T.T.T. diagrams. After 10 days all steels showed essentially a fully austenitic structure prior to quenching with slight signs of the nucleation of transformation visible at the austenite grain boundaries.

<u>500°C</u> All steels transformed at this temperature showed a mixed bainitic structure as would be expected from an examination of the T.T.T. diagrams.

<u>450° and 400°C</u> As previously determined, cobalt raises the M_s temperature of the basis 3M steel at a linear rate of 13.5°C /wt.% Co from 322 to 466°C for a 10% cobalt addition. In consequence, the structures obtained by isothermal transformation at 400 and 450°C showed a variety of structures from fully bainitic (Figure 43(k) and (m) on pages 109 and 110) to a partial martensite transformation (Figure 43 (l) and (n) pages 109 and 110) depending on the temperature of the transformation and the cobalt content of the steel. When transformed below their determined M_s temperatures, the steels were tempered immediately at 550°C

for 30 seconds before quenching to room temperature to distinguish between the martensite formed on isothermal holding and that formed on subsequent quenching.

5.2.2. Hardenability

With steels of high hardenability it is not possible to obtain meaningful results from the conventional Jominy test because the cooling rates along the bar are too rapid to reveal any hardenability differences. Many tests have been proposed to define hardenability in deep - hardening steels and an exhaustive survey has recently been compiled by Riley(99) but most of these tests require that large masses of metal be used for a single test. As a practical alternative the hardenability tests used in this investigation is a newly developed method devised by Etienne and Scheepens(100). This consists of cooling a rod shaped specimen $5^5/16$ - in. long and $1/4$-in. diameter in a refractory cone by means of a cooling ring as shown in Figure 44. (page 113).

In the apparatus used, the refractory cone was made by casting a slurry of graded chrome - magnesite refractory with a sodium silicate bonding into a waxed cardboard mould. The central hole was formed by a wax core which melted out on subsequent firing of the refractory cone and the hole dressed with a carbide tipped drill. The stainless steel sheath was made from a length of tube, closing the bottom by welding and welding a collar to the other end. The water cooled quenching cap was made of 70/30 brass fitted with two long copper tubes at the inlet and outlet.

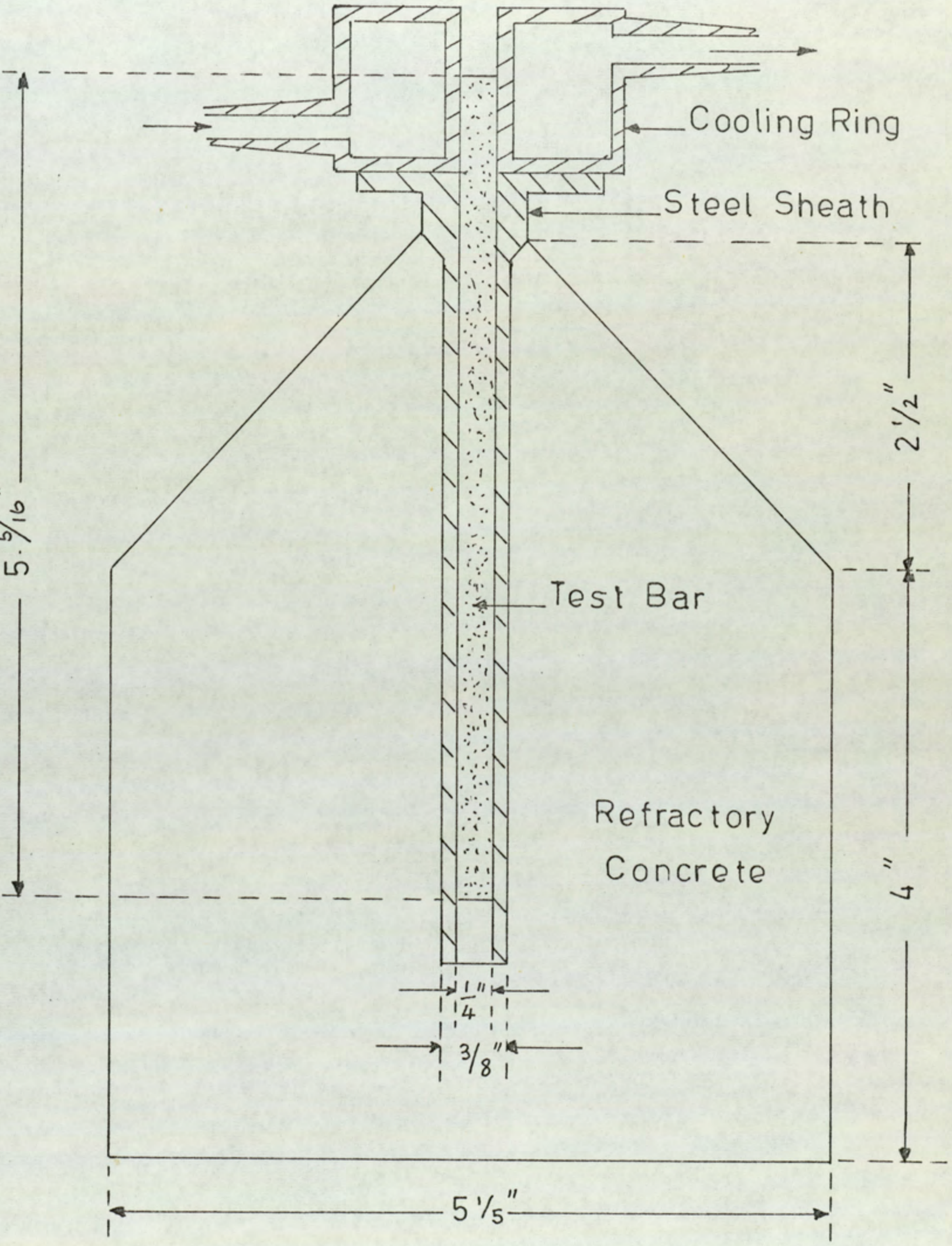

FIGURE 44

Refractory cone hardenability testing apparatus

To perform a test, the concrete cone was preheated in an electric furnace for three hours to a constant temperature of 1020°C. The specimen together with the stainless steel sheath was then inserted in the refractory cone and the whole assembly heated for a further 30 minutes to austenitise the sample. After removal from the furnace, the brass water cooled cap was quickly placed over the projecting end of the specimen and the whole block allowed to cool to room temperature which took about 4 hours. On removal from the refractory cone, two diametrically opposite flats were ground along the length of the specimen to a depth of 0.1 - in. and a Vickers hardness traverse made along the flats at 0.2-in. intervals. The results are shown in Figure 45 (page 115) each line representing the mean values from either side of the specimens.

Cobalt is seen to reduce hardenability by promoting the onset of the bainite transformation as illustrated in Figure 46 (page 116) which shows the structures obtained from the quenched and slow - cooled ends of the 0 and 10% cobalt specimens. The structures are not easy to analyse into separate components of martensite and bainite but as anticipated from the T.T.T. curves no transformation to pearlite was observed in any of the steels.

The method of measuring hardenability outlined above is a very recently devised test and to judge its applicability to commercial practice, it was thought necessary to determine the cooling processes taking place in the test piece. Holes were drilled through the concrete

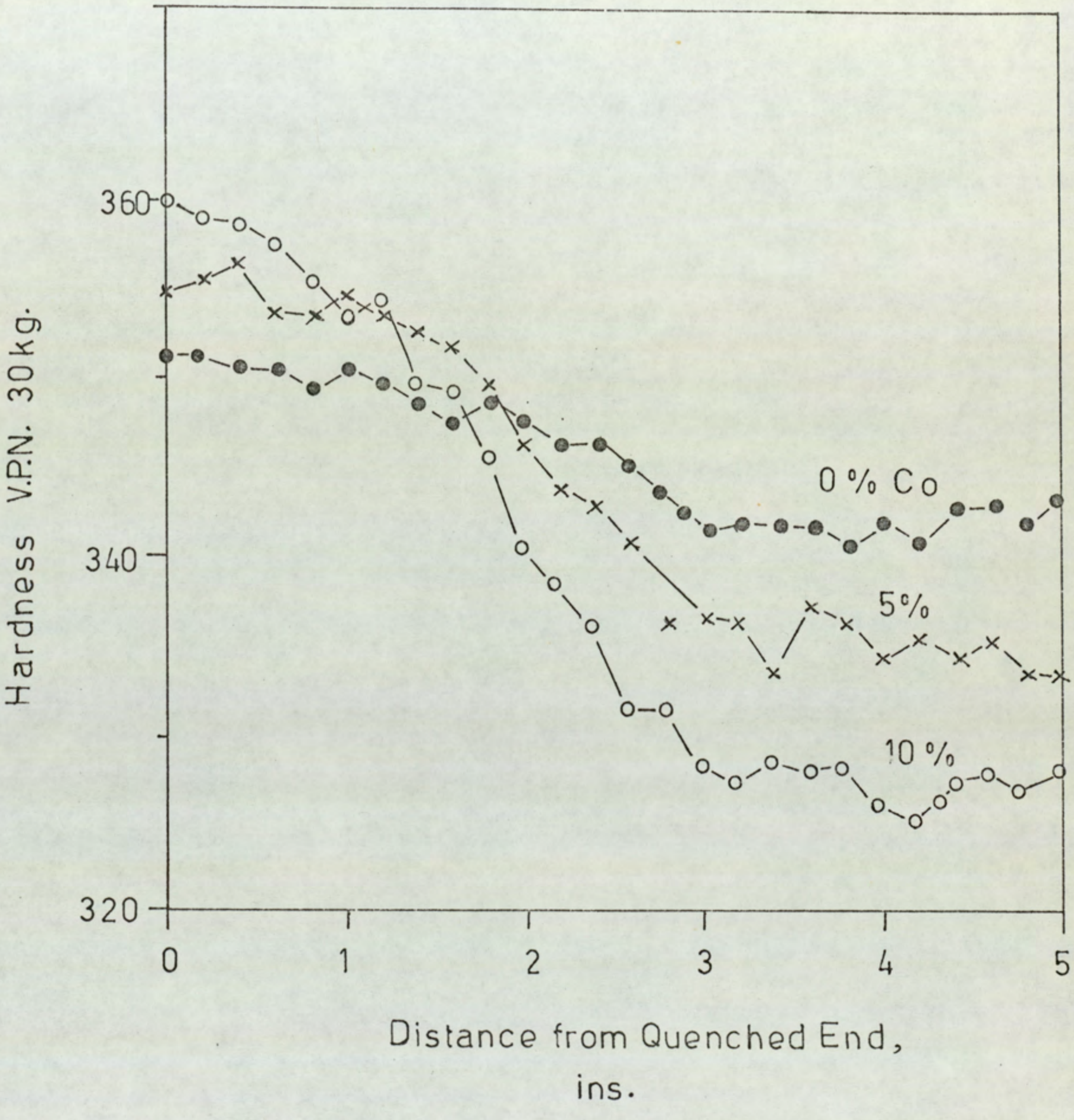

FIGURE 45

Effect of cobalt on hardenability

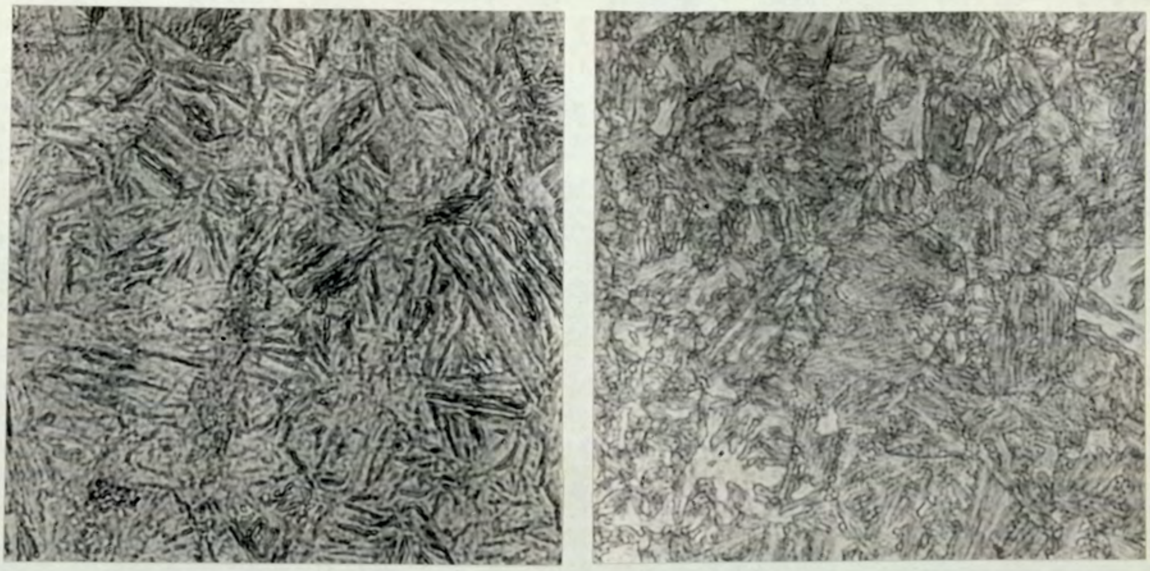

0% Co

10% Co

Water Cooled End

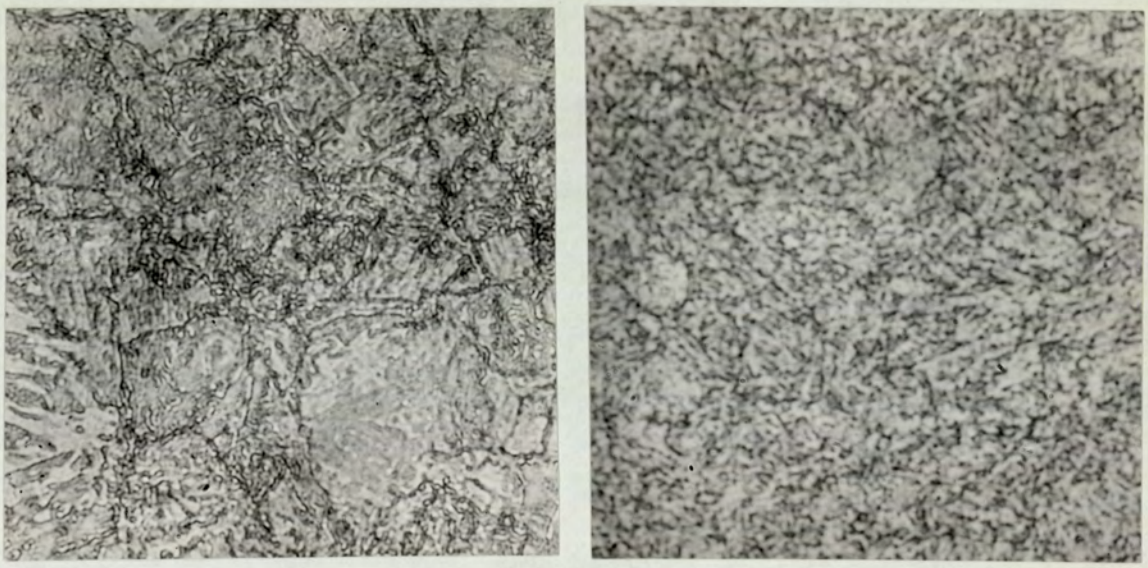

0% Co

10% Co

Slow Cooled End

FIGURE 46

Variation in structure along the length of the hardenability test bars of the 0 and 10% cobalt containing steels

Etched 2% Nital x 500

block and stainless steel sheath to accommodate fine chrome-alumel thermocouples which were seated in small holes drilled along the radius of the bar to its centre. At the end of the bar carrying the brass cooling ring, a hole was drilled in the axial direction to fix the thermocouple.

The refractory cone was heated for three hours at 850°C and a test performed in exactly the same manner as described previously. The cooling characteristics of the various positions along the bar were measured from the moment the cooling ring was fitted to the top of the bar. To follow the temperature changes easily and rapidly the thermocouples were attached to a 20 channel Solatron Digital Voltmeter initially scanning at a rate of 2 channels/sec. After the first hour the rate of scanning was reduced to 1 channel every 2 seconds and the cooling followed until the temperature at the centre of the cone had fallen to 200°C. From the print-out of the Digital Voltmeter the cooling curves illustrated in Figure 47 (page 118) were plotted neglecting recalescence effects originating from structural transformations. The pattern of curves determined in Figure 47 relate only to the cooling of this particular steel and will certainly be altered when other steels are tested and also when cooling starts from other temperatures. The influence of the hardening temperature can be reduced by introducing a cooling parameter which may be derived from a continuous cooling

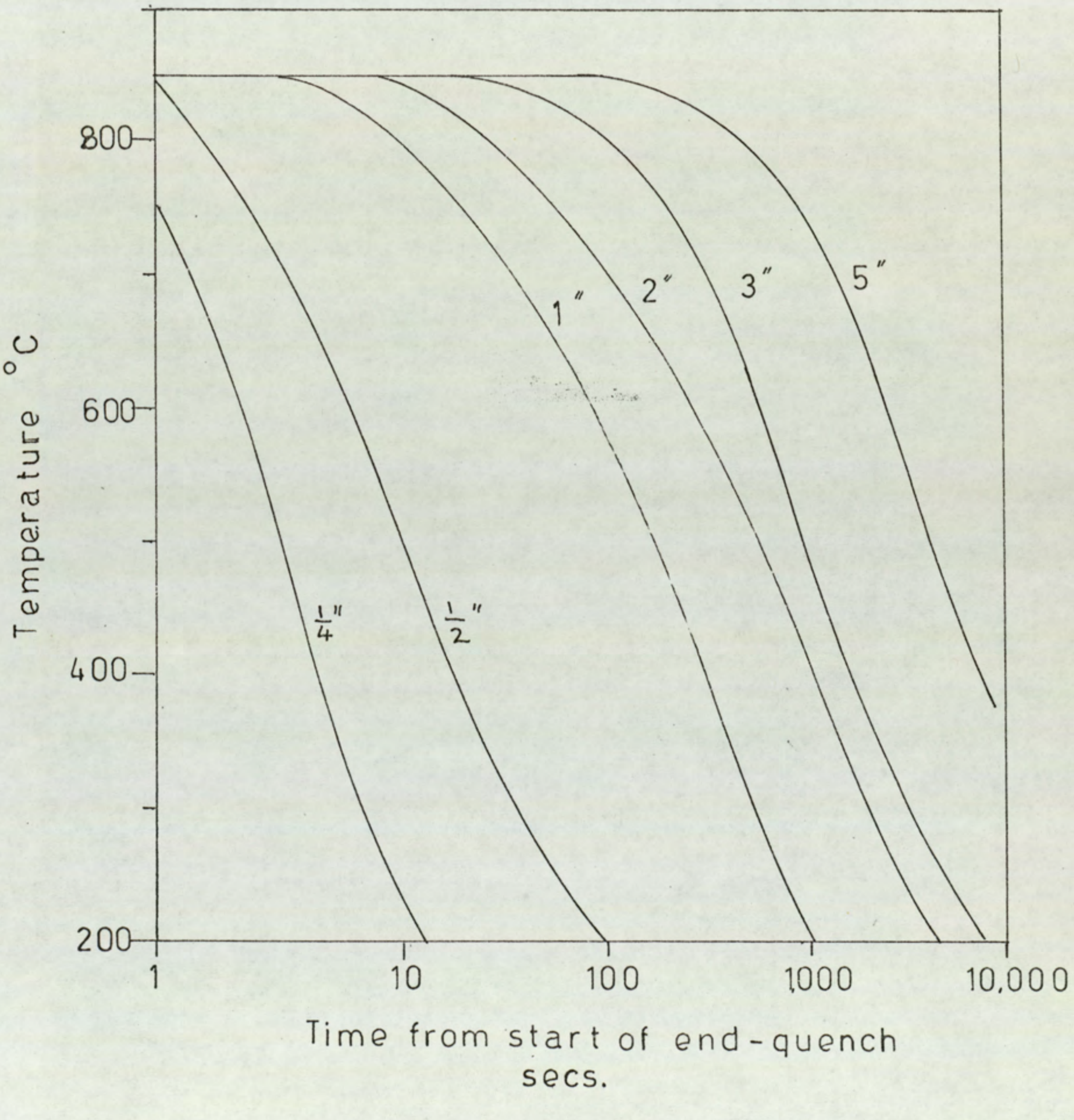

FIGURE 47

Cooling curves for indicated positions along the refractory cone hardenability test bar process by measuring the cooling speed at a given temperature, e.g. 700°C. This cooling parameter seems to be independant of the initial temperature of the test piece provided that the cooling curves follow Newton's law of cooling which states that the cooling speed is proportional to the difference in temperature between the steel surface and its surroundings. Although this assumption is only partially realised in cooling processes in practice, this method is frequently used in connection with the Jominy test and other hardenability tests.

From the heat flow analysis during the heating and cooling of steel formulated by Russell(101) it was possible to plot theoretical cooling curves for the centres of various diameter round bars and calculate the cooling rates at 700°C on air cooling and oil quenching. These results are shown in Figure 48 (a) (page 120). Analysis of the cooling curves in Figure 47 enabled the cooling rate at the same temperature to be computed for various positions along the axis of the refractory cone test bar and these are illustrated graphically in Figure 48 (b) (page 120). Also included in this diagram are the rates of cooling at 700°C for corresponding distances from the water cooled end of a Jominy test piece(102). It can be seen that the refractory cone hardenability test covers a far wider range of cooling rates than the Jominy test. The former test provides most of the cooling rates of the Jominy within the first 1.5-in. of the test bar whilst the remaining part of the test piece covers the slower cooling processes.

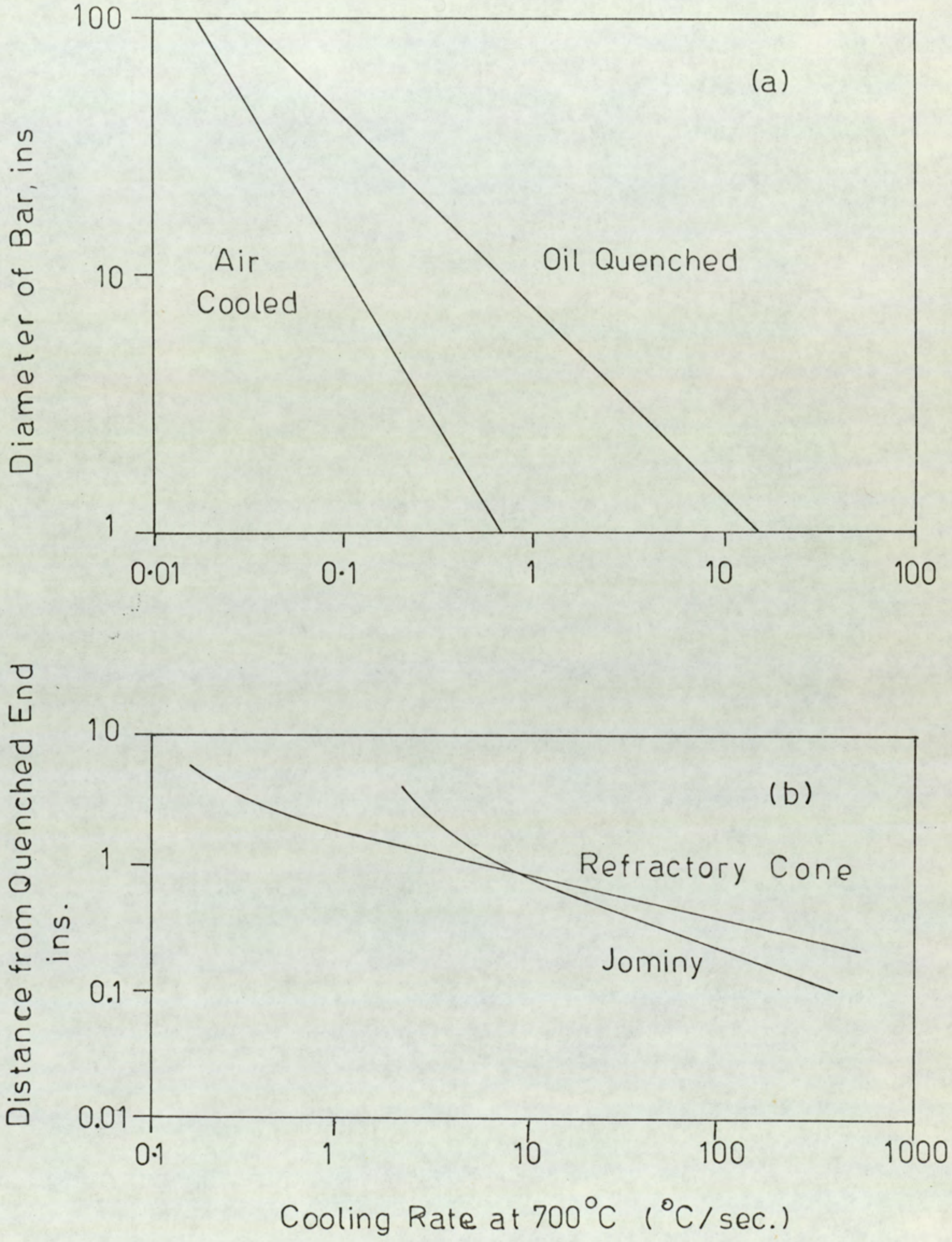

FIGURE 48

The computed theoretical cooling rates at the centres of various diameter bars (a) from data by Russell (101) and (b) the cooling rates at various positions along the axes of refractory cone and Jominy test bars

The relationship between the diameter of a quenched round bar and the distance from the water cooled end of the test bar can be found on the basis of identical cooling rates at a predetermined temperature, in this case, 700°C. From Figures 48(a) and (b) this relationship can be ascertained and summarised as in Figure 49 (page 122). Examination of Figure 49 reveals that the slowest cooling rate in the refractory cone hardenability test is equivalent to the cooling speed at the centre of an air cooled bar of approximately 6-ins. diameter or an oil quenched bar of almost 28-ins. diameter. The range of cooling rates for the Jominy bar is far narrower and reveals only particulars concerning oil quenched bars up to 3-ins. diameter and air cooled bars of less than 0.5-in. diameter.

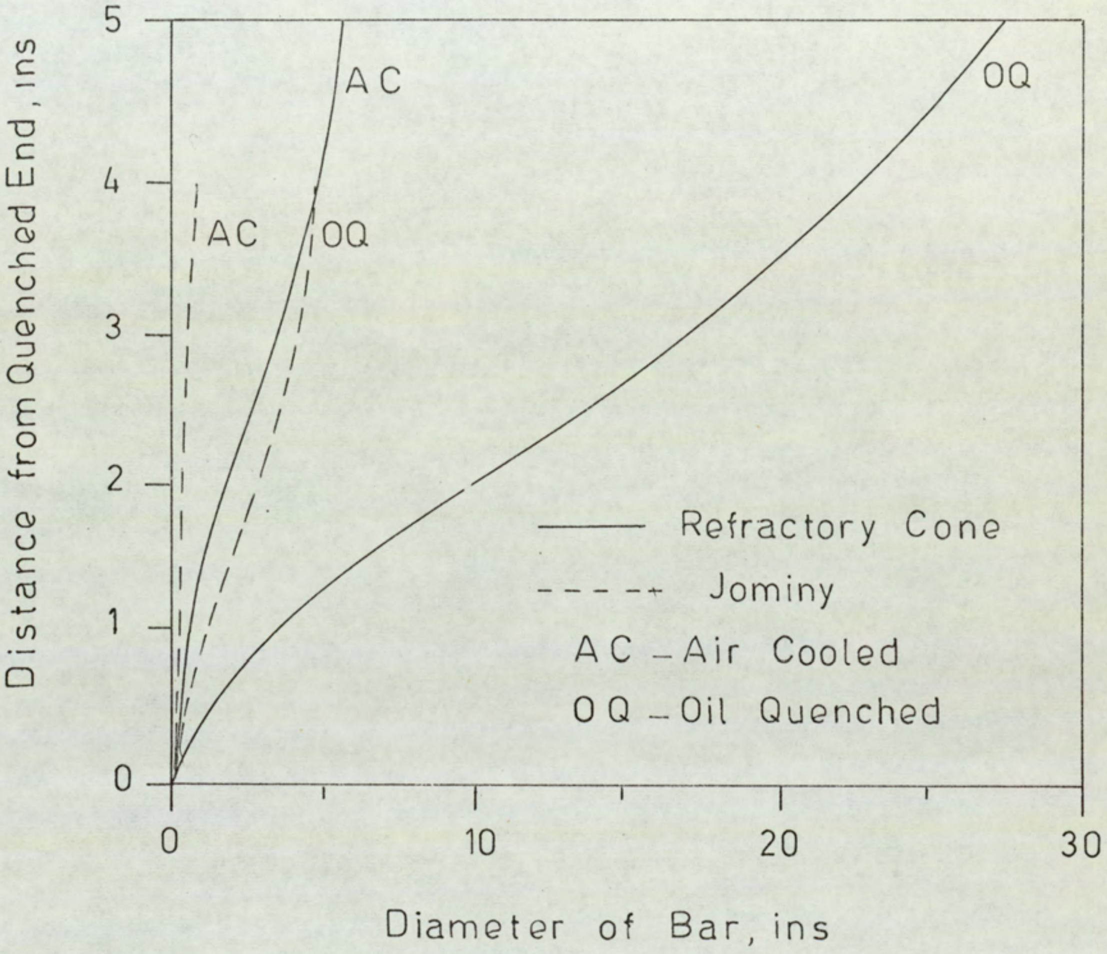

FIGURE 49

Relationship between the Jominy and refractory cone tests in simulating the cooling of various diameter bars on air cooling and oil-quenching

6. DIE WEAR PROPERTIES

6.1 Die Wear

As well as being one of the principal causes of die failure, er~~r~~osive wear is one of the more difficult material characteristics to study. For a wear test to be of significance, it must simulate the conditions of forging, in particular those of temperature, temperature gradient and impact loading. Early techniques involved the use of radioactive tracers but more recently a high degree of success has been achieved both at the University of Aston and the Drop Forging Research Association, Sheffield, using the material under test as small die inserts in experimental presses. The press used in this investigation is shown generally in Figure 50 (page 124) and is similar to that described by Lange and Meinert(103) and the one in use at D.F.R.A.(104). The structural and operational details of the press have been fully outlined elsewhere(105) and hence only a brief description will be included here.

The press was an old Sheffield cutlery press modified to run continuously, automatically feeding and upsetting $\frac{1}{2}$-in. diameter $\frac{3}{4}$-in. long En 3B slugs between the inserts. Each operation was controlled by a pair of cams which tripped microswitch contacts at the appropriate time and each pair of cams controlled a solenoid valve to switch compressed air to the relevent cylinder to activate the corresponding part of the feed mechanism. The component parts of the press are identified with reference to the schematic diagram, Figure 51 (page 125).

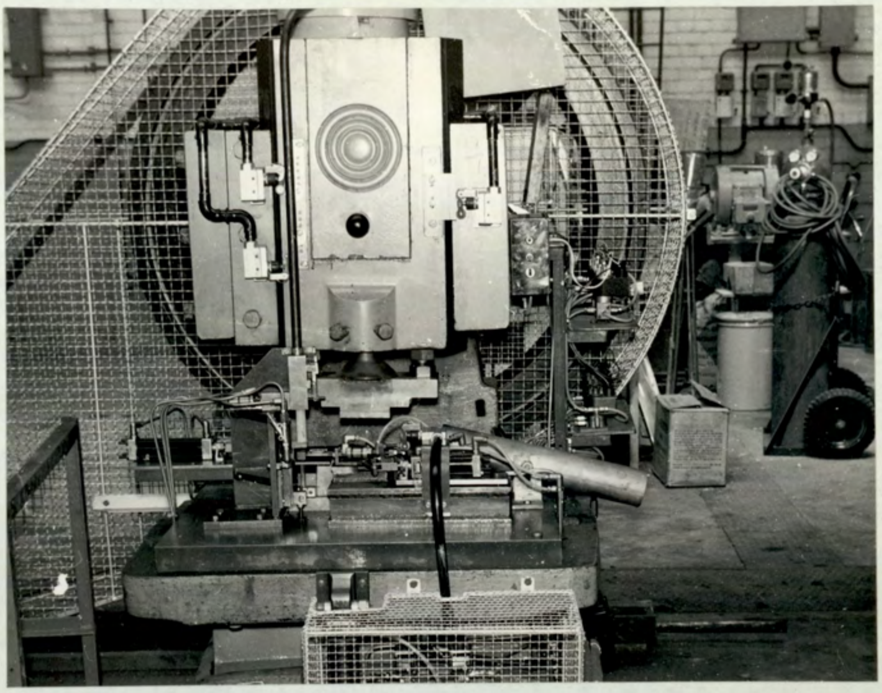

(a) General view

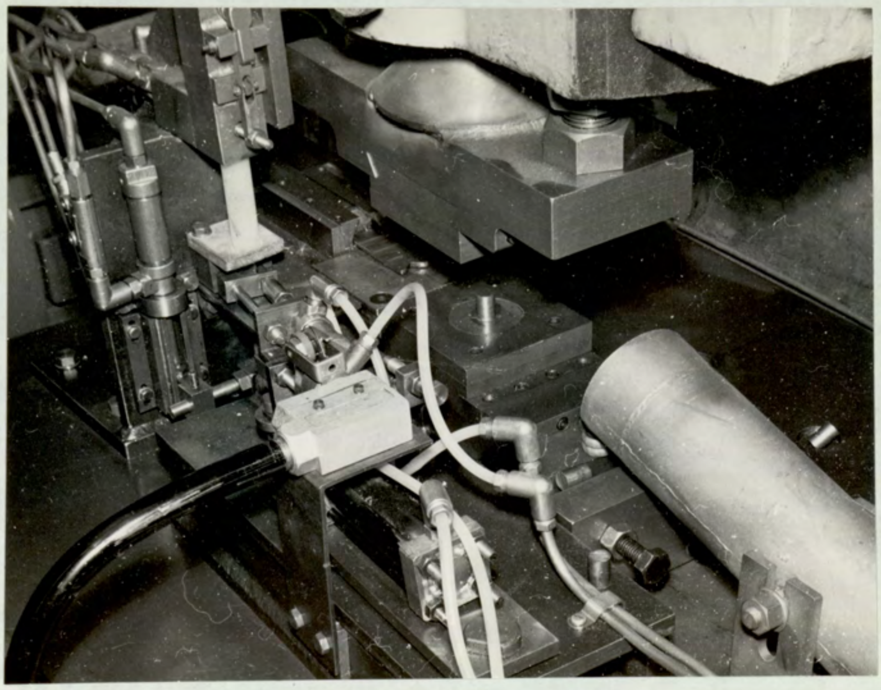

(b) The feeding mechanism

FIGURE 50

The Experimental Press

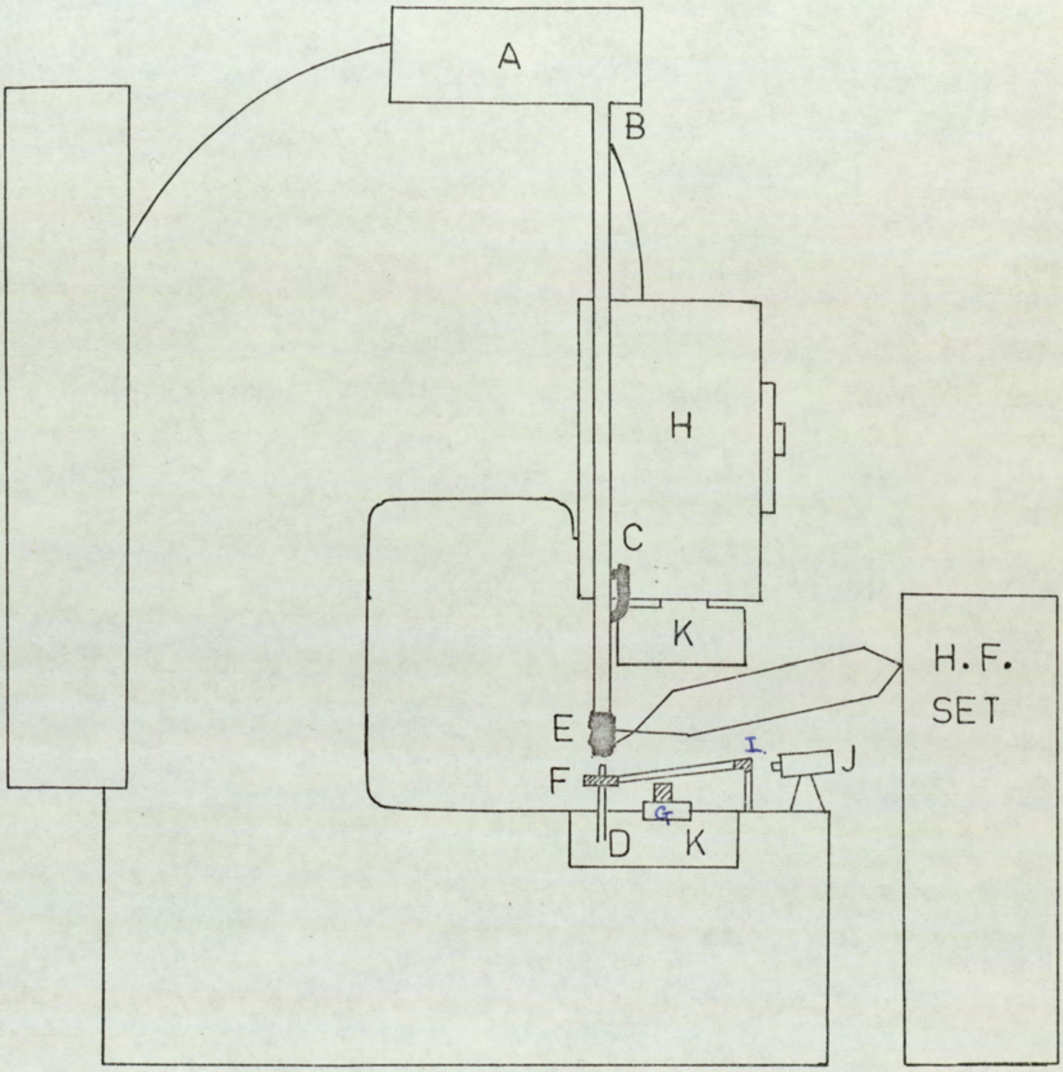

FIGURE 51

Schematic diagram of the experimental press

A rotary feeder (A) mounted on top of the press discharged in the form of slugs into the vertical feed pipe (B) where they fell into a pneumatically operated escapement mechanism (C). A ceramic peg (D) was raised to the silica tube surrounded by the high-frequency coil (E) and the escapement mechanism dropped one slug onto it. The H.F. set was left on throughout the cycle so heating began immediately. After the predetermined time, the ceramic peg was lowered to leave the hot slug between the jaws of a pair of feed tongs (F). These tongs pivoted through 90° to bring the slug to rest on the centre of the bottom die insert face (G). The finger of the tongs was withdrawn and they returned to their original position. As they came to rest, the finger returned to its gripping position and the tongs tripped a microswitch which operated a solenoid valve allowing high - pressure air to enter the clutch cylinder so engaging the clutch. The ram (H) therefore moved down and compressed the slug. In so doing it activated a microswitch on the side of the ram and opened an air inlet to the ejector (I) which moved forward until stopped by the presence of the ram. In this position air pressure built up behind the ejector so that, when the ram started to rise, it rapidly moved between the die faces and ejected the compressed slug into a bin. As the ram neared the top of its stroke, it activated two microswitches. One switched air to retract the ejector, the other switched air to the reverse side of the clutch cylinder, disengaging the clutch and allowing the ram to halt at top dead centre.

To increase the safety of the operation of the press, and to preclude the possibility of forging a cold slug, a photocell relay (J) was introduced which viewed the hot slug and if this was not present at the correct time (as determined by the cam timing device) cut off both the heating and the forging processes.

6.2 Testing Programme

From the forged stock were rough - machined two disc-shaped inserts 2-ins. diameter and ½-in. thick of each alloy. These blanks were austenitised for 1 hour at 1020°C and oil quenched. After finish - machining the dies were placed in the main die blocks and carefully levelled. The size of the stock relative to the mass of the die blocks is much smaller than that found in an industrial press and without auxiliary heating the bulk temperature would not rise above about 60°C. To simulate more realistic bulk temperatures therefore, Cressal cartridge type heaters were introduced into the main die blocks and the temperature attained by the inserts was recorded throughout the test. Periodic checks were made of slug temperature just before compression using an optical pyrometer and an "on-die" slug temperature of 1060 - 1080°C was maintained. Each test involved the forging of 750 slugs between the inserts, the compression being from 0.75 - in. to 0.25 - in.

After testing the inserts were removed and carefully descaled. The back faces and edges were coated with "Fortolac" stopping - off lacquer and made the cathode in a 5% H_2SO_4 solution at 76°C. A few drops of quinoline were added as inhibitor and a carbon rod made the anode to complete the cell. A current of 4.2 amps was passed for approximately ½-1 minute and the die removed and vigorously brushed with a small nylon brush. This operation was repeated until the dies were scale free when the "Fortolac" coating was removed with acetone and the dies examined for wear.

6.3 Evaluation of the Worn Inserts

A typically worn die insert is shown in Figure 52 (a) (page 129). In accordance with other evaluations of similarly worn inserts, profile traces were made across the die surface to determine the deviation from its initial flat state. Four traces were taken across each insert at 45°C to each other using a Taylor - Hobson Talylin I surface measuring machine connected to a chart recorder to give a graphical representation of the profile (Figure 52 (b) (page 129). This machine provided a choice of three horizontal magnifications, x 2, x5 and x 10 and six vertical magnifications, x 200, x 400, x 1000, x 2000, x 4000 and x 10,000 covering a range of depth to give full scale deflection on the trace from 0.01 - in. to 0.0002 - in. It was also possible to obtain simultaneously with the graphical trace the same output in digital form on punched tape, one point being recorded every 1/10 -sec.

The wear of the dies may be represented by the volume of metal removed. Since the volume is too small to be assessed accurately by direct methods such as the weighing of the insert before and after use, it was necessary

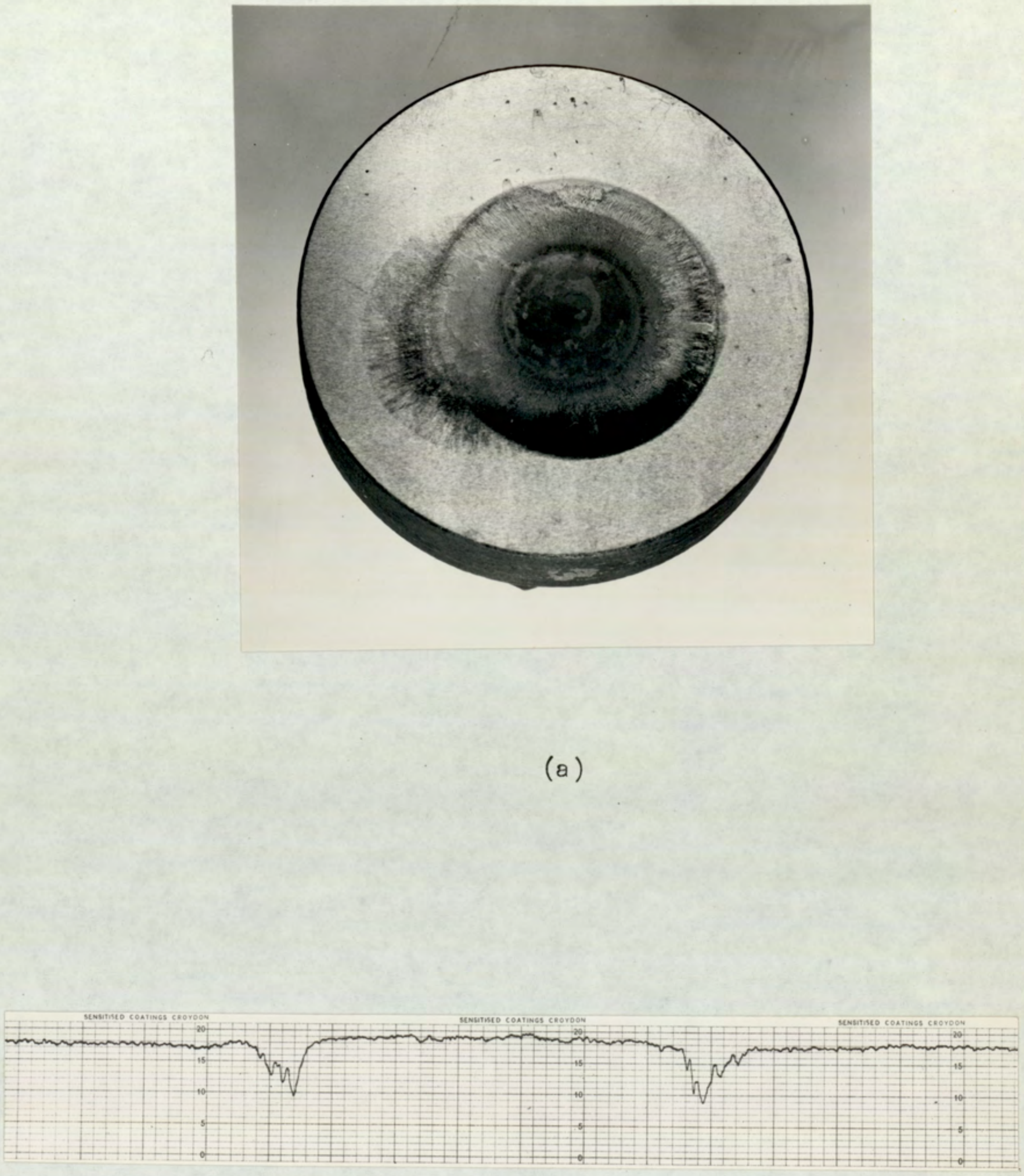

(a)

(b)

FIGURE 52

Typical worn die (a) and profile trace (b) across diameter it be calculated from the data provided by the contour trace. Advantage was taken of the digital output facilities of the Talylin I, the punched tapes being carefully edited and fed into an Elliott 303 computer together with a program established for the calculation of the wear volume.

6.4 Results

The results from the die wear tests are given in Table 8 (page 131) and represented diagrammatically in Figure 53 (page 132). A significant reduction in wear is observed on adding up to 3% cobalt, the wear volume being reduced by almost 50%. Further cobalt additions promote only a slight improvement in wear, the average reduction in wear volume being only some 0.25 cu. in. x 10^{-5} per wt.% Co over the range of cobalt additions 3-10%. A very similar trend has been recently reported by Bhattacharyya(106) in his work on No.5 die steel using the same equipment as used in this investigation.

Examination of the worn inserts showed that the 3% cobalt containing steel formed the boundary composition between two significant changes in die behaviour. Firstly, the shape of the wear profile changed from a dish - shaped impression for the lower cobalt steels to an annular wear pattern for the higher cobalt steels. This behaviour is exemplified in Figure 54 (page 133) where full scale deflection on the graphs represents 0.0005-in. Secondly, the 3% cobalt showed a network of fine cracks as shown in Figure 55 (page 134). This type of cracking was not observed in either the higher or lower cobalt-containing steels.

TABLE 8

DIE WEAR RESULTS FOR 3M ALLOY SERIES

Die Set		Nominal %Co	Hardness VPN	Wear Volume in³ x 10⁻⁵				AV. Wear Volume in³ x 10⁻⁵	Mean Wear Volume in² x 10⁻⁵
				1	2	3	4		
3M/0	Top	0	349	11.382	15.233	15.076	14.652	14.086	
	Bottom		352	13.427	13.609	15.323	14.013	13.702	13.894
3M/1	Top	1	354	10.545	13.417	6.620	9.291	10.870	
	Bottom		351	7.377	11.666	14.375	6.471	10.876	10.873
3M/3	Top	3	353	6.684	7.381	7.094	6.532	6.678	
	Bottom		355	9.950	10.015	9.041	8.413	9.348	8.013
3M/5	Top	5	358	8.683	7.673	3.455	-	6.604	
	Bottom		358	7.506	7.469	8.039	9.025	8.010	7.407
3M/7	Top	7	360	6.418	6.743	5.122	5.161	5.802	
	Bottom		361	8.213	7.636	5.966	6.250	7.016	6.409
3M/10	Top	10	365	4.304	5.493	6.353	4.376	5.131	
	Bottom		364	9.638	7.529	7.146	9.334	8.412	6.771

All dies tested in the as-quenched condition

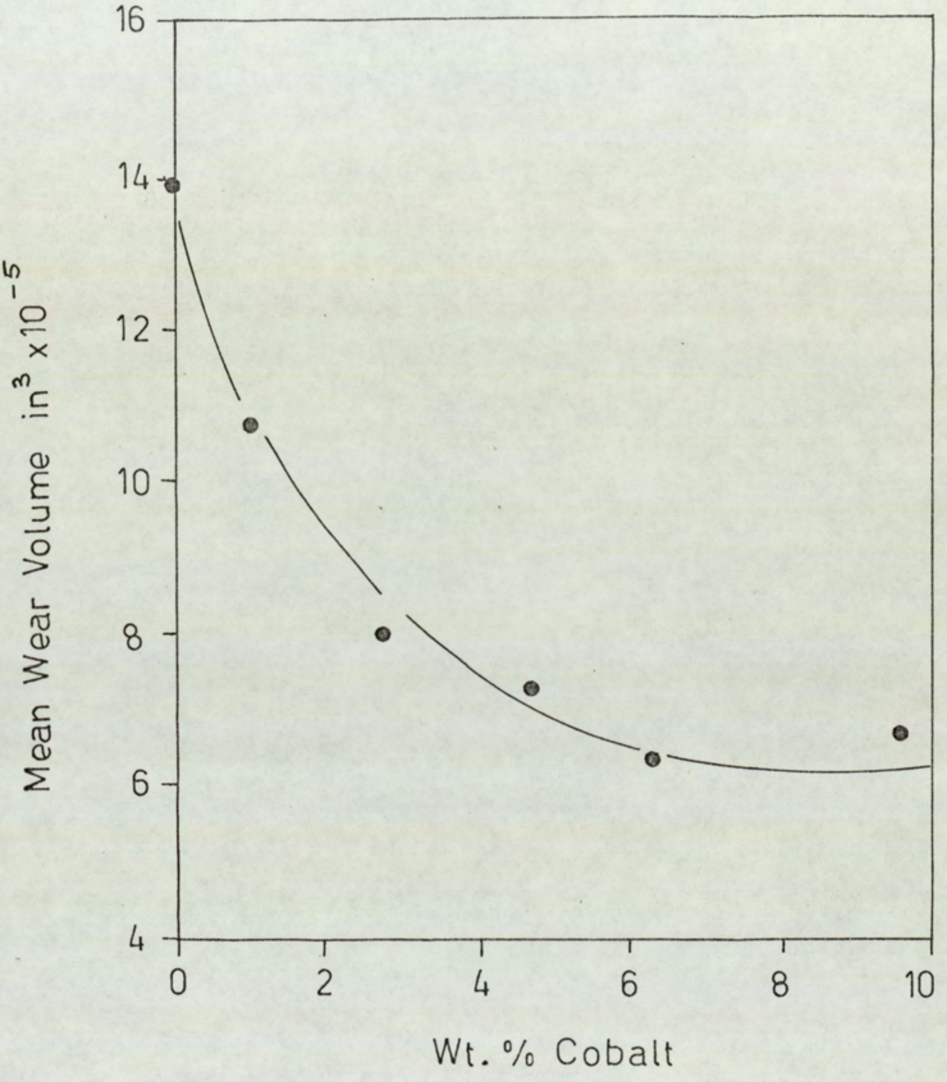

FIGURE 53

Influence of cobalt on die wear of the 3M steels

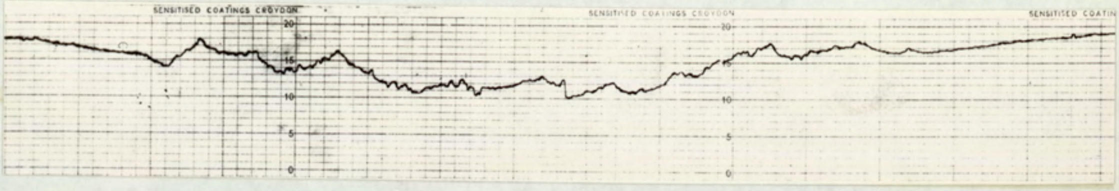

1% Co

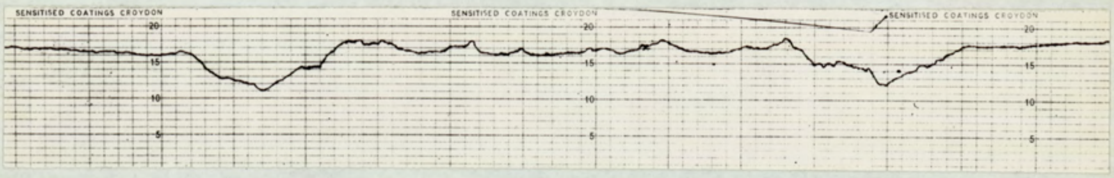

3% Co

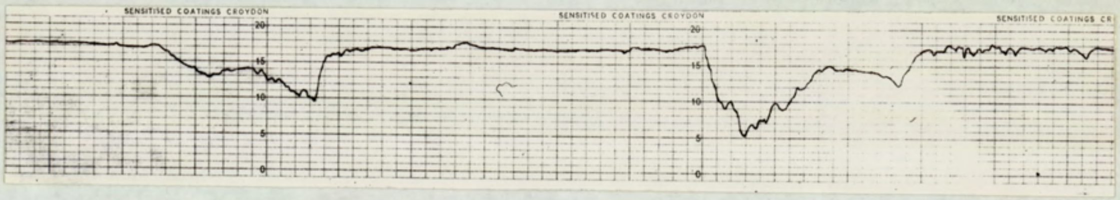

5% Co

FIGURE 54

Profile traces across worn die inserts of 1,3 and 5% cobalt steels showing transition from a dish - shaped to an annular wear pattern.

1% Co

3% Co

5% Co

FIGURE 55

Surface appearance of worn die inserts
showing cracking in the 3% cobalt steel

7. ALLOY DEVELOPMENT

In many investigations of this kind where a practical final product is required, the ultimate aim may be lost in the volume of results. The overriding factor in the development of these die steels is one of basic economics - the unit cost per forging produced. As far as possible this maxim was maintained during the development of new compositions, all alloying additions being considered on a cost basis rather than a theoretical concept.

At the time of this work (March 1969) the price of commercially pure (99.9%) cobalt was in the region of 16/9d per pound which meant that, as a general rule of thumb, a 2% cobalt addition was equivalent to a 1% molybdenum addition. It was decided, therefore, to cast a further two series of alloys in which the molybdenum content was reduced to 2% and 1% respectively. In each series three alloys were cast:-

i) a basic steel with the molybdenum reduced to the required level - no cobalt additions.

ii) an economically balanced steel where the molybdenum content was replaced by its cost equivalent of cobalt.

iii) a 10% cobalt containing steel as a comparison.

It may be recalled that, during the survey on the role of cobalt in tempering reactions (Section 3.2), reference was made to the work of Banerjee et.al.(64) who reported that cobalt increased the dislocation density in the steel and hence gave a much finer precipitate. It would appear that a logical extension of these results would be the utilisation of cobalt containing steels in the process of ausforming where the steel is mechanically worked in the metastable austenite region. This process yields a vastly improved steel basically it is thought because of the more highly faulted material resulting from the deformed austenite. For this reason a further three alloys were cast of 3M steel containing 0, 5 and 10% cobalt, and subsequently ausformed.

The compositions of these three series of alloys are given in Table 9 (page 137). All were melted and cast in the same way as described previously in Section 2, 3M steel scrap again forming the base charge of the 3M/AUS alloys. The 1M and 2M alloys were prepared from balanced charges of En 33 and En 24 steels, and forged in a similar manner to that outlined for the 3M alloys. The 3M/AUS alloys were ausformed by heating them to 1150°C, transferring to a furnace at 550°C and then reducing the ingots approximately 60% in a single squeeze operation on a 1200 ton press.

In general, the as-cast and forged structures of the 1M and 2M steels were similar to those observed and reported for the 3M series of alloys. The structures of the ausformed steels are shown in Figure 56 (page 138) which highlights the effect of cobalt already described on the isothermal transformation characteristics of the steel. All steels show a general precipitation of strain induced carbides but air cooling from the ausforming temperature has produced variations in the structure of the matrix from fully martensitic in the 0% cobalt

TABLE 9

CHEMICAL ANALYSIS OF 1M, 2M AND 3M/AUSF.ALLOY SERIES

Cast No.	Nominal Co	C	Ni	Mo	Cr	Mn	Si	Co
1M/0	0	0.24	3.28	0.97	0.51	0.66	0.27	<0.2
1M/4	4	0.25	3.41	0.98	0.58	0.68	0.22	4.06
1M/10	10	0.27	3.42	1.01	0.53	0.64	0.21	10.15
2M/0	0	0.26	3.33	2.07	0.60	0.67	0.20	<0.2
2M/2	2	0.28	3.34	2.08	0.57	0.70	0.23	2.11
2M/10	10	0.25	3.42	1.95	0.58	0.64	0.19	10.06
3M/0/AUSF	0	0.24	3.21	3.31	0.53	0.70	0.24	<0.2
3M/5/AUSF	5	0.26	3.09	3.29	0.54	0.60	0.21	4.53
3M/10/AUSF	10	0.26	3.16	3.36	0.53	0.66	0.29	10.03

All alloys contained less than 0.02% sulphur and phosphorus.

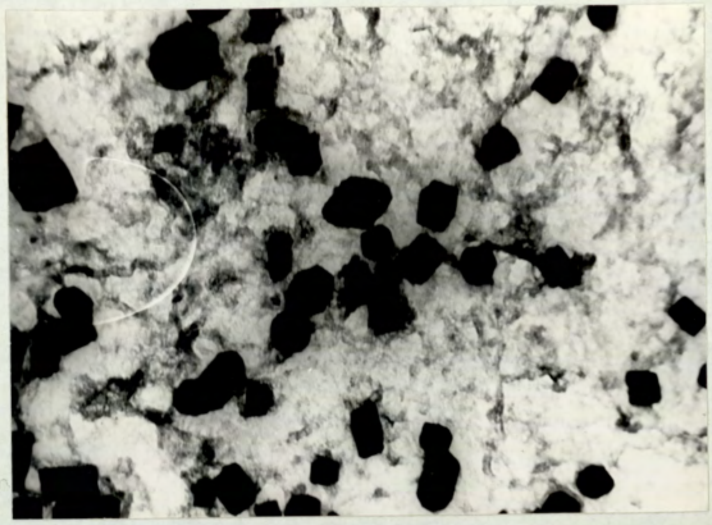

0% Co

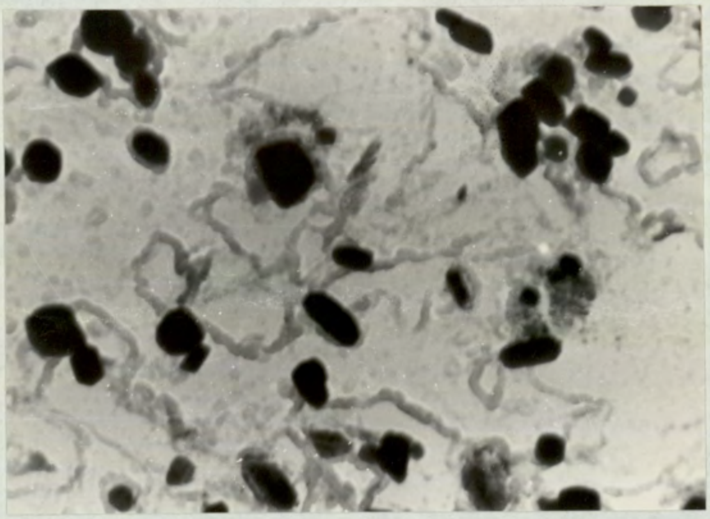

5% Co

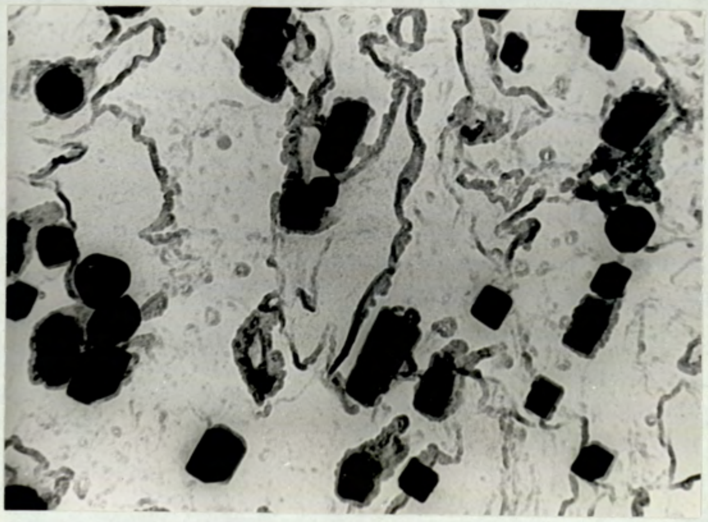

10% Co

FIGURE 56

Structures of ausformed steels
Carbon replicas x 5000

steel to bainitic in the 5 and 10% modification. The nature of the matrix variations is reflected in the ausformed hardness values, 560 VPN and 441 VPN for the 0% and 10% steels respectively.

Since insufficient time was available to evaluate each alloy to the same extent as were the 3M steels, it was decided to use the die wear test as the basis of comparison. The 1M and 2M steels were austenitised for 1 hour at 1020°C and oil quenched whilst the 3M/AUS alloys were tested as-ausformed. The bulk temperature of the dies was again controlled at 130°C and 750 slugs forged to a compression of 0.25 - in.

The results are given in Table 10 (page 140) and shown graphically in Figure 57 (page 141) together with the results from the 3M steels and those for No.5 die steel(106) tested under identical conditions. At all cobalt levels, reducing the molybdenum content of the steel leads to an increase in the wear values. The progressive addition of cobalt is again seen to promote a more wear-resistant material. From Figure 57 (page 141) the comparison of the steels may be divided into two sections - the reduced molybdenum steels and their 10% cobalt modifications and secondly the economically balanced steels.

In the first of these groupings it is observed that by merely reducing the molybdenum content the wear volume is increased in both the basis 3M and 10% cobalt containing steels. When the molybdenum content is reduced to 1% the wear resistance of the resultant material is reduced to such an extent that it is little better than the far cheaper No.5 die steel.

TABLE 10

DIE WEAR RESULTS OF 1M, 2M AND 3M/AUSF ALLOY SERIES

	Die Set	Nominal Comp^n	Hardness VPN	Wear Volume in^3 x 10^{-5}				Average Wear Volume	Mean Wear Volume
				1	2	3	4		
1M/0	Top	1%Mo	347	17.804	16.218	18.017	16.119	17.039	16.528
1M/0	Bottom	0%Co	348	15.872	14.988	17.809	15.413	16.018	
1M/4	Top	1%Mo	352	12.877	11.124	10.944	12.991	11.984	11.109
1M/4	Bottom	4%~~Mo~~Co	354	9.653	10.858	11.002	10.423	10.234	
1M/10	Top	1%Mo	357	6.914	8.893	6.723	7.906	7.906	8.543
1M/10	Bottom	10%Co	357	10.622	9.501	8.869	8.916	9.477	
2M/0	Top	2%Mo	348	13.701	12.398	12.025	15.924	13.512	15.158
2M/0	Bottom	0%Co	350	18.124	17.337	15.299	16.456	16.804	
2M/2	Top	2%Mo	352	12.556	10.204	9.886	7.806	10.113	11.562
2M/2	Bottom	2%Co	351	11.127	11.908	14.711	14.298	13.011	
2M/10	Top	2%Mo	359	8.111	6.983	8.814	4.136	7.011	7.497
2M/10	Bottom	10%Co	359	6.227	9.012	6.767	9.926	7.983	
3M/0/AUS	Top	3%Mo	563	6.710	5.979	6.768	7.323	6.695	6.770
3M/0/AUS	Bottom	0%Co	559	6.834	7.211	6.990	6.348	6.846	
3M/5/AUS	Top	3%Mo	467	4.011	3.724	4.291	3.042	3.767	3.798
3M/5/AUS	Bottom	5%Co	470	4.893	4.012	3.117	3.284	3.828	
3M/10/AUS	Top	3%Mo	443	1.470	2.234	2.509	2.131	2.086	2.553
3M/10/AUS	Bottom	10%Co	439	3.009	2.593	3.368	3.110	3.020	

1M and 2M alloys tested as-quenched
3M/AUS alloys tested as-ausformed

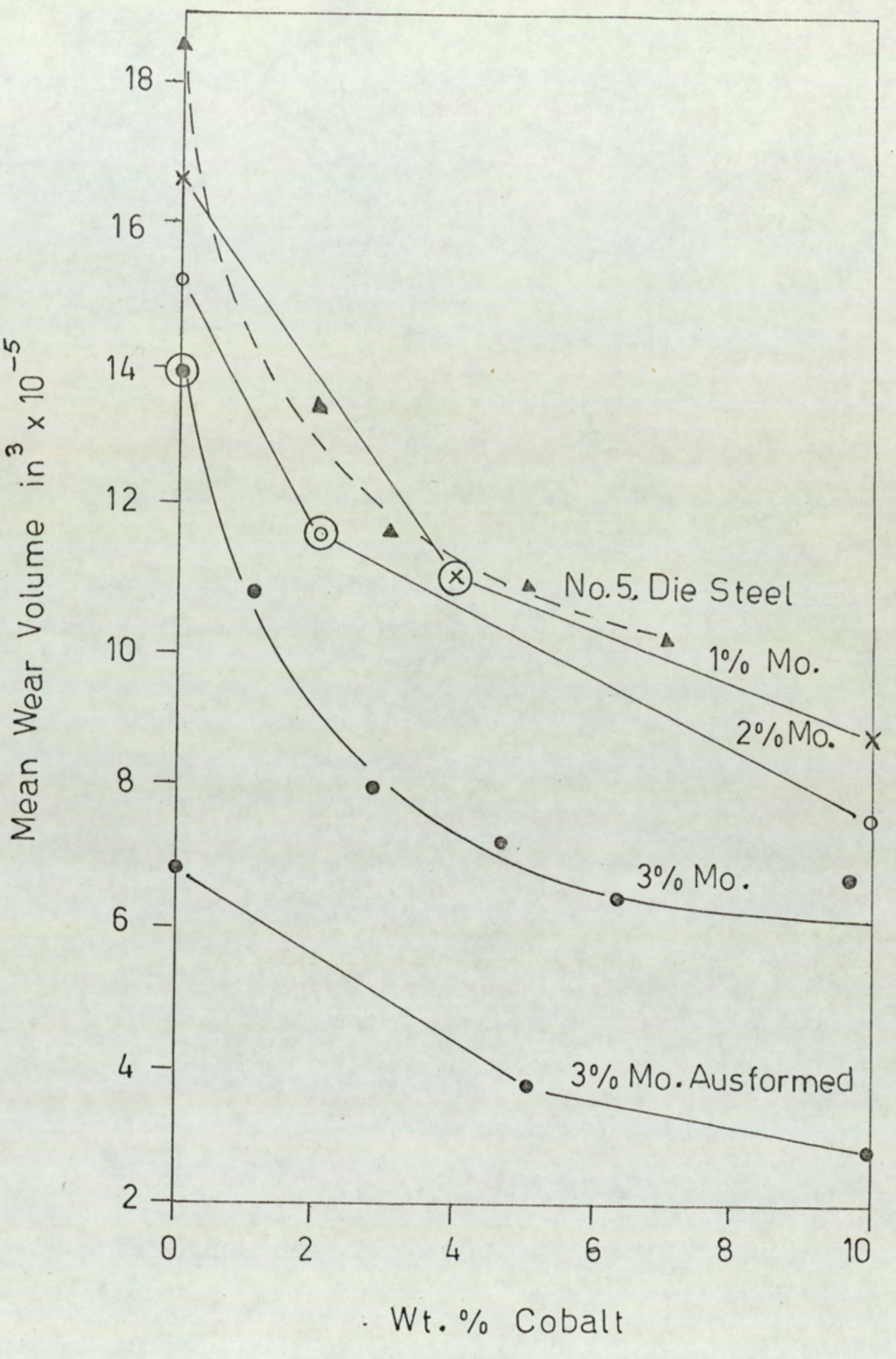

FIGURE 57

Effect of cobalt on the die wear of the 1M, 2M, 3M and 3M/AUS steels compared with No. 5 die steel

The economically balanced steels, on the other hand, offer some foundation for further development. For easy reference the points in Figure 57 (page 141) representing these steels are encircled. By reducing the molybdenum content from 3% to 1 and 2% with respective additions of 4 and 2% cobalt, the wear resistance of the resultant steel is improved above and beyond that of the original 3M steel.

8. DISCUSSION

The existing literature and experimental observations so far made have failed to reveal any general principles governing the behaviour of cobalt in low - and medium - alloy steels. Most other alloying elements that are added to steels usually influence a particular property of the steel in a specific and consistent manner. Cobalt, on the other hand, shows a marked discontinuity in its action and the diversity of its effects are almost as numerous as the research reports cited. The physical and chemical properties of iron and cobalt are so similar that it is difficult to appreciate why this inconsistency should exist. Both elements belong to VIII transitional group of the fourth period in the Periodic Table, cobalt having seven electrons in its 3d shell as opposed to the six of iron. At room temperature cobalt has a close packed hexagonal (ε) structure which transforms to a face centred structure (α) at 417°C. The atomic diameter of f.c.c. γ - iron and α - cobalt are 2.52 and 2.51 Å respectively and it is therefore not easy to envisage any other action for cobalt apart from that of a simple substitutional element.

In the present investigation it has been shown that cobalt additions to a nominal 3% nickel 3% molybdenum steel lead to a linear increase in the M_s temperature of 13.5°C/wt.% Co. This result is in agreement with the existing literature concerning the effect of cobalt on the M_s temperature of low - and medium - alloy steels. Many attempts have been made to produce a universal formula that would enable the M_s temperature to be computed from chemical composition but very few incorporate a factor to account for the action of cobalt. One that does however has been reported by Jaffe and Holloman$^{(107)}$ as follows:-

$$M_s = 549 - 350(\%C) - 40(\%Mn) - 35(\%V) - 20(\%Cr) - 17.2(\%Ni) - 10(\%Cu) - 10(\%Mo) - 5(\%W) + 15(\%Co) + 30(\%Al).^{\circ}C \quad \text{-------------(9)}$$

This formula was used to compute the values of M_s temperature for the 3M steels and the experimentally determined and calculated values were found to be in excellent agreement. For example, the 0 and 10% cobalt steels were calculated to have M_s temperatures of 316 and 466°C whilst experimentally determined temperatures were 322 and 456°C respectively. The value for the 0% cobalt steel was further compared with one of the most recent formula to be reported, that of Andrews$^{(108)}$ vis.

$$M_s = 539 - 423(\%C) - 30.4(\%Mn) - 17.7(\%Ni) - 12.1(\%Cr) - 7.5(\%Mo).^{\circ}C \quad \text{-----------(10)}$$

This again yielded a value of 315°C which is well within the 10% error margin advised by Andrews.

Cobalt has also been shown to increase the volume expansion associated with the martensite transformation. If this effect was consistent in all steels, then it might be anticipated that with the low alloy steels that rely on water quenching to produce a martensitic structure, this increase in the transformation volume might create warpage and cracking problems on hardening. Just how severe this problem would be in the higher alloy steels is difficult to assess. It might be anticipated that air cooling would reduce the temperature gradients in the steel and thus minimise the deformation arising from the martensite transformation. The die steel metallurgist, however, is concerned with the hardening of relatively large masses of steel which, even on air cooling, could develop quite steep temperature gradients from the surface to the centre. Consequently, the martensite transformation occurs over a considerable period of time and the increased volume expansion associated with cobalt-containing steels might still induce warpage and cracking even on air hardening.

One compensatory factor in this problem is that the martensite transformation occurs at a higher temperature when the material is more plastic and can absorb the extra volume expansion more readily. Although this behaviour may alleviate cracking in the steel, the resultant plastic deformation might necessitate the checking and final machining of finishing dies which are heat-treated after close tolerance machining.

The A_1 and A_3 temperatures are both raised linearly with cobalt additions at a rate of $6.5^{\circ}C/wt.\%$ Co , the difference between the A_1 and A_3 temperatures remaining essentially independent of cobalt content. These results are in accordance with the general effects of cobalt on the iron - carbon equilibrium diagram determined by Hawkes and Mehl(75). Since tempering and subsequent operating temperatures are dictated by A_1 values, raising the A_1 temperature is a decisive advantage. During the forging operation, the hot incoming stock material heats the die and, in extreme cases, may lead to the formation of austenite at the surface of the die.. By raising the A_1 temperature, cobalt minimises austenite formation and may thus lead to a reduction in die wear.

In addition to the elevation of the A_1 temperature, cobalt has also been shown to increase the volume contraction associated with the α to γ transformation. Whilst this behaviour would not be expected to cause undue difficulty during heat treatment, it is a factor that could increase die wear during service. If the forging conditions were such that the thermal cycle of the die surface involved the $\alpha \rightleftharpoons \gamma$ transformation then the increased volume change would lead to surface cracking of the die. Initially the cracking would lead to the forgings sticking in the dies and necessitate the removal and resinking of the dies. Alternatively, the cracking may occur in regions of high stress and might cause complete fracture of the die.

Small amounts of austenite are frequently retained in low - and medium - alloy steels at room temperature and it would appear that even when the carbon content is not high, the martensite reaction does not always proceed to completion above room temperature. This may be a normal characteristic of the martensite reaction or it may be a secondary effect due to other reactions. For example, the precipitation of ferrite prior to the martensite reaction will increase the carbon content of the parent austenite and thereby depress both M_s and M_f temperatures. It is very likely that the precipitation of pro - eutectoid ferrite or the formation of some upper bainite structure, which would have a closely similar effect, may be responsible for some of the retained austenite observed in quenched samples. The presence of appreciable amounts (in the order of 8-10%) of retained austenite in a quenched structure lowers hardness. Further, there is evidence to suggest that this phase is strain sensitive and that it may decompose to martensite when plastic deformation occurs during mechanical testing. Thus the presence of retained austenite in a steel tempered at less than 250°C may lead to elastic limit and yield stress values which are low in relation to the tensile strength. Tempering a hardened steel at these low temperatures does effect an improvement in its mechanical properties of course by relieving internal quenching stresses to a great extent. Tempering at temperatures above 250°C often results in isothermal transformation of retained austenite although in some types of steel the austenite may not transform at the tempering temperature but may undergo "conditioning" and then transform to bainite or martensite during cooling after tempering. The presence of martensite in the tempered steel structure would have a deleterious effect on its fracture toughness properties and in such cases the application of a second tempering treatment is desirable.

It is certainly advantageous therefore that the present results show that the amount of retained austenite in the 3M steel is well below any effective level (less than 1.5%) and that cobalt additions do not promote the retention of austenite in quenched or air cooled samples. This effect would be expected from the action of cobalt on the M_s temperature and is in agreement with the conclusions of Trusculescu(109) in his work on retained austenite in 9% nickel steels.

In accordance with other results, the progressive additions of cobalt have been shown to increase the resistance of the steel to tempering. Although cobalt does not increase the peak hardness temperature, it does increase the peak hardness value by considerably more than would be expected from mere solid solution hardening effects. It has been shown that the addition of cobalt to the steel produces a finer martensitic structure. One of the most recent explanations, forwarded by Banerjee and Hauser(64), to explain the effect of cobalt on tempering reactions is based on the hypothesis that cobalt reduces the stacking fault energy of austenite and hence produces extensive dislocation tangles which act as nucleation sites for carbides. This theory can be criticised on theoretical grounds but a finer martensite would certainly result from a more heavily faulted parent austenite, the martensite shear mechanism being repeatedly arrested and nucleated by these faults.

Electron microscopy has revealed that cobalt does not appear to alter the fundamental tempering sequences of the basis steel. All steels showed the same reactions, viz. -

> Precipitation of Fe_3C -- Re-solution of Fe_3C -- Highly strained structure at peak hardness -- Nucleation and growth of the secondary carbide Mo_2C.

In all the steels examined, the secondary carbide formed on tempering above 550°C was analysed as Mo_2C. The Mo/C ratio of the 3M steels is approximately 1.9 and thus the Mo_2C carbide is to be expected from the results of Kuo(28) who found that Mo_2C was the secondary carbide formed in steels with a Mo/C ratio greater than 1.5

Cobalt does, however, affect the extent to which these sequences occur and general structural morphology. Fe_3C growth is restricted in the cobalt-containing steels and the nucleation rate of the secondary carbide is greatly increased. In no steel could a precipitate be detected at peak hardness which indicates that the re - solution of Fe_3C was complete and that carbide nucleation sites were within the matrix. This would discount the possibility that the ferrite - undissolved Fe_3C interfaces might be present to act as nucleation sites for the Mo_2C. Results from the $(310)\alpha$ line breadth measurements would support this observation, the strain peak occurring at peak hardness where the coherency stresses are at a maximum.

The rate of agglomeration of the secondary carbides has been shown to be increased in the cobalt containing steels, an observation which is in contrast to that of Chandhok et.al.(58) From the results presented earlier however it can be demonstrated that an increase in the rate of agglomeration is to be expected. Apart from the simple rationalisation that the more numerous are the carbides and the smaller the mean free path between the precipitates, the faster they will agglomerate, it may also be presented in a more direct manner. Following the usual assumption that the rate is proportional to the free energy change in the process, the rate of agglomeration, $\dot{A}$, may be given by a basic expression of the form :-

$$\dot{A} \propto \sigma / (r_1 + r_2) \quad \ldots\ldots\ldots\ldots\ldots\ldots\ldots (11)$$

where σ is the surface energy of the carbide - ferrite interface and r_1 and r_2 are the principal radii of curvature of the particle. Since in the cobalt containing steels r_1 and r_2 are both much smaller than the corresponding values for carbides in the 0% cobalt steel then the rate of carbide agglomeration should be increased by cobalt additions. It is on this point that the proposed "interface control" mechanism detailed in Section 3.2 again falls down. If the action of cobalt could be rationalised solely on the basis of its preferential partitioning to the ferrite phase then it would be expected that the rate of carbide agglomeration would decrease rather than increase.

The proposal by Seal et. al.(42) that the formation of Co_3C was responsible for the beneficial effect of cobalt on tempering resistance appeared remarkable when it has such a high positive free energy of formation. During the initial carbide extraction experiments in this investigation, a similar cell was used to that described by Seal using a 5% HCl solution as the electrolyte. A great deal of difficulty was encountered on subsequent X - ray analysis of the extracted carbides due to their oxidation. Many of the iron oxide lines appeared on the film and some had "d" spacings very close to the values given in the A.S.T.M. Powder Data File for Co_3C. It would seem that these workers had also encountered oxidation of the extracted carbides, a fact which they seemed to accept later since a subsequent paper by the same authors made no mention of Co_3C precipitation.

The results from the carbide extraction experiments in this investigation would seem to indicate that little, if any, cobalt partitioning occurred to the carbide phase. Analysis of the observed "d" spacings for both the 0 and 10% cobalt steels showed very little variation from the standard "d" values found for the carbides Fe_3C and Mo_2C in the A.S.T.M. Powder Data File, and certainly no consistent distortion of the lattice parameter could be detected to indicate cobalt partitioning.

Perhaps the most interesting results to emerge from this investigation have come from the effect of cobalt on the fracture toughness values. Most of the previous workers have reported the effect of cobalt on impact transition temperature which, as already explained, is a rather vague parameter in the development of a new alloy. One of the very few reports dealing with the effect of cobalt on fracture toughness is by Priest and May(110) who investigated the effect of 1% cobalt in a series of low alloy steels. They found that K_{Ic} values after tempering were reduced by the cobalt addition which is generally in agreement with the present results although the reason for making only a 1% addition is not clear. Unfortunately their results were not supported by microstructural and fractographic studies.

The initial effect of cobalt after low temperature tempering is to increase K_{Ic} values which has been shown to be associated with a larger process zone size in the fracture. This is in accord with work recently recorded by Krafft(111) in which he correlated K_{Ic} values with process zone size and showed that a direct relationship could be established. The process zone size is related to the extent to which microvoids form ahead of the advancing crack and may be regarded as small regions of tensile fracture. Thus the greater the microvoidage the smaller will be the process zone size and hence the lower the K_{Ic} values.

Tempering in the range 200-400°C has been shown to greatly reduce the fracture toughness of the cobalt-containing steels, the extent of the reduction of the K_{Ic} values increasing with the cobalt content of the steel. Since the results from the retained austenite determinations would eliminate the possibility of austenite decomposition during tempering lowering the toughness, these results suggested that the addition of cobalt promoted the onset of either "350°C embrittlement" or "temper brittleness". Both types of embrittlement are encountered in some hardened and tempered steels depending on the heat treatment employed. The occurrence of temper-brittleness is controlled by both the tempering time and temperature, a sensitivity peak being found at approximately 550°C. The low tempering temperature, 400°C, and short time, 1 hour, used in this investigation would suggest that this form of embrittlement was not responsible for the drastic reduction in toughness resulting from the addition of cobalt to the steel.

"350°C embrittlement" is found in hardened steels which have been subsequently tempered in the range 200-400°C. It is exactly this tempering range over which cobalt has its most deleterious effect and it would therefore be convenient if the action of cobalt could be attributed to the promotion of this type of embrittlement. Capus and Meyer(112) have briefly reviewed the general theories proposed to account for "350°C embrittlement" and it is concluded that this form of embrittlement is characterised by an intergranular mode of fracture and the fall-off in toughness is not associated with impairment of ductility as shown by tensile properties. Fractographs from the broken fracture toughness specimens have already been presented on pages 79 to 84 and after tempering at 400°C, the temperature at which cobalt has its most profound effect, no evidence could be detected of an intergranular mode of fracture. This is perhaps more clearly illustrated in Figure 58 (pages 154 and 155) which illustrates the general fracture surfaces of the tempered samples of the 10% Co.steel. It can be seen quite clearly that the characteristic bright cleavage facets associated with intergranular fracture became visible only after tempering at 550°C and are certainly not present after treatment at 400°C.

Klingler et. al.(113) have suggested that "350°C embrittlement" was associated with localised precipitation of cementite platelets at prior austenite grain boundaries resulting in the formation of thin ferrite networks in an otherwise martensitic structure. If this were so, then it should

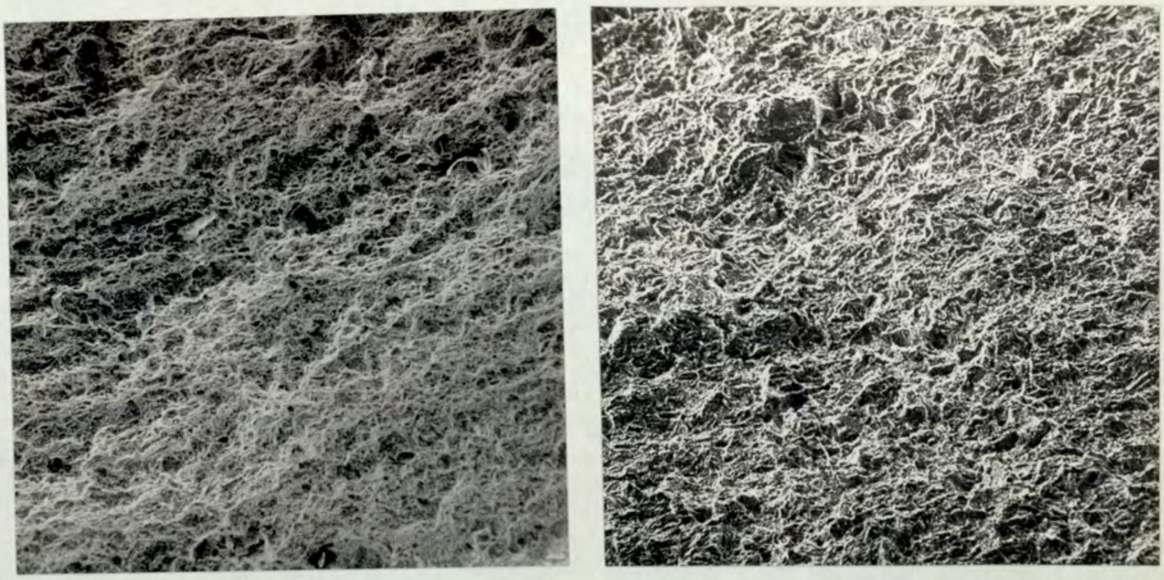

As-quenched

Tempered 200°C

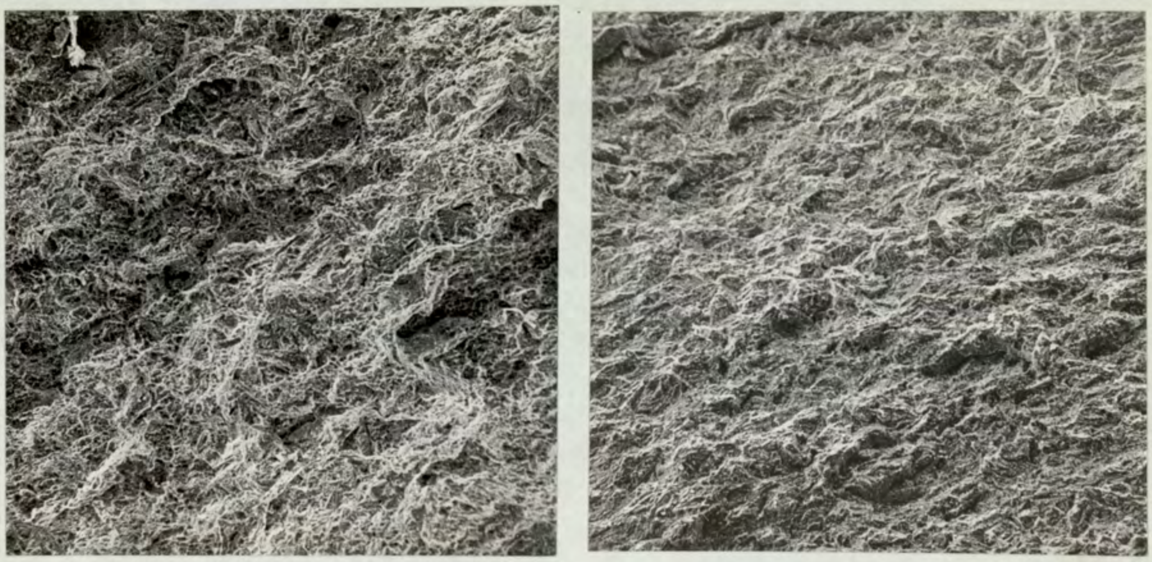

Tempered 400°C

Tempered 500°C

FIGURE 58

Fractographs from the 10% cobalt containing steel after various heat treatments illustrating the onset of the characteristic bright cleavage facets associated with intergranular brittle fracture

x 85

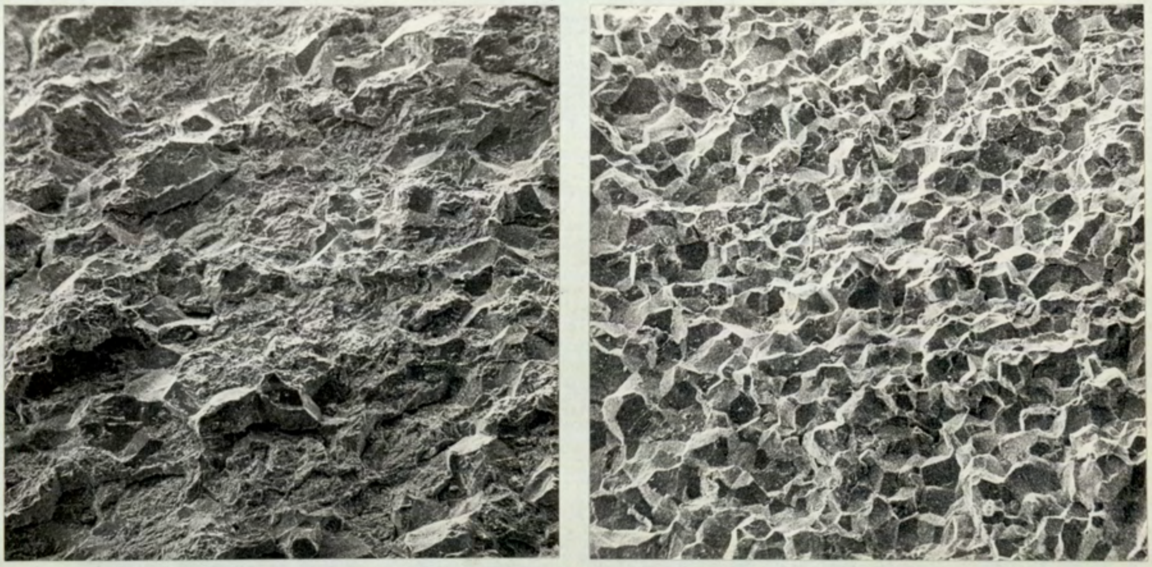

Tempered $550^{\circ}C$

Tempered $600^{\circ}C$

FIGURE 58 (continued)

be possible to define the cementite by the grain boundary etch technique proposed by Woodfine (114) to detect temper-brittleness in steels. The steels tempered at 400°C were consequently etched lightly in picral, repolished and re-etched in a saturated solution of picric acid in distilled water for ten minutes. In all the samples, no distinct preferential grain boundary attack could be observed which would indicate that no grain boundary precipitate was present.

To investigate this behaviour further, carbon replicas were prepared from the broken specimens tempered at 400°C and examined in detail under the electron microscope. The general structures were as already described in Section 3.5 but further examination revealed a very important action of cobalt on carbide morphology illustrated in Figure 59 (page 157). Whilst tempering at 400°C tended to spheroidize the Fe_3C in the 0% cobalt steel, as the cobalt content of the steel increased the degree of spheroidization decreased, the carbide remaining essentially as film associated with the martensite plate boundaries. This action of cobalt does not seem to have been reported previously and, apart from explaining the present fracture toughness results, it will be expanded further in subsequent pages in an attempt to explain the effects of cobalt on other properties.

With the carbide existing as discrete particles, fracture occurs by the cracking of the carbides ahead of the crack tip and a subsequent microvoid coalescence mechanism outlined in detail in Section 4.1.2. The crack must propagate, therefore,

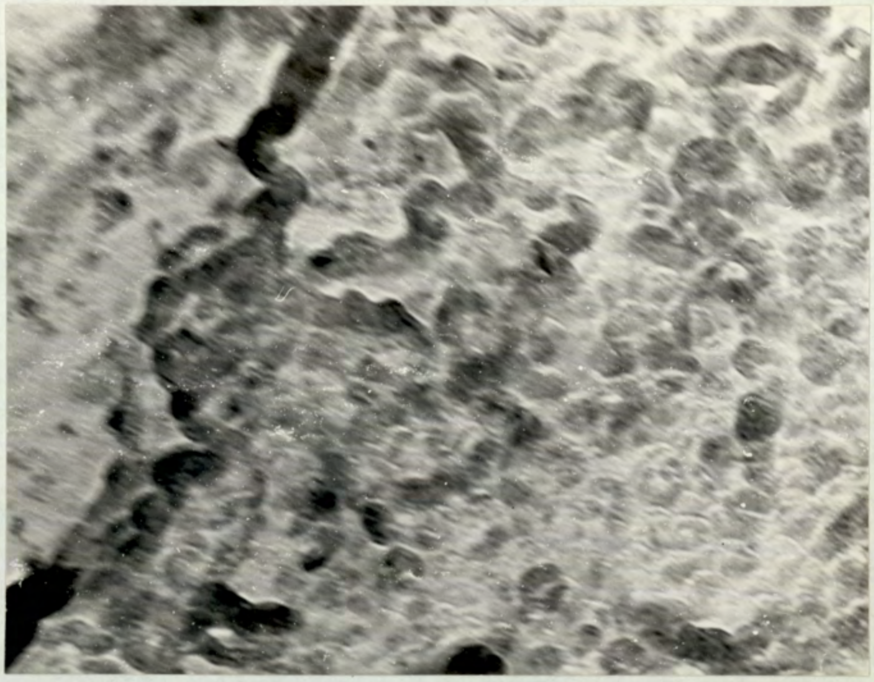

0% Co

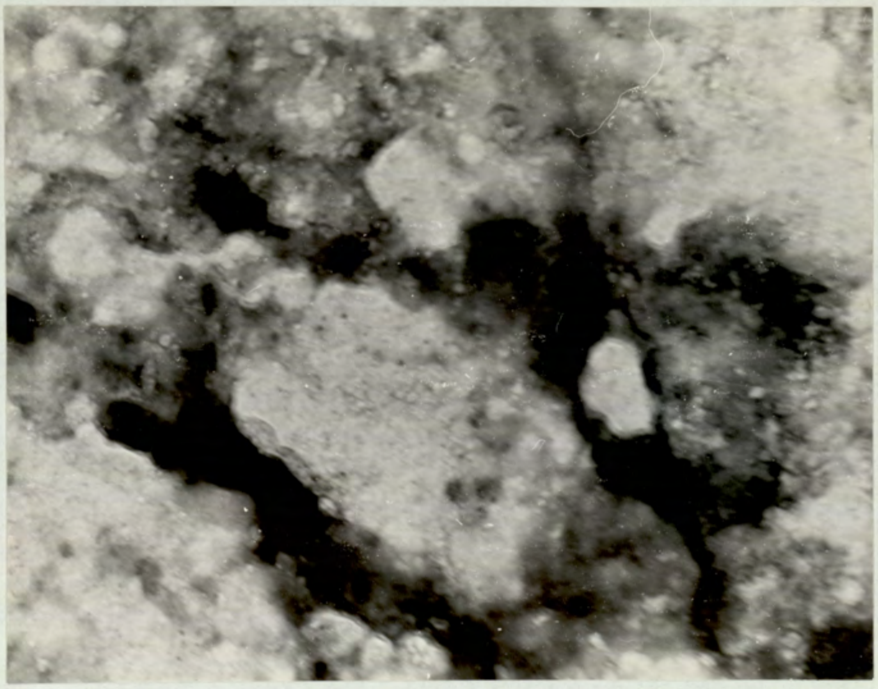

10% Co

FIGURE 59

Fracture toughness specimens tempered at 400°C

Direct carbon replicas x 27500

from the separate carbide particles through sound matrix ligaments and these will increase the energy for crack propagation and hence a high value of K_{Ic} will be recorded. When the carbide exists as a continuous film, however, it offers a brittle path for crack propagation and hence propagation energy and resultant K_{Ic} values will be low. It would seem, therefore, that the deleterious effect of cobalt on the fracture toughness properties of samples tempered in the region 400°C is due to the action of cobalt on carbide morphology and not to the onset of "350°C embrittlement".

A very similar explanation to that given above can be used to explain the action of cobalt on K_{Ic} values for samples tempered above peak hardness. It has already been shown that the addition of cobalt to the steel increases the number of secondary carbides produced on tempering above peak hardness. Again fracture occurs by the creation of microvoids by the carbide particles cracking ahead of the advancing crack. The fracture energy thus depends on the mean free path between the carbide particles. If this is high, as is the case with the low cobalt steels, then the matrix ligaments will act as barriers to the fast propagation of the crack and a high K_{Ic} value will be recorded. As the mean free path decreases, the matrix ligaments become smaller and less effective in blunting the propagation of the crack and a lower value of K_{Ic} will result.

As yet no strict universal relationship has been established between fracture toughness and tensile properties. As a general rule it is usually noted that increasing the tensile strength of a material has an adverse effect on fracture toughness properties. Certainly the results obtained in this work would tend to support this general conclusion because the drastic fall - off in toughness after tempering above 200°C is accompanied by a pronounced increase in tensile strength. A marked change is also observed in the values of ductility and reduction of area by tempering above 200°C. In the as-quenched and tempered 200°C conditions, cobalt increases these latter two values slightly which might also account for the observed increase in K_{Ic} values in these steels. The crack propagates through the matrix by microvoid coalescence and if the ductility of the matrix ligaments is increased then it will withstand the opening displacement of the crack to a greater extent and thus result in a higher toughness value. Mechanical test results are useful to supplement fracture toughness results but to what extent they can actually replace K_{Ic} values is uncertain. Kövesi(4) has suggested that reduction of area values less than 30% and elongation less than 8% indicate a susceptibility to brittle fracture. Examination of Figures 26 and 36 (pages 75 and 90) would certainly fail to indicate that any such empirical values could be quoted.

The results from the isothermal transformation experiments would further support the general view that cobalt reduces the incubation period and increases the transformation rate during the decomposition austenite in both the pearlite and bainite ranges. The T.T.T. diagrams are of direct practical value in such isothermal heat treatments as austempering and isothermal annealing, but they provide only a very broad qualitative means of differentiating between the hardening capabilities of various steels under continuous cooling conditions. Since the isothermal-transformation diagrams provide information on the progress of transformation at a specific temperature and not during cooling through a range of temperatures, they can not be used reliably to predict the heat treatment response of steels of slightly differing alloy contents cooled in air, oil or water. The limited attempts made to correlate isothermal- and continuous - cooling transformation characteristics do not give very satisfactory results due, in part, to the lack of adequate data on the respective transformation characteristics of a sufficiently wide range of steels. This is particularly true for the higher-alloy steels.

Hardenability experiments have revealed that cobalt has an adverse effect on hardenability by promoting the bainite transformation. The action of cobalt, however, is not uniform and additions of up to 3% cobalt do not seriously reduce hardenability. Since the extremely deleterious effects of relatively large percentages of cobalt on fracture toughness would almost certainly exclude the resultant steels from commercial use, the hardenability of these alloys becomes of only academic importance.

The refractory cone hardenability test used in this investigation is a relatively new test and the cooling processes occurring along the rod specimen have been determined. By calculating the cooling rate at 700oC from these cooling curves, it has been possible to correlate the cooling of various positions along the hardenability bar with that theoretically computed for the centres of different diameter bars on air cooling or oil quenching. A close approximation to the cooling rates encountered at the centres of other simple shapes is provided by the cooling rate for the centre of a cylindrical bar possessing the same ratio of volume to surface area. For the calculation of the cooling rates in rectangular blocks the work of Russell(101) is recommended.

It must be borne in mind that all the conversions used in determining the correlation data were based on average and calculated cooling rates and that the hardness after quenching is influenced in practice by other factors than the cooling rate only. In large die blocks, thermal stresses are created on cooling from the austenitic structure which can influence the speed of transformation of the steel. Similarly, segregation of alloying elements can also influence hardenability behaviour and this factor will be more pronounced in large sections.

From a practical point of view, the results from the die wear tests are particularly interesting. It has been shown that, when tested to simulate hot forging conditions, a 3% cobalt containing steel gave an improvement in wear properties of 50% over the basis steel. Bhattacharyya(106) found a very similar behaviour in his work on No.5 die steel using the same equipment as was used in this investigation but did not account for the improvement. It is difficult to explain how a 3% cobalt addition has such a profound effect on wear properties and that further cobalt additions only reduce wear marginally, and also why this pattern of behaviour should be observed in two different steels. Wear resistance is normally related to hardness and tempering parameters which show a progressive increase with cobalt additions and no discontinuity at the 3% level. Other factors which might be considered are oxidation resistance and thermal conductivity since both contribute to the complex wear resistance property. Cobalt has already been shown to increase the oxidation resistance of the basis 3M steel and it has been suggested that oxide scale is a major factor in die wear acting as abrasive particles on the die surface. The thermal conductivity of the steel controls the surface temperature and temperature gradient of the die and is increased by the addition of cobalt(2, 115). Both of these properties, although generally improving die wear, do not account for the sharp discontinuity at 3% cobalt.

Examination of the worn inserts showed extensive cracking in the 3% cobalt steel and it is this observation which provides a clue to the wear behaviour. It was thought that the surface cracking might have resulted from the surface layers of the insert continually undergoing the $\alpha \rightleftharpoons \gamma$ transformation. In the 0 and 1% cobalt steels the surface was heated by the hot stock to a temperature above their respective A_1 temperatures and the austenitic surface layers gave rise to a high wear volume. This hypothesis was supported by the dish - shaped wear pattern observed for these steels where the relatively soft and weak central region had worn during forging. The addition of 3% cobalt to the steel raised the A_1 temperature to a point where it was just equal to that of the die surface and hence during forging the surface layers are continually undergoing the $\alpha \rightleftarrows \gamma$ transformation. Above 3% cobalt, the A_1 temperatures of the steels are all above the surface temperature attained by the die and consequently the wear is considerably reduced and then becomes dependant on a host of variable factors that might influence die wear.

To test this basic hypothesis, it was decided to retest the 0, 3 and 7% cobalt containing steels and attempt to make allowances for the effect of cobalt in raising the A_1 temperature. In the first series of tests, the bulk die temperature was controlled at 130°C for all steels. To a first approximation it can be assumed that the forging operation will cause a constant temperature rise of the die surface and that this temperature rise is independant of the bulk die temperature. In effect, the die surface temperature can be controlled by preselecting the bulk die temperature. Results have shown that cobalt raises the A_1 temperature of the steel by approximately 6.5°C/wt.% Co and when selecting the bulk die temperature, this effect was taken into account. Thus, if the bulk die temperature of the 0% cobalt steel is maintained at 130°C as before, then the corresponding temperatures for the 3 and 7% cobalt steels should be 150 and 176°C respectively.

Using these controlled bulk die temperatures, the three steels were retested and evaluated in exactly the same way as described in Section 6. The original wear pattern on the dies was completely ground off and the discs subjected to die-penetrant crack detection testing to ensure a perfectly sound surface. The results from these tests are given in Table 11 (page 165) and compared graphically with the first series of tests in Figure 60 (page 166). It can be seen that the original hypothesis of cobalt improving die wear basically due to its action of increasing the A_1 temperature is generally correct, although the wear volume decreases somewhat more than would be expected if the increase in A_1 temperature had been fully compensated. It will be remembered, however, that in determining the bulk die temperatures, it was assumed for convenience that the heat input to the die from the hot forging stock was constant and remained unaffected by the bulk die temperature. This is a very much simplified case and the die surface temperature will certainly be affected by its bulk temperature. Consequently, an increase of $T^{o}C$ in the bulk die temperature will not be complimented by an increase of $T^{o}C$ at the die surface, rather by an increase of $(T - \Delta T)^{o}C$. If, therefore, it is accepted that the actual die surface temperature of the 3 and 7% cobalt steels might still have been slightly lower relative to their A_1 temperatures than was the 0% cobalt steel then this would reduce the slope of the die wear line for these tests in Figure 60 and an even better correlation between wear volume and A_1 temperature

TABLE 11

RETESTING 3M SERIES OF ALLOYS AT COMPENSATED BULK DIE TEMPERATURES

	Die Set	Nominal % Co	Hardness VPN	Bulk Die Temp. °C	Wear Volume in3 x 10-5				Av. Wear Volume $in^3 \times 10^{-5}$	Mean Wear Volume $in^3 \times 10^{-5}$
					1	2	3	4		
3M/0	Top	0	347	130	13.899	14.782	13.203	12.713	13.649	13.625
	Bottom		350		14.286	14.002	13.011	13.109	13.601	
3M/3	Top	3	354	150	11.792	10.039	12.445	10.801	11.269	11.489
	Bottom		351		11.498	13.624	12.009	9.711	11.710	
3M/7	Top	7	362	176	8.413	9.982	11.459	11.012	10.216	10.081
	Bottom		359		10.807	9.583	8.992	10.402	9.946	

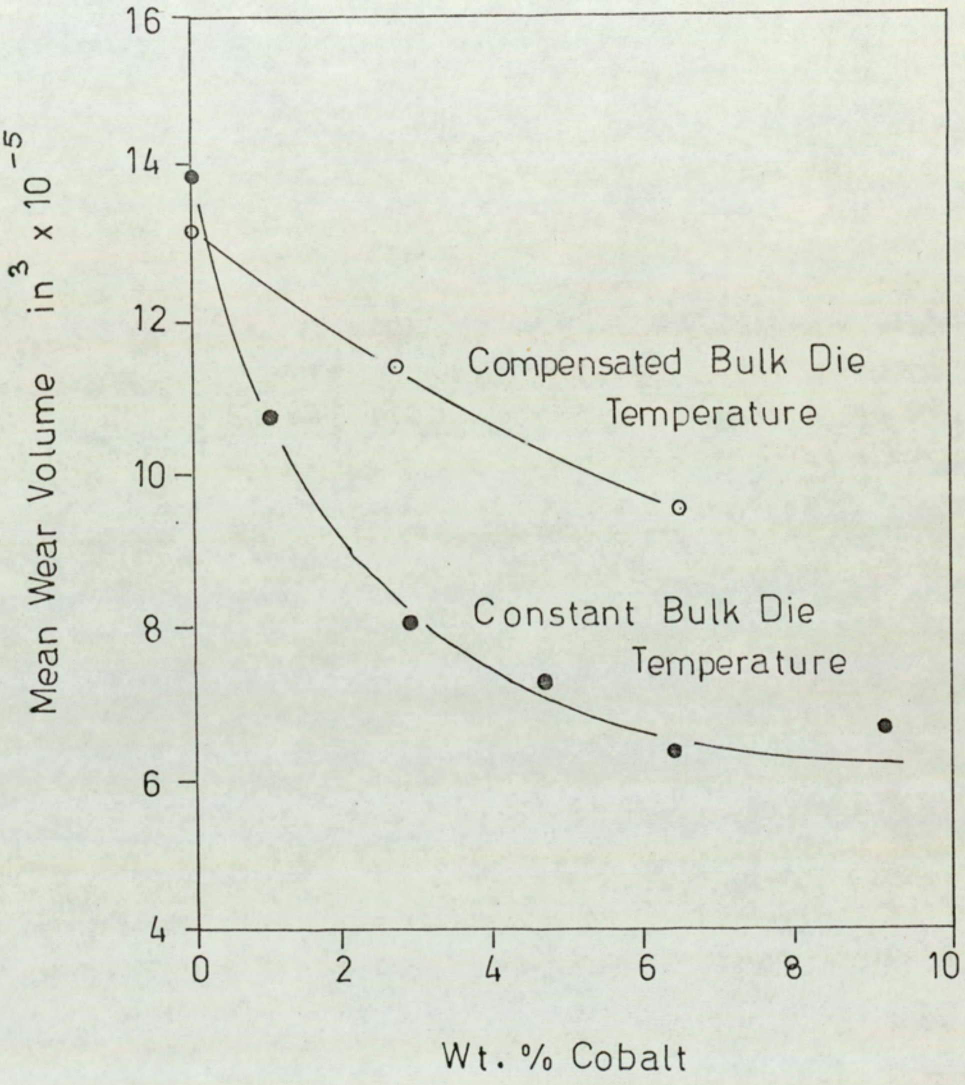

FIGURE 60

Effect on die wear of compensating for the higher A_1 temperatures of the cobalt modified steels could be obtained.

Above a cobalt content of 3%, the steels show a gradual reduction in wear volume of approximately 2.5 x 10^{-4} cu ins. wt.% Co. All these steels are operating under conditions whereby the surface layers remain ferritic and, since the as-quenched hardness values are similar, the increased wear resistance must be attributable to the variation in the elevated temperature properties. The addition of cobalt has been shown to produce a stronger steel which would reduce gross deformation in the die, but it seems that the controlling factor in wear resistance is the differences observed in the tempered structures. Wetter(116) attempted to relate wear to the structure of several W-V-Mo steels and found that wear decreased as the number of carbides left undissolved after tempering at the working temperature increased. In the series of tests on the 3M steels, the inserts were tested in the as-quenched condition and were subsequently tempered to the same degree by the forging operation. Cobalt promotes a more dense precipitation of carbides and consequently the dies contained an increasing number of carbides in their structures to reduce wear.

The first series of results on die wear amply illustrate the importance of the A_1 temperature in hot forging die materials. It may be that many steels would show a vastly improved life by merely increasing the A_1 temperature by the addition of a few per cent cobalt. The actual percentage of cobalt added would obviously depend on the chemical composition of the steel, and service conditions such as bulk die temperature, stock temperature, nature of the forging operation and coolant, but it is interesting to break down the figures into a cost per unit forging to see the advantage of cobalt additions. In this anlysis the addition of 3% cobalt to the basis steel has been shown to improve die wear by 50%. The basis 3M steel costs approximately 4/- per pound and the addition of 3% cobalt would increase the cost of the steel by 12.5% so that the cost per unit forging can be derived as shown in Table 12 (page 169). This cost analysis is based on a comparison with a common standard, No.5 die steel. The cost of No.5 die steel is arbitrarily fixed at 10.0 units and the price of 3M steel is thus represented by 21.0 units. It is tentatively assumed that cobalt does not alter machining costs although a slight increase might be anticipated from the hardening effect of cobalt. Two factors which, although not included in this analysis, must be taken into account are the cost of breakdown and die replacement. The interruption in production brought about each time a die fails means a machine idle and the result is an effective increase in the overall cost per unit forging. Any improvements in the life of complex dies, for example pressure die casting or plastic moulding dies, will be far~~e~~ more rewarding because of the high machining costs. It is not unusual in the production of complex dies for the cost of the finished tool to be ten times that of the steel.

TABLE 12

ANALYSIS OF THE COST PER UNIT FORGING FOR 3M AND 3M + 3% Co STEELS

	3M	3M + 3% Co
Cost of Inserts	21.0 units	22.8
Cost of Sinking	36.6	36.6
Total Die Cost	57.6	59.4
Mean Die Life	19,000	28,500
Mean Die Cost Per Unit Forging x 1000	3.03	2.09

Results of this analysis show a substantial reduction in the cost per unit forging produced. It must be remembered however that this improvement relates only to this forging process which is unique in its operating conditions. Much of this improvement would be lost if the stock material was forged at a higher temperature or a different forging cycle was used since this would lead to a higher die surface temperature and the beneficial effect of an increased A_1 temperature would be lessened. In any production forging run it would certainly be advantageous to analyse the operating conditions and determine whether a cobalt - modified cheap steel could not replace a more expensive steel. It is important however that the industrial operating conditions are simulated as closely as possible in these tests in particular to ensure the stock temperature and stock/die mass ratio relate to projected industrial use.

Before the results of the alloy development trials are discussed, an attempt must be made to explain the action of cobalt on the various properties determined. The literature survey has revealed two main theories to account for the influence of cobalt in steels; Banerjee(64) asserts that the role of cobalt in nucleation reactions during tempering is to create a more heavily faulted material and thereby provide the sites for precipitate nucleation whilst Chandhok et. al.(58) propose an interface control mechanism based on their findings that cobalt increases the activity of carbon in steels. Neither of these theories account for the full observed effects of cobalt and both are open to considerable criticism. An important observation has been noted in this investigation, however, in that cobalt inhibits the spheroidisation of the Fe_3C carbide~~s~~ during tempering. Since the degree of spheroidisation depends principally on the carbide/ferrite interfacial surface energy, by limiting spheroidisation cobalt acts to reduce the surface energy value and this effect may be used in part to explain the action of cobalt on other properties.

The main influence of cobalt has been found to be in nucleation processes both in tempering and in the isothermal decomposition of austenite. The surface energy of an interface is a controlling factor in nucleation phenomena, the ease of nucleation increasing as the surface energy value decreases. This behaviour can be illustrated by reference Equation 1, viz:-

$$\dot{N} \;\alpha\; \exp\left[-C\sigma^{3}/RT(\Delta F_{V})E^{2}\right]\ldots\ldots\ldots\ldots(1)$$

from which it can be seen that reducing the surface energy of the carbide/ferrite interface, σ, then the nucleation rate, $\dot{N}$, is consequently increased. The present investigation has demonstrated the influence that cobalt has on the surface energy of the carbide/ferrite interface and would explain the precipitation of more numerous carbides during tempering. The reduction in the incubation period prior to the isothermal decomposition of austenite could also be explained in a similar manner if the influence of cobalt on interfacial surface energies is extended to the carbide/ferrite/austenite interfaces.

With reference to Equation 1, it was thought that the results from the $(310)\alpha$ line breadth measurements might have also given information on the value of E, the strain energy accompanying critical nucleus formation. The total strain in the ferrite matrix was certainly found to be increased by cobalt but a much higher nucleation rate was also observed in these steels. It is thus impossible to determine from these results whether the extra strain is due to a higher value of E or merely a consequence of the enhanced nucleation rate.

In the cobalt modified steels, the growth rate of the alloy carbides was found to be slower than that for the basis 3M steel. An equation of the form -

$$\bar{r}^3 - \bar{r}_o^3 = k\ t \qquad \dots\dots\dots\dots\dots\dots\dots\dots\dots\ (12)$$

can be used to describe the theoretical growth rate of a particle,(118) where $\bar{r}$ is the average particle radius at time t and $\bar{r}_o$ is the average particle radius prior to the onset of growth. The rate constant, k, is given by

$$k = \frac{2\,\sigma\,D\ \ c_e\ V_m^{\ 2}}{\rho_c^{\ 2}\ \ R\ \ T} \qquad \dots\dots\dots\dots\dots\dots\dots\dots(13)$$

where σ is the interfacial surface energy between the particle and the matrix, D is the coefficient of diffusion of the solute in the matrix, c_e is the concentration of solute in equilibrium with a particle of infinite size, V_m is the molar volume of the precipitate, ρ_c is a numerical constant related to the distribution of particle sizes (theoretically ρ_c is $3/2$) and RT has its usual meaning. Although Equations 12 and 13 are essentially for spherical particles growing in fluid matrices, they well illustrate the influence of interfacial surface energy on growth characteristics. Equation 13 predicts that any reduction in σ would lead to a consequential reduction in the rate constant k and thus growth would be diminished.

Earlier it was noted that cobalt increased the rate of agglomeration of the alloy carbides and this was explained on the basis of cobalt promoting smaller and more numerous carbide particles. A simple equation was invoked of the form -

$$\dot{A} \propto \sigma / (r_1 + r_2) \quad \ldots\ldots\ldots\ldots\ldots\ldots\ldots (11)$$

It was stated that the agglomeration rate, $\dot{A}$, was higher in the cobalt steels because the principal radii of curvature of the carbide particles, $r1$ and r_2 were reduced. On the basis of the observed effect of cobalt on the carbide/ferrite interfacial surface energy a decrease in agglomeration rate would be expected. The actual rate of agglomeration of the carbides is therefore a balance between the two counteracting effects of surface energy and particle size. Certainly the agglomeration rate was increased in the cobalt steels and it would thus appear that in these cases the influence of cobalt on particle size is the predominant factor.

The action of cobalt on the surface energy of the carbide/ ferrite interface can be used to explain the influence of cobalt on most of the observed phenomena but the raising of the M_s temperature is not accountable on this basis. The martensite transformation is akin to other transformations in that it is a process of nucleation and growth of a new phase although it is a diffusionless reaction. Most martensitic transformations exhibit athermal characteristics, the amount of transformation product being a function of temperature and the transformation rate independant of temperature. The onset of the austenite to martensite transformation is thus a nucleation controlled reaction and the degree of supercooling represents the ease of nucleus formation. In a 70/30 iron - nickel alloy for example, martensite begins to form at - 30°C whereas the reverse transformation begins at a temperature designated A_s (austenite start temperature) which is 420°C higher than the M_s. The 420°C temperature difference is indicative of the large driving force needed in this alloy to nucleate the transformation.

Much less is known about the nucleation of martensite than about its growth. Calculations by Bilby and Christian(118) and Cohen(119) indicate that nuclei of martensite could not be formed by random fluctuations in a defect-free region of solid solution, at least in transformations where the shape deformation is reasonably large such as is the case with steels. Thermal nucleation must therefore be catalysed in some way making use of existing defects, heterogeneities or internal stress fields. There is thus some difficulty in formulating a nucleation theory if the growth of embryos is thermally activated whilst that of stable plates is not. Athermal nucleation of martensite however may envisage a beginning from structural defects or from embryos formed at a higher temperature when a critical driving force is exceeded. It is in this context that the effect of cobalt on the fault energy of austenite becomes of real significance. The present investigation has shown that cobalt additions to a steel promote the formation of a finer martensite, an observation that would support the Banerjee hypothesis(64) of cobalt reducing stacking fault energy. If the austenite is highly faulted, nucleation is greatly facilitated and hence a rise in the M_s temperature would be anticipated. It would be expected therefore that any element that reduced the stacking fault energy of the austenite would raise the M_s temperature, but this is not entirely correct. The hypothesis falls into some difficulty when the effects of alloying elements such as nickel and manganese are evaluated. Both elements lower the M_s temperature of steel yet manganese lowers the fault energy of austenite whilst the nickel has the opposite effect(120, 121). Moreover, low stacking fault energy in steels is known to lead to the metastable product - martensite and also seems to favour untwinned rather than twinned martensite. The available evidence is that twinned martensite is more brittle than untwinned martensite because the number of possible slip systems common to both twin orientations in a twinned plate is only a quarter of that of an untwinned plate. Generally, therefore, manganese might be expected to increase the toughness and ductility of martensite and nickel to reduce these values. As Nutting(122) has remarked, the observed effects are opposite to those predicted. Although the internal structure of the martensites produced were not examined using thin film techniques, cobalt additions are shown to yield a finer martensite and increase both the as-quenched fracture toughness and tensile ductility values. The results obtained from the present investigation would therefore indicate that the theory is generally correct in predicting the effect of cobalt on these properties.

The extent to which the M_s temperature is raised by cobalt additions varies with the base composition of the steel under investigation, but to account for the whole range of increments quoted it may be that it is the influence of cobalt on carbon, the most potent element affecting the M_s temperature, that is of importance. By raising the M_s temperature, cobalt makes the steel behave as if it had an effectively lower carbon content and the vacancies in the austenite could act as sinks to which the carbon atoms could diffuse. Removal of carbon from solid solution by this method would mean that the martensite formed from a lower carbon austenite and hence a rise in the M_s temperature would result. The existence of high carbon regions would also explain the effect of cobalt on nucleation processes since the areas of high carbon segregation could act as nucleation centres for the precipitating carbide. This mechanism would agree with the results of Irani and Honeycombe(39) who found that the activation energy associated with peak hardness in a 0.2% carbon 4% molybdenum alloy was 65 kcal./mole which approximates to that for the diffusion of molybdenum in α - iron. This activation energy remained unaltered by cobalt additions.

It must be argued however as to the effectiveness of this mechanism for removing carbon from solid solution. In the results presented earlier in Section 5 it was shown that the M_s temperature is raised quite linearly by cobalt at some 13.5°C/wt.% Co. From the Andrews formula for the determination of M_s temperature from chemical composition given at the beginning of this discussion (page 144), the carbon factor is 423 which means that if the M_s temperature were based on carbon alone then an increase of say 100°C would correspond to a reduction in carbon content of over 0.2%. This means that with the steels in this investigation the effective carbon remaining in solid solution in the 10% cobalt material would be only slightly over 0.05% giving a martensitic hardness of approximately 290 VPN. To counteract this, the solid solution hardening effect of cobalt would need to be in the order of 12 VPN/wt.% Co or an order of magnitude in excess of the experimentally determined value.

The hardness of martensite is not solely dependant on the carbon content however. The as-quenched hardness of the steel is due to four main factors, viz -

i) solid solution strengthening by cobalt
ii) solid solution strengthening by carbon
iii) work hardening due to the transformation itself
iv) hardening due to numerous twin interfaces

Cobalt has been shown to increase both the volume associated with the martensite transformation and the fineness of the resultant martensitic structure. These two observations will increase factors (iii) and (iv) respectively and hence increase the as-quenched hardness of the steel. Thus the high faulted regions could remove carbon from solid solution as detailed above without the drastic reduction in as-quenched hardness that might be expected.

The heavily faulted regions may not remove the carbon from solid solution in a homogeneous manner but instead create around themselves a low carbon austenite envelope which could nucleate the martensite transformation. This would overcome the nucleation barrier in the martensite transformation and correlate with the previous discussion, but the effectiveness of these low carbon trigger spots is uncertain.

In conclusion, it must be stated that a consistent model to explain all the effects of cobalt in steels has still to find both theoretical and experimental justification. This work has shown that cobalt inhibits the spheroidisation of the Fe_3C carbide during tempering and this behaviour has been attributed to a reduction of the carbide/ferrite interfacial surface energy. Since the fundamental action of cobalt is to alter nucleation characteristics, this theory can be successfully extended to explain most of the observed phenomena in cobalt modified steels. The elevation of the M_s temperature, however, can not be rationalised on this basis. A finer martensitic structure has been suggested to support the Banerjee theory of cobalt promoting a more heavily faulted austenite and the full effects of cobalt on other properties explained from this. It would seem that further work is needed on this point to determine the nature of the dislocations in b.c.c. materials and the influence of cobalt on their occurrence and properties.

To supplement the argument concerning the effective removal of carbon from solid solution by the higher faulted regions, preliminary trials were undertaken in an attempt to try to establish this data by measurement of the c/a ratios for the quenched steels. The three lowest order lines on a powder photograph of b.c.c. iron are line 2 having indices (110), line 4 having indices (200) and line 6 having indices (211), the line number being equal to the sum of the squares of the indices. As martensite is tetragonal with the c-axis greater than the a - axis, the "ℓ" indices are not interchangeable with the others so that the (110) for example has a different angle of reflection from the (101). Thus instead of a single line 2 that ferrite gives there are two lines, one being equal (110) the other the (101) and (011) which overlap. Similarly twin lines occur for the (002) and (200) + (020) and (112) and (211) + (121). The carbon content of the steels investigated was only 0.25% and the displacement of the twin peaks was not sufficient to enable accurate measurements of the c and a parameters to be determined. It may be, however, that internal friction measurements could help resolve this problem.

An attempt has been made to improve the basic 3M steel composition by the systematic substitution of cobalt for molybdenum on an economic basis. Results have indicated that a deterioration in wear resistance accompanies any reduction in molybdenum content. Indeed, when the molybdenum content is reduced to only 1%, the wear resistance of the resultant steel is only slightly better than the much cheaper No.5 die steel. Using a similar die test apparatus as the one outlined for use in this project, Thomas at D.F.R.A. has used a multiple regression analysis technique to demonstrate that wear and composition can be related by an equation of the form -

$$\text{Wear, } W = \text{Constant} - a(\text{Mo})^{1/2} - b(\text{SS}) - c(\text{H}) \quad \ldots\ldots\ldots\ldots (14)$$

a, b and c are experimentally determined coefficients, (Mo) is the equivalent molybdenum content of the alloy, (SS) is the sum of the elements present in solid solution and (H) is the hardness of the alloy. This is a very general formula and an example of its oversimplification has been demonstrated in this work with the effect of cobalt in reducing wear by raising the A_1 temperature. Further, in the ausformed series of alloys, the cobalt free steel was over 100 VPN harder than its 10% cobalt modification yet still showed a higher wear volume. Nonetheless, this formula does predict a reduction in wear when the molybdenum content of the steel is lowered and this trend has been found in the present results.

Cobalt additions to these reduced molybdenum steels improved their wear resistance as was noted for the 3M alloy series. In general it must be concluded that a substantial reduction in the molybdenum content of the steel would not be advantageous even with a 10% cobalt addition. In this work, however, the molybdenum content has been reduced in increments of 1%. At the 2% level, the wear resistance of the material, although lower than the wear resistance of the 3M steel, is still much higher than No.5 die steel. It may be worthwhile to investigate the effect of reducing the molybdenum content by only 0.5% since even this small reduction could lead to very high cost savings on a high - tonnage material such as the 3M steel.

When the economically balanced steels are analysed on the other hand, it seems that there may be some cause for their further investigation. Results from the die wear test have indicated that an improvement in the wear resistance results from replacing some of the molybdenum with cobalt. The respective wear volumes for the 3M/0,2M/2 and 1M/4 steels are 13.894, 11.562 and 11.109. If a similar analysis is followed as outlined in Table 12 (page 169) then these values would yield cost per unit forging prices of 3.03, 2.65 and 2.52 units respectively. Thus the reduced molybdenum, cobalt-balanced steels would lead to a lower cost per unit forging produced. It will be remembered, however, that by making a straight addition of 3% cobalt to the basis 3M steel, the cost per unit forging was reduced to only 2.09 units and it would appear that this is perhaps the best overall composition. On the basis of these results, it is suggested that the following three steels are investigated further and perhaps put into an experimental/industrial trial press.

i) 3% molybdenum + 3% cobalt
ii) 2% molybdenum + 2% cobalt
iii) 1% molybdenum + 4% cobalt

Perhaps the most fitting summary to this section of the work can be made by reference to a paper by Mathews (123) entitled "Modern High Speed Steels". Writing on the role of cobalt as an alloying element in steels he states:-

"It was always present as an addition to types of steels that would have given remarkably good results if the cobalt had been omitted. I have never seen anything to indicate that it could be used as a substitute for any of the other elements regularly present".

The results from the die-wear tests clearly indicate that cobalt can be used not only to replace some of the molybdenum in the basis 3M steel but the resultant steel could effect a lower unit forging cost. A degree of caution must be exercised, however, in extrapolating these results to commercial forging operations and a great deal of work is needed to evaluate the full properties of the cobalt modified steels.

By ausforming steels containing 0, 5 and 10% cobalt at 550°C, the wear volume is considerably reduced below that recorded for steels of a similar composition heat treated in the conventional way. The action of cobalt in reducing wear might again be rationalised on the basis of the elevation of the A_1 temperature, but with the ausformed steels, wear resistance becomes a rather more complex parameter than was applicable to the conventionally treated steels. In the present work the 1M, 2M and 3M alloys were all tested in the as-quenched condition and thus at the beginning of the wear test, all steels had the same basic structure and very similar hardness values. With these alloys, the forging operation tempered the dies and consequently the wear properties of the steel could be generally related to its tempering characteristics. With the ausformed steels on the other hand, the steels were tested with different initial structures and also a corresponding variation in hardness values. Empirical rules and the formula of Thomas in Equation (14) predict a reduction in wear volume with increased hardness, and this trend is evident in the results from the die wear experiments given previously. The importance of initial hardness has been demonstrated in Figure 57 (page 141) where an increase in hardness of the 10% cobalt steel of approximately 100 V.P.N. has reduced the wear volume by 3.5×10^{-5} cu.ins. Whilst an hardness increase of 200 V.P.N. in the basis 3M steel has reduced wear by almost 7×10^{-5} cu.ins.

The inter-relationship between hardness and structure in the wear parameter has so far been unresolved. Rule-of-thumb guides attribute reduced wear to an increase in hardness of the steel but as the variation in hardness generally implies a corresponding difference in structure, the contribution of each is almost impossible to define. With the ausformed steels, this hardness difference is due to a variation in the structure of the matrices and it would certainly be instructive to be able to assign hardness and structure separate contributary coefficients. Bainitic structures in steels have received scant attention from die steel metallurgists in the past, but it might be of significance to run several exploratory tests on the die-wear apparatus on bainitic steels to see just how wear resistant these steels are in service.

Although ausforming has been shown to yield a far more wear resistant steel it is questionable as to how far this method of fabrication can be applied to die production. Power requirements and the need for considerable (at least 50%) plastic flow, would immediately limit this practice to only small dies but two applications might be investigated. Firstly the production of relatively small die inserts might be considered for ausforming. The 3M steel has already been used very successfully in this way(124) and with such a pronounced increase in wear properties to be gained, ausforming might be seriously considered. Secondly, with the production of larger dies, a method of ausform-hobbing might be feasible. In this approach the die could be prepared for ausforming in the normal way, i.e. heat to 1020°C and cool to 550°C and then the impression formed in the block by a shaped former. The resultant block would then effectively have an ausformed cavity in a conventionally quenched jacket. In both of these applications there are considerable practical difficulties to be overcome before ausforming can be considered as a serious alternative to conventional heat treatment methods. Apart from the greatly increased press or forge capacity required, the ausformed impression or insert will need final machining and since the hardness of the material might well exceed 600 V.P.N. this will present a severe limitation on the acceptance of ausforming to general practice.

As a final comment in this discussion, it is pertinent to critically examine the nickel content of the 3M steel. When planning this work it was the molybdenum content of the basic steel that seemed to be the most attractive proposition for further development and its subsequent replacement by cobalt. At this time the price of nickel was some £700/ton - it is now £1220/ton and all nickel containing steels carry a surcharge. The 3% nickel content of the 3M steel for example carries a surcharge of over £70. Thus, having shown that, as a result of die wear tests, it might be advantageous to either add 3% cobalt to the basic steel or modify the composition with cobalt it now seems that a critical appraisal must be made of the relatively high nickel content of the steel. Certainly with the adverse effect of cobalt on hardenability and toughness it cannot be envisaged that any substantial reduction of nickel could be effected with cobalt additions to the steel. It would seem to be a natural extension of this work, therefore, to examine the nickel content of the steel and determine the effectiveness of possible substitutes.

Nickel fulfills a dual role in the 3M steel in that it increases both hardenability and toughness. If hardenability were the only requirement, then several alternatives exist to replace nickel as illustrated in Figure 61 (page 186). To achieve a similar hardenability factor, nickel might be successfully replaced by molybdenum, chromium, manganese and, to a lesser extent, silicon. This is perhaps more clearly demonstrated in Figure 62 (page 187) where the alloying elements are compared on an effective-cost basis. From this diagram it can be seen that to achieve a hardenability factor of, for example, 2, then additions of approximately £8 molybdenum or £2 manganese or chromium are required as opposed to £25 nickel. This obvious economic advantage of nickel substitution is further enhanced by the reduction in the surcharge which is at present imposed on nickel-containing steels.

Unfortunately, a reduction in the nickel content is usually complemented in practice by a lowering of toughness. Pick(125) has demonstrated this effect in a low-alloy steel in which manganese was used to substitute for the nickel. He quotes the following results:-

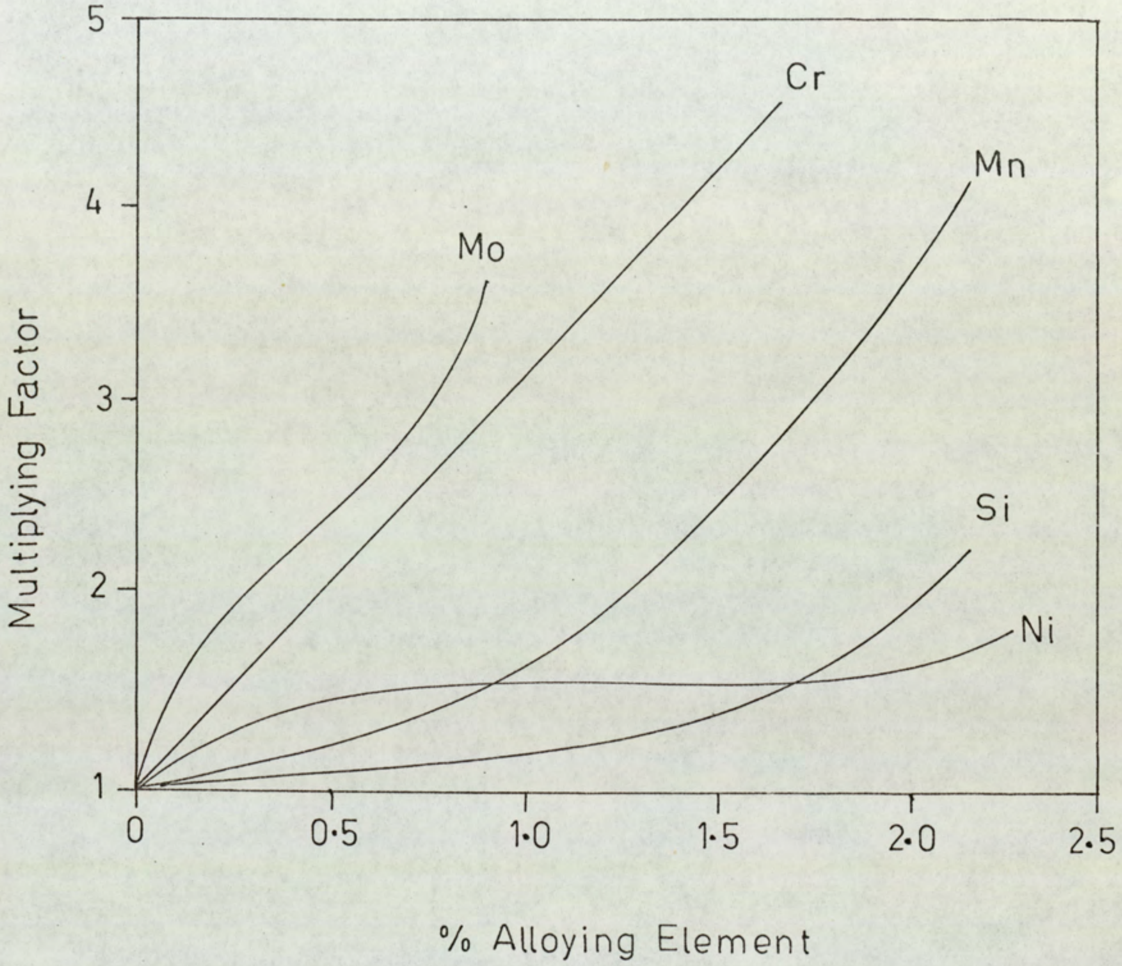

FIGURE 61

Hardenability multiplication factors for several elements

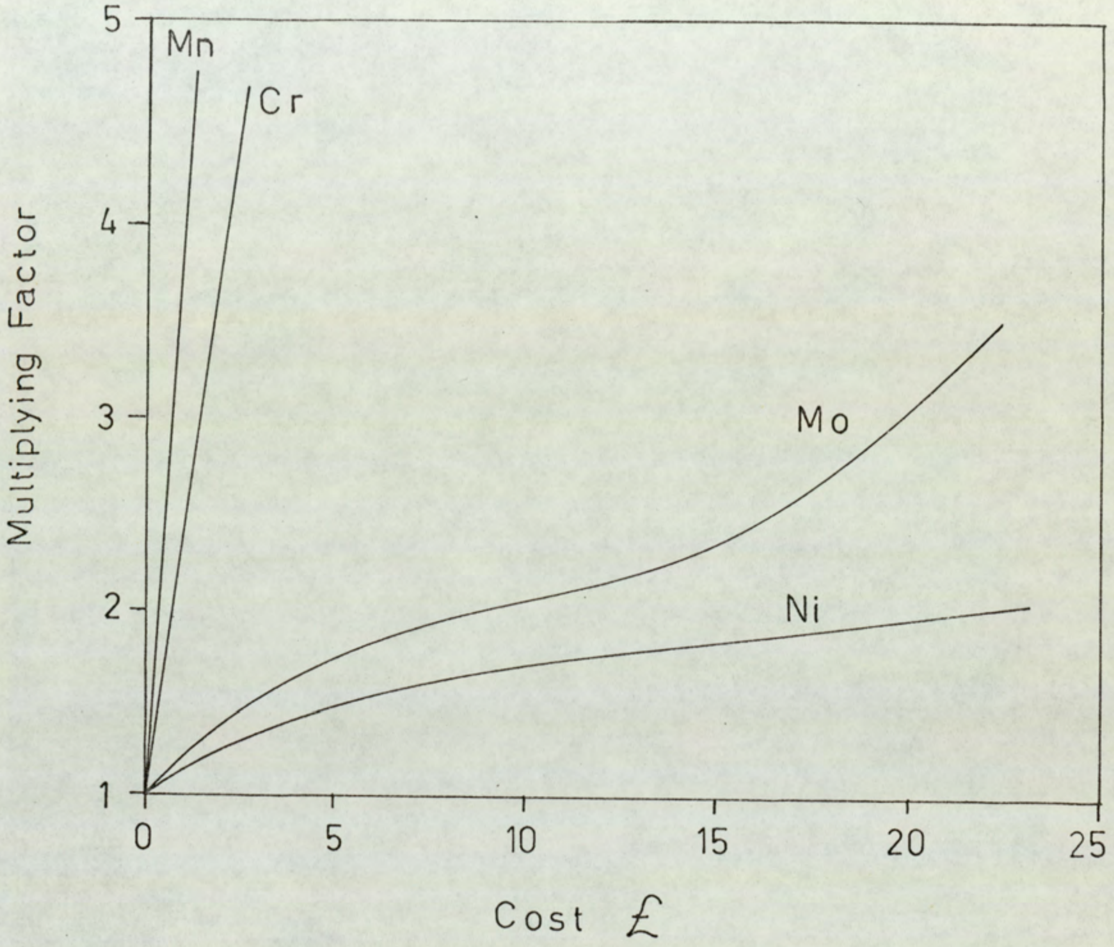

FIGURE 62

Hardenability multiplication factors for several common alloying elements compared on a cost - effective basis

	Specification	
Chemical composition (%)	En 354	CM 70
Carbon	0.15 - 0.20	0.16 - 0.21
Manganese	0.5 - 1.00	1.1 - 1.4
Nickel	1.5 - 2.0	0.6 max (total)
Chromium	0.75-1.25	
Molybdenum	0.1 - 0.2	
Mechanical properties of core, 0.46-in.dia. test bar.		
U.T.S.	80tonf/in^2	80 ton/in^2
Izod	30 ft.lb.	15 ft.lb.

In this analysis, the hardenability and strength of the steel are maintained by replacing the nickel with manganese and the cost is greatly reduced - from £136 per ton for the En 354 steel to £84 per ton for the CM 70 steel. Examination of the Izod properties, however, reveals that toughness is reduced to only one half of its original value.

Priest and May(110) have recently published results that are inconsistent with most views on the properties of nickel-containing steels. In a series of fracture toughness tests, they found that the real effect of nickel on toughness was, in fact, negative. It may be that this effect could be related to the use of a constant austenitisation temperature although this explanation is rather doubtful since manganese lowers the A_3 temperature more than nickel yet does not suffer from this defect. It may be, therefore, that nickel has been overestimated as an alloy addition due to the use of impact testing procedures which show nickel to have a positive effect. The need for further investigation into this apparent anomaly is abundantly clear.

CONCLUSIONS

(i) Cobalt is essentially neutral in its effect on the retention of austenite after quenching and air cooling.

(ii) Tempering resistance is increased by cobalt additions. Electron microscopy has revealed that cobalt produces higher nucleation and agglomeration rates of the alloy carbides but the growth rate is decreased.

(iii) Analysis of carbides extracted electrolytically from the steels have shown that cobalt does not alter the general form of carbides precipitated during the tempering process. This reaction may be summarised as:-

Precipitation and growth of Fe_3C - Re-solution of Fe_3C

Precipitation and growth of secondary carbide Mo_2C.

Determination of the 'd' spacings of the extracted carbides has led to the conclusion that no appreciable cobalt partitioning occurs to the carbide phase.

(iv) The total strain in the matrix prior to the nucleation of the secondary carbide is increased by cobalt although it is not clear whether this is due to an increase in the coherency strains or simply a consequence of a greater number of nuclei~~i~~ being formed.

(v) Cobalt greatly reduces the fracture toughness of the 3M steel after tempering above 200°C. Fractographic studies indicate that cobalt does not promote the onset of "350°C embrittlement" and the embrittlement is due to the action of cobalt on inhibiting spheroidisation of Fe_3C during tempering.

(vi) Cobalt greatly increases the tensile strength of the steel tempered above 200°C and severely reduces elongation and reduction of area. At elevated temperature cobalt containing steels maintain their increased strength over the basic steel.

(vii) Cobalt raises the transformation temperatures A_1, A_3 and M_s of the basic steel. The rate of increase of the A_1 and A_3 temperatures is uniform at 6.5°C/wt.% cobalt whilst the M_s temperature is raised at a higher rate, 13.5°C/wt.% cobalt.

(viii) Cobalt increases the volume changes of the steel when it undergoes the α-γ and martensite transformations.

(ix) The incubation period for the isothermal decomposition of austenite to pearlite and bainite and hardenability are all reduced by the addition of cobalt although the transformation rate is increased.

(x) The remarkable reduction in die wear by the addition of 3% cobalt is attributed to the action of cobalt in raising the A_1 temperature such that during forging the die surface does not undergo the α-γ transformation.

(xi) An attempt to develop the basis 3M steel further by replacing molybdenum with cobalt on a cost equivalent basis has met with some success. The cost per unit forging is successively lowered by reducing the molybdenum content either to 2 or 1% with corresponding cobalt additions of 2% and 4%. The most economic steel, however, would seem to be one based on the original steel with a 3% cobalt addition. Consequently three steels are suggested for further examination:-

(a) 3% molybdenum + 3% cobalt

(b) 2% molybdenum + 2% cobalt

(c) 1% molybdenum + 4% cobalt

(xii) Ausformed steels have greatly improved wear properties over the conventionally treated steels but this method of fabrication would be of limited use in the production of hot forging dies. It may be applicable to the production of die inserts or the impression may be produced by an ausform-hobbing technique.

ACKNOWLEDGEMENTS

The author is indebted to his tutor, Mr. A. D. Hopkins, for his support and guidance during this project.

Appreciation is also expressed to many members of Staff and technicians at the University of Aston for their help in several aspects of this work, in particular, Mr. S. Cross for his assistance in the die - wear testing.

Finally, thanks are recorded to Mr. R. N. Bayliss of Walter Somers Limited for providing the 3M steel scrap for re-melting and arranging the forging of the cast billets.

REFERENCES

1. Settle (D), Met. Treat. and Drop Forging, 1963, v.30, p.177.

2. Hopkins (A.D.) and Williams (E), Cobalt, 1966, No.31, p.69.

3. Bayliss (R.N.), Metal Forming, 1967, Aug., p.229.

4. Kövesi (P), Alloy Metals Review, 1963, v.11, p.2.

5. Glenny (E), Met. Rev. 1961, v.6, No.24, p.387.

6. Davenport (E.S.), Trans. A.S.M. 1939, v.27, p.837.

7. Corbett (R.B.), Succop (J.A.) and Feduska (A), Ibid, 1954, v.46, p.1599.

8. Habraken (L) and Contsouradis (D), Cobalt, 1958, No.2, p.11.

9. Urbain (M), Ibid 1961, No.12, p.11.

10. Irvine (K.J.), "Journees Internationales des Applications du Cobalt", Brussels, June 1964.

11. Habraken (L) and Contsouradis (D), Cobalt, 1965, No.26,p.18.

12. Lacy (C.E.) and Gensamer (M), Trans. A.S.M., 1944, v.32, p.88.

13. Allen (N.P.) "Iron and its Dilute Solid Solutions", Interscience Publ., New York, 1963.

14. Smoluchowski (R), Phys. Rev. 1942, v.62, p.539.

15. Blanter (M.E.), Z.Technitscheskoi Fiziki SSR., 1950, v.20, p.1001.

16. Ivanov (A.G.), Symposium "Trud Tsent Nauchoissled Inst. Chem. Metallurgy", 1960, Issue 17, p.107.

17. Appleton (A.S.), Trans. A.I.M.E., 1964, v.230, p.893.

18. French patent No. 1,139,865 (8.7.1957).

19. Michel (E), "Les Aciers a-Outils", Dunod, Paris, 1950.

20. Roos (A), 16th Int. Congress of Pure and Applied Chemistry, Paris, 1957.

21. M^{c}Murray (J.G.), Unpublished report, University of Aston,1968.

22. Tucker (R), Unpublished report, University of Aston, 1970.

23. Thomas (A), Tribology Conference, September 1969, I.S.I. Preprint 125, p.55.

24. Bayliss (R.N.), M.Sc Thesis, University of Aston, October 1957.

25. Jack (K.H.), J.I.S.I., 1951, v.169, p.26.

26. Goldschmidt (H.J.), Ibid, 1948, v.160, p.345.

27. Goldschmidt (H.J.), Ibid, 1952, v.170, p.189.

28. Kuo (K), Ibid, 1953, v.174, p.223-228 and 363.

29. Woodhead (J.H.) and Quarrell (A.G.), "The Role of Carbides in Low-Alloy Creep-Resisting Steels" Climax Molybdenum Publ.

30. Seal (A.K.) and Honeycombe (R.W.K.), J.I.S.I., 1958, v.188, p.9 and 343.

31. Raynor (D), Whiteman (J.A.) and Honeycombe (R.W.K.), Ibid, 1966, v.204, p.1114.

32. Dyson (D.J.), Keown (S.R.), Raynor (D) and Whiteman(J.A.), Acta Met., 1966, v.14, p.867.

33. Allten (A.G.) and Payson (P), Trans. A.S.M., 1953, v.45, p.498.

34. Cohen (M), Metal Progress, 1947, v.51, p.781.

35. Balluffi (R.W.), Cohen (M) and Averbach (B.L.), Trans. A.S.M., 1951, v.43, p.497.

36. Hultgren (A), Rev.Met., 1953, v.50, p.737 and 847.

37. Sato (T) and Nishizawa (T), Tech.Report Tohuku University, 1960, v.25, p.65.

38. Kenneford (A.S.) and Williams (T), J.I.S.I., 1957, v.185, p.467.

39. Irani (J.J.) and Honeycombe (R.W.K.), Ibid, 1965, v.203, p.826.

40. Biswas (S.K.) and Seal (A.K.), J.of Tech.,1965, v.10,p.41.

41. Irvine (K.J.), Journees Internationales des Applications du Cobalt, Brussels, June 1964.

42. Seal (A.K.), Roy (J) and Roy (R), Trans. Ind.Inst.Met., 1965, v.18, p.159.

43. Loria (E.A.), Trans. A.S.M., 1945, v.34, p.407.

44. Houdremont (E) and Schrader (H), Krup.Monatshefte,1942, v.13, p.1.

45. Geller (Y.A.), and Novikova (O.A.), Stal, 1947, v.1, p.239.

46. Kayser (F) and Cohen (M), Metal Progress, 1952, v.61, p.79.

47. Gulyaev (A.P.), Stanki i Instrument, 1946, v.17, p.14.

48. Gudsov (N.T.) and Gelfand (K.M.), Bull.Acad.Sci.URSS. Classe Sci. Tech., 1947, p.93.

49. Oertal (W) and Poelzguter (F), Stahl und Eisen, 1924, v.44, p.1165.

50. Ruff (O) and Keilig (F), Zeitschrift für anorganische und allgemeine Chemie, 1914, v.88, p.410.

51. Schenck (R) and Klas (H), Ibid, 1929, v.178, p.146.

52. Bahr (H.A.) and Jessen (V), Berichte der deutschen chemischen Gesellschaft, 1930, v.63, p.2226.

53. Meyer (W.F.), Metall Wirtsch, 1938, v.17, p.413

54. Morrogh (H) and Williams (W.J.), J.I.S.I., 1947, v.155, p.321.

55. Hofer (L.J.E.) and Peebles (W.C.), J.Amer.Chem.Soc., 1947, v.69, p.893.

56. Nagakura (S), J.Phys.Soc.Jap., 1961, v.16, p.1213.

57. Richardson (F.D.), J.I.S.I., 1953, v.175, p.33.

58. Chandhok (V.K.), Hirth (J.P.) and Dulis (E.J.), Trans. A.S.M., 1963, v.56, p.677.

59. Chandhok (V.K.), Hirth (J.P.) and Dulis (E.J.), Trans. A.I.M.E., 1962, v.224, p.858.

60. Smith (R.P.), Ibid, 1965, v.233, p.397.

61. Hollomon (J.H.) and Turnbull (D), "Nucleation", Progress in Metal Physics, Pergammon Press, New York, 1953, v.4, p.333.

62. Heckel (R) and Paxton (W), Ibid, 1960, v.218, p.709.

63. Darkens (L.S.), Ibid, 1961, v.221, p.654.

64. Banerjee (B.R.) and Hauser (J.J.), Symposium "Transformation and Hardenability in Steels", Climax Molybdenum Publication 1967, p.133.

65. Pellissier (G.E.), D.M.I.C. Report No.210, p.173.

66. Seeger (A), "Stacking Fault in Close-Packed Lattices", Bristol Conf. Defects in Crystalline Solids, Phys.Soc., 1955, p.328.

67. Votava (E), Acta Met., 1960, v.8, p.901.

68. Stoloff (N.S.), Davies (R.G. and Ku (R.C.), Trans. A.I.M.E., 1965, v.223, p.1500.

69. Fourdeaux (A) and Berghezau (A), J.I.M., 1960, v.89, p.31.

70. Demny (J), Phys.Stat. Solidi, 1967, v.22. p.K1.

71. Miles (D.E.), Fourth Regional Conference on Electron Microscopy, Rome 1968, v.1, p.419.

72. Nutting (J), I.S.I. Centenary Preprint 1969, p.123.

73. Ohr (S.M.) and Beshers (D.N.), Phil.Mag., 1964, v.10, p.219.

74. Griffith (A.A.) and Phil.Trans. 1921, v.A221, p.163.

75. Barnby (J.T.), Welding and Metal Fabrication, 1969,Feb. p.71.

76. May (M.J.) and Walker (E.F.), "Low Alloy Steels" I.S.I. Report 114, p.149.

77. Greenwood (G.W.), "Fracture Toughness of High Strength Materials - Theory and Practice", Symposium, University of Sheffield, 25-27th March,1968, p.A1.

78. Walker (E.F.), Ibid. p.D1.

79. Brown (W.F.) and Shrawley (J.E.), A.S.T.M., STP 410.

80. Chiswick (H.H.) and Greninger (A.B.), Trans. A.S.M.,1944, v.32, p.483.

81. Hawkes (M.F.) and Mehl (R.F.), Trans. A.I.M.E., 1947, v.172, p.467.

82. Cohen (M), Trans. A.S.M., 1949, v.41, p.35.

83. Yamanaka (N) and Kusaka (K), Tetsu-to-Hague, 1960,v.46,p.46.

84. Roberts (G.A.), Hamaker (J.C.) and Johnson (A.R.), "Tool Steels", A.S.M. Publication, 3rd.Edition, 1962.

85. Irvine (K.J.), J.I.S.I., 1962, v.200, p.820.

86. Yeo (R.B.G.), Trans. A.I.M.E., 1963, v.227, p.884.

87. Connor (L.P.)and Dabkowski (D.S.), Tech.Report 429139, January 2, 1964.

88. Dolby (R.E.) and Ginn (B.J.), B.W.R.A. Report C153/5/66. December 1966.

89. Hopkins (A.D.), Unpublished Report, University of Aston,1967.

90. Hammond (C.M.), Cobalt, 1964, No.25, p.15.

91. Allison (F), Trans. A.I.M.E., 1927, v.75, p.234.

92. Scherer (R), Archivfür das Eisenhüttenwesen, 1927, v.1, p.325-329.

93. Houdremont (E) and Schrader (H), Ibid, 1932, v.5, p.523-534.

94. Esser (E), Eilander (K) and Majert (C), Ibid, 1933, v.7,p.367.

95. Davenport (E), Trans. A.S.M., 1939, v.27, p.837.

96. Hagel (W.C.), Pound (G.M.) and Mehl (R.F.), Acta.Met., 1956, v.4, p.37.

97. Kramer (J.J.) and Pound (G.M.), Final Report O.O.R. Cont.No. DA-36-961-ORD-543. 30th September,1956.

98. Aaronson (H.I.), Domain (H.A.) and Pound (G.M.), Trans. Met.Soc. A.I.M.E., 1966, v.236, p.768.

99. Riley (D.), M.Sc Thesis University of Aston,September 1967.

100. Etienne (C.F.) and Scheepens (C.P.), Metal Progress,1962, December, p.77.

101. Russell (T.F.), First Report of the Alloy Steels Research Committee, I.S.I. Special Report No.14, 1936, p.149.

102. Jominy (W.E.) and Boegehold (A.L.), Trans. A.S.M., 1938, v.26, p.574.

103. Lange (K) and Meinert (H), Werkstaffstechnik und Maschinenban, 1956, v.46, p.81.

104. D.F.R.A., Metal Treatment, 1965, v.32, p.47.

105. Kirkham (K.E.), M.Sc Thesis, University of Aston in Birmingham, September 1968.

106. Bhattacharyya (J), M.Sc Thesis, University of Aston in Birmingham, April, 1969.

107. Jaffe (L.D.) and Hollomon (J.H.), Trans. A.I.M.E.,1946, v.167, p.

108. Andrews (K.W.), J.I.S.I., 1965, v.203, p.721.

109. Trusculescu (H), Revue Roumaine des Sciences Techniques Sevie de Metallurgie, 1966, v.11, p.169.

110. Priest (A.H.) and May (M.J.), B.I.S.R.A. Report MG/E/404/66, 1966.

111. Krafft (J.M.), Applied Materials Research, 1964,April,p.88.

112. Capus (J.M.) and Meyer (G), Metallurgia, 1960, v.61-62, October, p.133.

113. Klingler (L.J.), Barnett (W.J.), Frohmberg (R.P.) and Troiano (A.R.), Trans. A.S.M., 1954, v.46, p.1557.

114. Woodfine (B.C.), J.I.S.I.,1953, v.173, p.240.

115. Uddeholmes Aktiebolag, Hagfors Jarnverk, Hagfors Laboratoriemeddelande, 1958, August, 15874-F.

116. Wetter (E), Dissertation, T.H. Hannover, 1964.

117. Ardell (A.J.), "The Mechanism of Phase Transformations in Crystalline Solids", I.M. Monograph No.33, 1969, p.111.

118. Bilby (B.A.) and Christian (J.W.), Symposium "Mechanism of Phase Transformations in Metals", Inst. of Metals, 1956, p.121.

119. Cohen (M), Trans. A.I.M.E., 1958, v.212, p.171.

120. Dulieu (D) and Nutting (J),"High Alloy Steels", I.S.I. Report 86, 1964, p.140.

121. Christian (J.W.) and Swann (P.C.), Symposium "Properties of Solid Solutions", A.I.M.E., 1963.

122. Nutting (J), Ref (121), p.160.

123. Mathews (J.A.), Proc. A.S.T.M., 1919, v.19, p.141.

124. "Inco Nickel", 1966, No.16, July, p.16.

125. Pick (H.J.), "Conservation of Nickel in Alloy Steels", Symposium, University of Aston in Birmingham,February 1970.